OFFICE OF CIVILIAN RADIOACTIVE WASTE MANAGEMENT
SPECIAL INSTRUCTION SHEET

1. QA: QA

Complete Only Applicable Items

This is a placeholder page for records that cannot be scanned.

2. Record Date	3. Accession Number
06/18/2001	MOL.20010625.0306
4. Author Name(s)	**5. Author Organization**
ROBERT FITCH	N/A

6. Title/Description
SECONDARY URANIUM-PHASE PARAGENESIS AND INCORPORATION OF RADIONUCLIDES INTO SECONDARY PHASES

7. Document Number(s)	8. Version Designator
ANL-EBS-MD-000019	REV. 0, ICN 01

9. Document Type	10. Medium
REPORT	OPTIC/PAPER

11. Access Control Code
PUB

12. Traceability Designator
DC #27136

13. Comments
THIS IS A ONE-OF-A-KIND DOCUMENT DUE TO THE COLORED GRAPHS ENCLOSED AND CAN BE LOCATED THROUGH THE RPC

OFFICE OF CIVILIAN RADIOACTIVE WASTE MANAGEMENT
ANALYSIS/MODEL COVER SHEET

1. QA: QA

Page: 1 of: 65

Complete Only Applicable Items

2. ☒ Analysis — Check all that apply

Type of Analysis:
- ☐ Engineering
- ☐ Performance Assessment
- ☒ Scientific

Intended Use of Analysis:
- ☐ Input to Calculation
- ☐ Input to another Analysis or Model
- ☒ Input to Technical Document
- ☐ Input to other Technical Products

Describe use:

Input to Waste Form PMR

3. ☒ Model — Check all that apply

Type of Model:
- ☒ Conceptual Model
- ☐ Abstraction Model
- ☐ Mathematical Model
- ☐ System Model
- ☐ Process Model

Intended Use of Model:
- ☐ Input to Calculation
- ☐ Input to another Model or Analysis
- ☒ Input to Technical Document
- ☐ Input to other Technical Products

Describe use:

Alternative conceptual model for use in TSPA

4. Title:

Secondary Uranium-Phase Paragenesis and Incorporation of Radionuclides into Secondary Phases

5. Document Identifier (including Rev. No. and Change No., if applicable):

ANL-EBS-MD-000019 REV 00 ICN 01

6. Total Attachments:

3

7. Attachment Numbers - No. of Pages in Each:

I-17, II-11, III-4

	Printed Name	Signature	Date
8. Originator	Robert Finch	Christine Stockman for Robert Finch	6/5/01
9. Checker	Terry Steinborn		6/5/01
10. Lead/Supervisor	Patrick Brady	Christine Stockman for Pat Brady	6/5/01
11. Responsible Manager	Christine Stockman	Christine Stockman	6/5/01

12. Remarks:

Reproduction of figures in either black + white or color is acceptable. CJS 6/5/01

OFFICE OF CIVILIAN RADIOACTIVE WASTE MANAGEMENT
ANALYSIS/MODEL REVISION RECORD

Complete Only Applicable Items

2. Analysis or Model Title:

Secondary Uranium-Phase Paragenesis and Incorporation of Radionuclides into Secondary Phases

3. Document Identifier (including Rev. No. and Change No., if applicable):

ANL-EBS-MD-000019 REV 00 ICN 01

4. Revision/Change No.	5. Description of Revision/Change
REV 00	Initial Issue
REV 00 ICN 01	Re-evaluate experimental results from dissolution studies on spent fuel, as well as analyze expected in-package chemistries, in order to develop a secondary-phase-based model for estimating dissolved Np concentrations in a breached waste package. Substantial changes were made to Sections 6.7.1, 6.7.2, and 7.1; Section 6.7.2.3 was added (including Subsection 6.7.2.3.1). Section A2.1 was inserted (having been moved from the main text). Minor editorial corrections and clarifications were also made to the text, none of which affected the analysis, conclusions or recommendations.

CONTENTS

Page

1. PURPOSE 8

2. QUALITY ASSURANCE 8

3. COMPUTER SOFTWARE AND MODEL USAGE 8

4. INPUTS 9
   - 4.1 DATA AND PARAMETERS 9
   - 4.2 CRITERIA 10
   - 4.3 CODES AND STANDARDS 11

5. ASSUMPTIONS 11

6. ANALYSIS/MODEL 12
   - 6.1 INTRODUCTION 12
   - 6.2 SOLUTION BEHAVIORS OF KEY RADIONUCLIDES DURING CORROSION OF SPENT UO_2 FUELS 14
   - 6.3 OXIDATIVE ALTERATION OF SPENT UO_2 FUELS–EXPERIMENTAL OVERVIEW 16
     - 6.3.1 Experimental Corrosion and Dissolution of Fuel 16
   - 6.4 SUMMARIES OF SELECTED FUEL EXPERIMENTS 16
     - 6.4.1 ANL Unsaturated Drip and Humid-Air Tests (CRWMS M&O 2000b; Finch et al. 1999) 16
     - 6.4.2 Nevada Nuclear Waste Storage Investigations (NNWSI) Series 2 and 3 Fuel Dissolution Tests (Wilson 1990a, 1990b) 20
     - 6.4.3 Swedish Nuclear Fuel and Waste Management Company (SKB) Series 11, Clad-Fuel Experiments (Forsyth and Werme 1992) 21
     - 6.4.4 CANDU Dissolution Experiments (Stroes-Gascoyne et al. 1997) 22
   - 6.5 THERMODYNAMIC PARAMETERS FOR U(VI) SOLIDS 22
     - 6.5.1 System CO_2-CaO-UO_3-H_2O 25
     - 6.5.2. Systems SiO_2-CaO-UO_3-H_2O and SiO_2-Na_2O-UO_3-H_2O 28
   - 6.6 KINETIC PARAMETERS FOR U(VI) COMPOUNDS 31
   - 6.7 DISCUSSION 33
     - 6.7.1 Water Contact and In-Package Chemistry 33
     - 6.7.2 Neptunium 35
     - 6.7.3 Technetium 44
     - 6.7.4 Plutonium 44
     - 6.7.5 Iodine 45
     - 6.7.6 Selenium 45
     - 6.7.7 Americium 45
     - 6.7.8 Protactinium 46
     - 6.7.9 Carbon 46

CONTENTS (Continued)

Page

6.7.10 Codisposal Waste Packages (Defense Spent Nuclear Fuel and High-Level Waste Glasses) 46
6.7.11 Estimating RN Concentrations Over the Very Long Term (to ~10^6 years) 47

7. CONCLUSIONS 49
7.1 RECOMMENDATIONS 50
7.2 EFFECTS OF UNCERTAINTIES 51

8. INPUTS AND REFERENCES 54
8.1 DOCUMENTS CITED 54
8.2 CODES, STANDARDS, AND REGULATIONS 64
8.3 SOURCE DATA 65

ATTACHMENT I - OVERVIEW OF SELECTED RADIONUCLIDE RELEASE DATA FROM ANL UNSATURATED DRIP AND HUMID-AIR TESTS I-1

ATTACHMENT II - PARAGENESIS OF URANIUM MINERALS IN NATURE II-1

ATTACHMENT III - USE OF EXEMPT SOFTWARE IN AMR.ANL-EBS-MD-000019 ..... III-1

FIGURES

Page

1. Actinide Concentrations in Leachates In ANL HDR Tests on Spent Fuel 18
2. Solution Molar An/U Ratios in ANL HDR Tests on Spent Fuel 18
3. Activity-Activity Diagram for the System CO2-CaO-UO3- H_2O 26
4. Activity-Activity Diagram for the System SiO2-CaO-UO3- H_2O 29
5. Activity-Activity Diagram for the System SiO_2-Na_2O-UO_3-H_2O 31
6. Schematic Representation of Alteration-Phase Paragenesis 33
7. Activity-Activity Diagram for the System SiO_2-CaO-UO_3-H_2O 35
8. Distribution of Reported log[Np] Values for Hydrologically Unsaturated and Batch Experiments with Spent Fuel 42
9. Distributions of Np Concentrations Versus pH Calculated from the Model Proposed Here and Compared with Measured Np Concentrations Reported from Dissolution Studies on Spent Fuel 43

A1. Back Scattered-Electron Images of Corroded Spent Fuel from ANL Drip Tests I-2
A2. Cumulative Releases of U and Np in HDR Tests I-8
A3. Cumulative U, Np, and Tc Releases in ANL Drip Tests I-8
A4. Molar Concentrations of Np and U in Solution, ANL HDR Tests I-9
A5. Molar Ratios Np/U in Solution for All ANL Unsaturated Tests I-9
A6. Comparisons of U, Np, and Tc Releases in ANL HDR and LDR Tests I-10
A7. Np Releases in ANL LDR and Humid-Air Tests I-10
A8. Cumulative Tc Release as Fraction of Inventory in HDR Tests and LDR Tests at ANL I-13
A9. Cumulative Releases of Pu (fraction of inventory) for all ANL Unsaturated Tests I-14
A10. Cumulative Releases of I (fraction of inventory) for all ANL Unsaturated Tests I-15
A11. Cumulative Releases of Am in Unsaturated Tests at ANL I-16

TABLES

Page

1. Reference Data Used as Input for This Analysis 10
2. Priority Radionuclides and Their Sources in Fuel and Potential Sinks During Fuel Corrosion[b] 15
3. Priority Radionuclides and Their Crystal-Chemical and Aqueous-Chemical Analogues 15
4. Release Behaviors of Some Radionuclides in ANL Drip Tests 16
5. Uranium Corrosion Products Identified in Tests on Spent UO_2 Fuel Reacted in Groundwater and Humid Air 20
6. Molar Contributions of Structural Components to $\Delta G^0_{f,298}$ and $\Delta H^0_{f,298}$ of U(VI) ($kJ.mol^{-1}$) 24
7. $\Delta G^0_{f,298}$ and $\Delta H^0_{f,298}$ for U(VI) Minerals Indicated in Figures 3 and 4 ($kJ.mol^{-1}$) 25
8. Intrinsic Dissolution Rates for Uranophane, Schoepite, and Soddyite 32
9. Range of In-Package Fluid Compositions (mol/L, except for pH and Eh)[a] 34
10. Statistics Calculated from Np Concentrations Reported from Fuel Studies[a] 42
11. Data Required for Understanding the Role of Corrosion Products in Radionuclide Release 53

ACRONYMS AND ABBREVIATIONS

AMR	analysis/model report
ANL	Argonne National Laboratory
ASTM	American Society for Testing and Materials
ATM	Approved Testing Material
BSE	back-scattered electron
CSNF	commercial spent nuclear fuel
DIW	de-ionized water
DOE	U.S. Department of Energy
DS	dehydrated schoepite
DTN	data tracking number
EBS	Engineered Barrier System
EDS	energy dispersive spectroscopy
EELS	electron energy loss spectroscopy
HDR	high drip rate
ICPMS	inductively coupled plasma mass spectrometry
LDR	low drip rate
LWR	light water reactor
NNWSI	Nevada Nuclear Waste Storage Investigations
NRC	U.S. Nuclear Regulatory Commission
PA	performance assessment
QA	Quality Assurance
REE	rare earth element
RN	radionuclide
SEM	scanning electron microscope
Simfuel	simulated spent UO_2 fuel
SKB	Swedish Nuclear Fuel and Waste Management Company
TEM	transmission electron microscope
wt.%	weight percent
YMP	Yucca Mountain Site Characterization Project

1. PURPOSE

The purpose of this analysis/model report (AMR) is to assess the potential for uranium (U) (VI) compounds, formed during the oxidative corrosion of spent uranium-oxide (UO_2) fuels, to sequester certain radionuclides and, thereby, limit their release. The "unsaturated drip tests" being conducted at Argonne National Laboratory (ANL) provide the basis of this AMR (Table 1). The ANL drip tests on spent fuel are the only experiments on fuel corrosion from which solids have been analyzed for trace levels of radionuclides. Brief summaries are provided of the results from other selected corrosion and dissolution experiments on spent UO_2 fuels, specifically those conducted under nominally oxidizing conditions. Discussions of the current understanding of thermodynamic and kinetic properties of U(VI) compounds is provided in order to outline the scientific basis for modeling precipitation and dissolution of potential radionuclide-bearing phases under repository-relevant conditions. Attachment I provides additional information on corrosion mechanisms and behaviors of radionuclides in the tests at ANL. Attachment II reviews occurrence, formation, and alteration (collectively known as paragenesis) of naturally occurring U(VI) minerals because natural mineral occurrences can be used to assess the possible long-term behaviors of U(VI) compounds formed in short-term laboratory experiments and to extrapolate experimental results to repository-relevant time scales.

This AMR develops a model for calculating dissolved concentrations of radionuclides that are incorporated into U(VI) compounds, which is an alternative to models currently used in TSPA to calculate dissolved concentration limits for certain radionuclides. In particular, the model developed in this AMR applies to Np (neptunium) concentrations being controlled by solid uranyl oxyhydroxides that are known to contain trace levels of Np. The results of this AMR and the conceptual model developed from it and presented in Section 6.7.2.3 are primarily intended to support sensitivity evaluations in performance assessment.

This AMR was developed in accordance with the *Technical Work Plan for Waste Form Degradation Process Model Report for SR* (CRWMS M&O 2000a). The scope of this AMR is outlined in the section "Mixed Phase Dissolved Radionuclide Concentration Limits" of the technical work plan.

2. QUALITY ASSURANCE

An activity evaluation (CRWMS M&O 2000a, Enclosure 1), which was prepared per AP-2.21Q, *Quality Determinations and Planning for Scientific, Engineering, and Regulatory Compliance Activities*, determined that the Quality Assurance (QA) program (DOE 2000) applies to the activity under which this AMR was developed. Control of the electronic management of data was accomplished in accordance with the controls specified by CRWMS M&O (2000a, Enclosure 4).

3. COMPUTER SOFTWARE AND MODEL USAGE

Microsoft Excel 97 SR-1 was used to generate several figures in this AMR. No macros or subroutines were used. All calculations performed (e.g., addition, subtraction, division, squares, etc.) can be performed without the aid of Excel. Several figures simply display data taken from

tables in DTN: LL991001251021.090, and no calculations were performed for displaying such information. Figures 1, 2, 9, and A4 display solution-concentration data taken directly from DTN: LL991001251021.090 (additional corroborative data plotted in Figure 9 are from Wilson 1990a, 1990b). Figure A5 shows the molar ratios of Np and U in solution, calculated by dividing the dissolved Np concentration at each sampling interval by the total dissolved U concentration for the same sampling interval (all U and Np solution data are taken from DTN: LL991001251021.090 for Figure A5). Figures 3, 4, 5, and 7 are thermodynamic stability diagrams, for which phase-field boundaries were calculated according to the method described in Attachment III with free-energy data in Table 7; the hachured field in Figure 7 displays the range of solution compositions indicated by CRWMS M&O (2000c, Table 3). Figure 9 shows the modeled concentration of total dissolved Np as a function of pH, calculated by multiplying the result of Equation 3 in CRWMS M&O (2000d) (i.e., [U]total) by the Np/U proportionality in Equation 5 of this AMR. Figures A2, A3, and A6-A11 display cumulative release fractions, taken directly from DTN: LL991001251021.090; these figures also show linear least-squares fits through the radionuclide-release data (calculated by using standard least-squares techniques), and report the slopes of the lines through the data as "release rates." Additional information about how figures in this report were generated is provided in Attachment 3. The computer platform on which the software was executed was a Dell Corporation 'OptiPlex GXa' personal computer with an Intel Pentium II processor (ANL property number CSI319029) running on a local-area network (Windows NT, version 4.0).

4. INPUTS

4.1 DATA AND PARAMETERS

Data used to directly support this AMR are derived from the *Unsaturated Dissolution and Release Rate (Reaction) Tests on Spent Fuel and UO2* (Stout 1998) performed at ANL under activity number D-20-43, as part of the Lawrence Livermore National Laboratory Yucca Mountain Site Characterization Project (YMP) Scientific Investigation Plan for Spent Fuel Waste Form Testing (YMP WBS Element 1.2.2.3.1.1). Work for this test plan was conducted under a QA Level I quality assurance plan that is listed as YMP-02-001 in records maintained at ANL for the Lawrence Livermore National Laboratory YMP program. This work is described in *Test Plan for Reactions Between Spent Fuel and J-13 Well Water Under Unsaturated Conditions* (Finn et al. 1993).

This AMR, as well as the conceptual model for calculating dissolved Np concentrations that is developed from it, is primarily intended for use in sensitivity evaluations. This AMR draws upon information that may be superseded in the future, and the potential impact any superseded documents have on this AMR will be evaluated as needed.

This document may be affected by technical product input information that requires confirmation. Any changes to the document that may occur as a result of completing the confirmation activities will be reflected in subsequent revisions. The status of the technical product input information quality may be confirmed by review of the DIRS database.

The data used as input in this report are appropriate because the experiments from which the data are derived are technically relevant to the processes being addressed in this report. The ANL experiments on fuel corrosion are also the only experiments available for which solid uranium compounds (U secondary phases) have been analyzed directly for minor and trace levels of incorporated radionuclides.

Data reported here in direct support of this AMR are derived from the following sources (Table 1). Additional corroborating data, described in Section 6, were obtained from the open literature (see Section 8).

Table 1. Reference Data Used as Input for This Analysis

Reference Data/Document	Input Description	Cited In
Data Tracking Number (DTN): LL991001251021.090	Dissolution and alteration of spent fuel by ground water	Section 6.4.1 and Attachment I:
DTN: LL010305512241.024, pp. 148-149, ANL-CMT Scientific Notebook 1355	Transmission electron microscope (TEM) analyses and electron energy loss spectroscopy (EELS) and energy dispersive spectroscopy (EDS) compositional analyses of Pu-rich residue in ANL unsaturated drip tests	Section 6.4.1
DTN: LL991110351021.100, pp. 173-174, ANL-CMT Scientific Notebook 867 and 1528	TEM analyses (micrographs, EDS, and EELS) of colloids from spent fuel	Section 6.4.1
DTN: LL010305312241.022, pp. 36-38, 40, pp. 108-109, ANL-CMT Scientific Notebook 1528	TEM analyses and EELS and EDS compositional analyses of Pu-rich residue in ANL unsaturated drip tests	Section 6.4.1
DTN: LL010109312241.021 (pp. 2-3, 6, 16) ANL-CMT Scientific Notebook 1635	Altered fuel analyses by inductively coupled plasma mass spectrometry (ICPMS)	Section 6.4.1

4.2 CRITERIA

This report is not related to system description documents or design criteria.

One of the objectives of this AMR is to document progress in addressing the applicable U.S. Nuclear Regulatory Commission (NRC) key technical issues in the NRC's *Issue Resolution Status Report, Key Technical Issue: Container Life and Source Term* (NRC 1999) and *Issue Resolution Status Report Key Technical Issue: Total System Performance Assessment and Integration* (NRC 2000). These documents give acceptance criteria to be applied for reviewing the U.S. Department of Energy (DOE)'s License Application. The general acceptance criteria in each of these documents were used as general guidance, and the specific acceptance criteria directly relevant to this AMR are listed below.

Container Life and Source Term, Subissue 3 (Section 4.3 of NRC 1999):

4. DOE has identified and considered likely processes for SNF degradation and the release of radionuclides from the Engineered Barrier System (EBS), as follows: dissolution of the irradiated UO_2 matrix, with the consequent formation of secondary minerals and colloids; prompt release of radionuclides; degradation in the dry air environment; degradation and

failure of fuel cladding; preferential dissolution of intermetallics in DOE SNF; and release of radionuclides from the WP emplacement drifts.

5. DOE has demonstrated that the numerical models used for SNF degradation and radionuclide release from the EBS are adequate representations, including consideration of uncertainties, of the expected SNF performance. They are not likely to overestimate the actual performance in the repository environment.

8. DOE has conducted a consistent, sufficient, and suitable SNF corrosion and radionuclide release testing program at the time of the license application submittal. In addition, DOE has identified specific plans for further testing to reduce any significant area (or areas) of uncertainty as part of the performance confirmation program.

Total System Performance Assessment and Integration (NRC 2000, Criterion T3 and T4), Subissue 3, Radionuclide Release Rates and Solubility Limits:

3. Alternative waste form dissolution and radionuclide release modeling approaches consistent with available data and current scientific understanding are investigated and results and limitations appropriately factored into the radionuclide release rates and solubility limits abstraction.

4. Radionuclide release rates and solubility limits abstraction outputs is supported by comparison to outputs of detailed process models or empirical observations (field, laboratory, and natural analog data).

4.3 CODES AND STANDARDS

Data collection and analyses for data used directly to support this AMR followed the American Society for Testing and Materials (ASTM) standard for service condition tests, *Standard Practice for Prediction of the Long-Term Behavior of Materials, Including Waste Forms, Used in Engineered Barrier Systems (EBS) for Geological Disposal of High-Level Radioactive Waste* (ASTM C 1174-97 1997).

5. ASSUMPTIONS

In order to calculate dissolution rates reported in Table 8, Section 6.6, it has been assumed that the surface area of schoepite remained constant during the duration of the dissolution study reported by Casas et al. (1994). This assumption is based on the fact that only a small fraction (< 9%) of the original mass of schoepite dissolved during the experiment by Casas et al. (1994). This assumption is unlikely to affect the derived result within the error of the originally reported data; however, the degree to which this is true cannot be ascertained and needs no verification at this time. However, the values cited in Table 8 do not support this AMR directly but provide additional input for how to apply the results of this AMR.

6. ANALYSIS/MODEL

6.1 INTRODUCTION

Unused UO_2 fuel is nearly stoichiometric UO_2. During irradiation, fission and neutron capture create fission products and transuranic actinides. Nevertheless, even after irradiation, spent UO_2 fuel remains greater than 95% UO_2 (Finch et al. 1999). UO_2 is virtually insoluble in water under reducing conditions (Eh at or below approximately 0 mV at near-neutral pH values), and natural UO_2 (uraninite) is known to persist in natural reducing environments for many millions of years. In an oxidizing environment, such as exists at the site of the proposed Yucca Mountain repository, UO_2 and, therefore, spent UO_2 fuel are not stable. The U(IV) in fuel oxidizes to U(VI), destroying the UO_2 structure. The rate at which UO_2 and fuel oxidize and decompose in dry air is strongly dependent on kinetics of both oxygen diffusion in UO_2 and crystallization of higher oxides, including U_4O_9, U_3O_7 (unirradiated UO_2 only), and U_3O_8 (Thomas et al. 1993; McEachern and Taylor 1998). In the presence of an aqueous phase (water), U oxides above cubic U_4O_9-type oxides are irrelevant because dissolution dominates, and the kinetics of UO_2 dissolution in oxidizing aqueous media are orders of magnitude faster than those of dry-air oxidation (Shoesmith and Sunder 1991).

Most actinides and lanthanides (rare earth elements [REE]) are soluble in crystalline UO_2 and probably replace U in structural sites. The release of these compatible elements from UO_2 requires decomposition of the UO_2 structure (the fuel matrix); e.g., by dissolution. Many fission products are relatively insoluble in UO_2, including Cs, Rb, Ba, Te, Mo, Tc, Ru, Rh, Pd, halides (e.g., Cl and I), and noble gases (e.g., Xe and Kr). These incompatible elements may exsolve from the UO_2 matrix and precipitate as separate phases during in-reactor operation. The extent of exsolution and the location of these elements in unoxidized spent fuel depend largely on irradiation history, burn up, and in-reactor temperatures. Incompatible elements may precipitate as inclusions within the fuel matrix, diffuse to and precipitate along grain boundaries and other defects, or migrate to the gap between the UO_2 fuel and the cladding. Many fission products can combine with other elements in the fuel to form phases stable at reactor temperatures (e.g., CsI, $BaUO_4$, ε-Ru). Knowledge of the locations and dissolution behaviors of these exsolved phases under repository-relevant conditions is critical for understanding how radionuclides (RN) contained within them may be released to solution. Some of these phases may dissolve in water rapidly upon contact (e.g., CsI), whereas the decomposition of others may be governed by oxidation and dissolution kinetics that are independent of those of the fuel matrix (e.g., ε-Ru particles) (Forsyth and Werme 1992; Johnson and Werme 1994).

The immediate fate of radioelements released from dissolving spent fuel will depend on the solubilities of compounds in which radioelements become incorporated under oxidizing conditions. Some radioelements, such as noble gases or, perhaps, halides, do not form stable solids in water except at unrealistically high concentrations. Many other radioelements can reprecipitate as components of solid corrosion products. These so-called "secondary" phases may be "pure," containing only one radioelement and elements derived from groundwater (e.g., metaschoepite, $(UO_2)_4O(OH)_6(H_2O)_5$, or Na-boltwoodite, $(Na,K)(UO_2)(SiO_3OH)(H_2O)_{1.5}$). Some radioelements may recombine into new, more stable compounds (e.g., $Cs_{2-2x}Ba_x(UO_2)_5(MoO_4)\cdot nH_2O$, identified by Buck et al. 1997) or, perhaps most commonly,

minor radioelements may form limited solid solutions by substituting for major elements in stable secondary phases (e.g., . Ba substitution for Ca in uranophane, $Ca_{1-x}Ba_x(UO_2)_2(SiO_3OH)_2(H_2O)_5$; Finn et al. 1998). The most abundant radioelement in spent fuel is U, which forms a myriad of solid U(VI) (uranyl) compounds, depending on solution composition, the concentration of dissolved U, as well as crystallization kinetics of various uranyl phases. Therefore, when exposed to humid air or relatively small volumes of dripping or standing groundwater, the oxidative corrosion of spent UO_2 fuel is a complex, heterogeneous process involving dissolution and precipitation of multiple radioelement-bearing solids, many of which may be metastable (Wronkiewicz et al. 1992; 1996). Incorporation of radioelements into solids formed during the corrosion of spent nuclear fuel may reduce radioelement concentrations in waters that have contacted fuel and its corrosion products, although the degree to which this applies to most specific radioelements remains poorly understood.

U(VI) solids formed during corrosion of both unirradiated UO_2 and spent UO_2 fuel are closely similar to solids formed where natural UO_2 has been corroded by oxidizing groundwaters (Finch and Ewing 1992; Pearcy et al. 1994), suggesting that solids formed in fuel experiments are likely to form in a geologic repository under similar conditions. In nature, uranyl minerals may persist for many thousands of years under some geochemical conditions (Finch et al. 1996), including those conditions relevant to Yucca Mountain (Murrell et al. 1999). Thus, evidence from studies of natural U occurrences suggests that U(VI) solids with radionuclides in stable structural sites are potentially long-term radionuclide hosts.

In order to quantify and model radionuclide sequestration by U(VI) solids we need to know the following:

(1) Identity of solids that sequester Np and other radionuclides

(2) Radionuclide partition coefficients between U(VI) solids and aqueous solutions as a function of solution composition

(3) Solubilities and stability ranges of relevant U(VI) solids (i.e., thermodynamic parameters)

(4) Rates of precipitation and dissolution for relevant U(VI) solids (i.e., kinetic rate laws).

Without this kind of information, strictly empirical evidence that radionuclides are incorporated into solids formed on corroded fuel under select experimental conditions provides only limited confidence that these same solids will limit radionuclide releases over repository-relevant time scales.

The analysis and model presented in this report address processes relevant to understanding radionuclide concentration limits in water, one of the principle factors for the repository post-closure safety case. The model and analyses presented here are, therefore, assigned Level-1 importance.

6.2 SOLUTION BEHAVIORS OF KEY RADIONUCLIDES DURING CORROSION OF SPENT UO_2 FUELS

The emphasis of this analysis is on eight radionuclides considered in the TSPA-VA Base Case Performance Analysis (DOE 1998, Section 3.5.1, Table 3-14), which are of special concern because of their long half-lives, radiological toxicities, and potential mobilities. These are the three actinides: Np-237, Pu-239, and Pa-231 and the four fission products: Tc-99, I-129, Se-79, and C-14. In addition, Am-241 is discussed in this analysis because it is a parent of Np-237 (Tables 2 and 3). These radionuclides can also be loosely categorized by their release behaviors according to how fast they are released to solution relative to U, the predominant radioelement in the fuel (Table 4) with the fission products generally being released more rapidly than the actinides.

We can look to nature to help us understand potential long-term behaviors of radionuclides in nature. A few of these radionuclides have naturally occurring isotopes, and some radionuclides in Tables 2 and 3 may behave in ways comparable to other more common naturally occurring elements that may serve as chemical analogues for their behaviors. For example, non-radioactive isotopes of I, Se, and C occur in many natural waters at concentrations that may be relevant to concentrations attainable in a repository. Also, Se and S are chemically similar in many respects. Americium, which has no naturally occurring counterpart, is chemically similar to yttrium and trivalent REE. Protactinium has been well studied because of its importance to U-series age-dating techniques; it is chemically similar to Ta and occurs as a trace constituent in U-bearing minerals. Technetium, Pu, and Np have no good chemical analogues, nor do they occur naturally (at least in substantial quantities; see Curtis et al. 1999 for a discussion of natural Tc-99 and Pu). The best chemical analogues for Pu and Np are Th and U, but the stable oxidation states and redox sensitivities of these actinides can differ dramatically under similar geochemical conditions (Ce^{4+} has been used as a surrogate for Pu^{4+} in some solid-state studies).

In terms of potential mobility in groundwater, several elements listed in Tables 2 and 3 can only form solids in water when their concentrations reach levels higher than those considered likely in or near the repository (CRWMS M&O 2000d); these are potentially mobile elements. For example, Tc (as TcO_4^-), I (as I^- or IO_3^{2-}), C (as bicarbonate HCO_3^-) and Se (as selenite, SeO_3^{2-}, or selenate, SeO_4^{2-}) can all form anionic solution species and are unlikely to form pure phases at concentrations likely to be reached in groundwaters contacting a repository (CRWMS M&O 2000d; Chen et al. 1999b). Recent studies suggest that the mobility of Am in groundwater such as J-13 well water from near Yucca Mountain may be most strongly influenced by Am-carbonate solution complexes (Clark et al. 1995). Under sufficiently oxidizing conditions, Pu is also potentially mobile as PuO_2^+ or PuO_2^{2+} ions, possibly including plutonyl carbonate complexes (Clark et al. 1995). Neptunium (as NpO_2^+) is considered potentially mobile because pure neptunyl solids are believed to be sufficiently soluble in most natural waters, including J-13 well water (Efurd et al. 1998), that Np mobility is considered problematic; however, relatively few thermodynamic data are available to confirm this. The potential for sorption of anions and singly valent cations to existing minerals in the surrounding country rocks is considered small. Colloidal transport is also considered potentially important for several radionuclides. Colloids are addressed in the analysis model reports, *Colloid-Associated Radionuclide Concentration*

Limits: ANL (CRWMS M&O 2001a) and *Waste Form Colloid-Associated Concentration Limits: Abstraction and Summary* (CRWMS M&O 2001b).

Table 2. Priority Radionuclides and Their Sources in Fuel and Potential Sinks During Fuel Corrosion[b]

Element	Primary Source	Sinks		Limits to Release
		Solution	Solids	
Tc	ε-Ru particles (GB and matrix)	~100%	*trace*	Reaction Rate
I	Grain Boundaries	~100%	*trace*	Reaction Rate
Se	*unknown*	*unknown*	*unknown*	*unknown*
C	*unknown*	*unknown*	*unknown*	*unknown*
Actinides				
Np	UO_2 Matrix	minor (~10%)	*unknown*	Saturation (?)
Pu	UO_2 Matrix	*trace*	Residuum [a]	Saturation
Am	UO_2 Matrix	minor (1-3%)	Residuum [a]	Saturation
Pa	UO_2 Matrix	*unknown*	*unknown*	Saturation (?)

NOTE: [a] Ill-defined phase identified by transmission electron microscopy and interpreted as an insoluble residue remaining after bulk fuel-matrix dissolution.

Source: [b]Based on data from Finn et al. (1998) and CRWMS M&O (2000b)

Table 3. Priority Radionuclides and Their Crystal-Chemical and Aqueous-Chemical Analogues

Element	Valence	Ionic Radius (pm)[b]	Crystal-Chemical Analogue [a]	Aqueous Chemical Analogue [a]
Tc	+7	37-56	Re	Re
I	-1 +5	220 95-42	Br-, At- *none*	Br-, At- *none*
Se	+4, +6	50-28	Si^{4+}, S	(S)
C	+4	15	B, N	*none*
Actinides				
Np	+4, +5 (+6)	98-75	U	U
Pu	+3, +4, +5, +6	100-71	U	Ln^{3+}, Ce^{4+}, U
Am	+3	109	Ln^{3+}	Ln^{3+}
Pa	(+4) +5	78-95	(Th) Ta	(Th) Ta

NOTE: [a]Ln^{3+} refers to the trivalent lanthanide-series elements ($57 \leq Z \leq 71$).

Source: [b]Shannon (1976)

Table 4. Release Behaviors of Some Radionuclides in ANL Drip Tests

Radionuclide Release Rate	Element
Rapid (>> U)	Tc, I, (Mo), Xe, Kr
Moderate (≥ U)	Cs, Sr, (Mo)
Slow (≤ U)	Pu, Np, Am, REE, Zr
Uncertain	Se, Pa, ^{14}C

Source: Based on data from Finn et al. (1997) and CRWMS M&O (2000b)

6.3 OXIDATIVE ALTERATION OF SPENT UO_2 FUELS–EXPERIMENTAL OVERVIEW

6.3.1 Experimental Corrosion and Dissolution of Fuel

Numerous experiments have been conducted on the oxidative corrosion of unirradiated UO_2, spent UO_2 fuels and simulated spent UO_2 fuel (Simfuel). Because the emphasis in this report is on the potential roles of secondary U(VI) corrosion products in sequestering radionuclides, only a few studies that either report the formation of U(VI) solids and those for which the specific radionuclides addressed here are reported will be discussed. Only one series of experiments on spent fuel corrosion has analyzed and reported trace-level radionuclide concentrations in solids formed during corrosion: the ANL unsaturated drip and humid-air tests. The ANL tests provide the only available information for the incorporation of most radionuclides in U(VI) corrosion products. Therefore, the ANL tests provide the basis for this analysis; other experiments are described for completeness and provide some corroborating evidence for our interpretations of certain radionuclide behaviors in the ANL tests. Reviews of dissolution experiments on UO_2 and spent fuel conducted before 1990 are provided by Grambow (1989) and Finch and Ewing (1990).

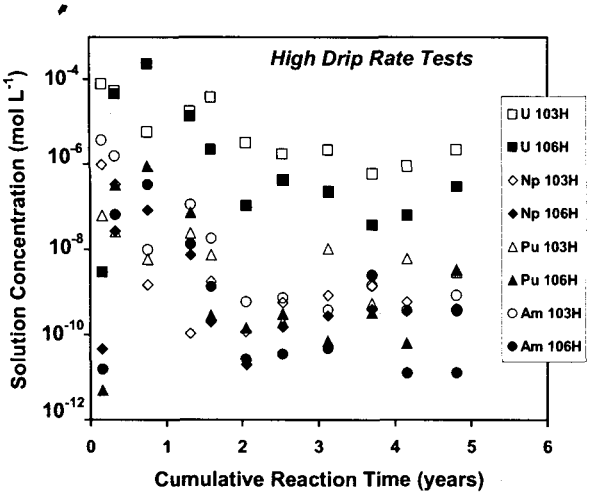
6.4 SUMMARIES OF SELECTED FUEL EXPERIMENTS

6.4.1 ANL Unsaturated Drip and Humid-Air Tests (CRWMS M&O 2000b; Finch et al. 1999)

A modified (Si-saturated, Na-bicarbonate) groundwater is periodically injected onto light water reactor (LWR) fuel fragments (~8 g) within Zircaloy cups inside stainless-steel reaction vessels at 90°C. The water used in these experiments ("EJ-13" water) is a modified groundwater (groundwater originally taken from the J-13 well near Yucca Mountain and then heated at 90°C for 21 days with crushed Topapah Springs tuff). The rationale for using the EJ-13 modified groundwater is that when groundwater re-enters the repository, it will have been in contact with hot tuff; 90°C is believed to be the approximate temperature at which groundwater may first re-enter the repository. In addition, experiments are conducted at 90°C in order to enhance reaction kinetics for reactions that are too sluggish to observe on laboratory time scales. Some validation

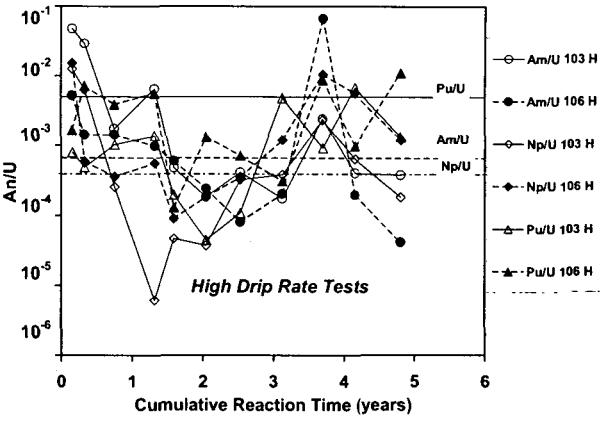
for using higher-than-ambient temperatures is obtained from studies of analogous natural systems (e.g., uraninite alteration), which commonly produce alteration products similar to those found in UO_2 and fuel experiments conducted at elevated temperatures (see Attachment 2). Two injection (drip) rates are employed: low drip rate (LDR) experiments receive, nominally, 0.15 mL of groundwater each week; high drip rate (HDR) experiments receive approximately ten times that amount. Tests are maintained at 100% relative humidity (RH). Experiments in humid air are also conducted at 90°C and 100% RH, but no additional groundwater is injected in humid-air experiments. Two pressurized-water reactor (PWR) fuels with burnups of ~30 MWd/kg-U and ~45 MWd/kg-U, are used, designated Approved Testing Material (ATM)-103 and ATM-106, respectively. Six unsaturated drip and humid-air corrosion experiments have been running for more than six years. Experiments are periodically interrupted, vessels opened, and both solid and solution samples are analyzed.

Actinides–In HDR tests, U, Np, Am, and Pu have all achieved nearly constant rates at which radionuclides are released into solution recovered from the base of test vessels in HDR experiments, following some early erratic releases during the first year (Figure 1). Solution concentration ratios, Np/U, Am/U, and Pu/U indicate that Np and Am are released more or less congruently with U, whereas Pu is not (Figure 2). However, all three ratios are similar, varying about a ratio of approximately 0.001, with excursions during the first year (rapid initial releases) and during the 3.7 year sampling interval when U solution concentration dropped for both tests (Figure 2). Solution concentrations for U decreased by approximately two orders of magnitude during the first two years (from $\sim 10^{-4}$ to $\sim 10^{-6}$ M) (Figure 1). Solution concentrations of Pu, Am, and Np decreased by nearly four orders of magnitude over the same interval (from $\approx 10^{-6}$ to $\approx 10^{-10}$ M) (Figure 1). These trends are consistent with actinide behaviors in batch tests (see Sections 6.4.2 and 6.4.3); however, the ANL drip tests are dynamic flow tests, and solution concentrations are controlled by the combination of flow rate, fuel dissolution rates, and possible saturation with secondary actinide-bearing solids. Solution concentrations of Am, Pu, and Np in the ANL drip tests are one to two orders of magnitude lower than corresponding concentrations in batch tests (Wilson 1990a, 1990b; Forsyth and Werme 1992). Releases for each actinide are discussed in more detail for the ANL drip and humid-air fuel-corrosion tests in Attachment I. No data are available for Pa.



Source: Actinide concentrations in leachates as a function of cumulative reaction time in high drip-rate tests on spent fuel (includes dissolved and acid-strip components) (DTN: LL991001251021.090)

Figure 1. Actinide Concentrations in Leachates In ANL HDR Tests on Spent Fuel



Source: Solution molar ratios An/U (where An = Am, Np, and Pu) as a function of cumulative reaction time in high drip-rate tests on spent fuel. Horizontal lines labeled Pu/U, Am/U, and Np/U indicate corresponding An/U ratios in the fuel (based on the ratio in fuel specimen, ATM-103) (DTN: LL991001251021.090).

Figure 2. Solution Molar An/U Ratios in ANL HDR Tests on Spent Fuel

Fission products–In the HDR tests Tc, I, Sr, Cs, and Mo display nearly constant release rates over time, with overall average rates decreasing approximately in the order Tc ≥ Mo ≥ I ≥ Cs > Sr. Tc, Mo, and I release rates have remained approximately constant over time. Specific releases are described in Attachment I, and more detail on the behaviors of fission products in the ANL tests is provided by CRWMS M&O (2000b). No data are available for releases of Se or C.

Solids–After approximately five years, the surfaces of all fuel fragments in all drip and humid-air experiments had developed yellowish to white crusts, obscuring the underlying (black) fuel. These crusts are predominantly uranyl oxyhydroxides and uranyl silicates (Table 5) with uranyl silicates (Na-boltwoodite and β-uranophane) dominating in the HDR tests and oxyhydroxides (metaschoepite and dehydrated schoepite [DS]) dominating in the humid-air tests (Finch et al. 1999). Similar phases were identified during corrosion studies of unirradiated UO_2 (Wronkiewicz et al. 1992; 1996) and occur at many oxidized uraninite deposits in nature (Finch and Ewing 1992; Pearcy et al. 1994). One novel uranyl phase has also been identified in the ANL fuel-corrosion tests, $Cs_{2x}Ba_{1-xz}(UO_2)_5MoO_6(OH)_6(H_2O)_n$ (Buck et al. 1997), a phase with a composition similar to that of the mineral tengchongite, $Ca(UO_2)_6(MoO_4)_2O_5(H_2O)_{12}$. Barium and Sr are important substituents in β-uranophane (Finch et al. 1999), where they likely replace Ca in structural sites. Ruthenium and, to a lesser degree, Tc have also been detected as trace components of β-uranophane by TEM (Finch et al. 1999). Ruthenium and Tc may replace Si in very small amounts, although the substitutional mechanism(s) has not been confirmed. Cesium has been detected in Na-boltwoodite (Finch et al. 1999), and recent ion-exchange experiments (Burns 1999) indicate that Cs^+ can exchange with Na^+ and K^+ in natural boltwoodite exposed to

Cs-rich solutions. The large surface area associated with fine-grained corrosion layers makes Na-boltwoodite a potentially important sink for Cs in HDR experiments.

Analyses by scanning electron microscope (SEM) of solids removed from the surface of fuel at the 5.2-year reaction interval revealed numerous golden-brown spherules of an unidentified U-Zr oxide (Finch et al. 1999). Trace-element analyses have not yet been completed on these particles. A Pu-bearing U-Zr oxide was detected during transmission electron microscope (TEM) analyses of samples from the 4.9-yr sampling interval of the HDR experiment on ATM-103 (CRWMS M&O 2000b; Finch et al. 1999). This solid is electron-diffraction amorphous and appears to be a chemically heterogeneous oxide (DTN: LL010305512241.024; LL991110351021.100; LL010305312241.022). This solid occurs as thin layers (~100 nm thick) in contact with corroded fuel grains. It is currently considered to be a residual solid of "insoluble" elements that precipitates near the fuel surface after dissolution of the UO_2 matrix; however, this remains to be confirmed. In addition to Pu, U, and Zr, this residuum contains Am, Ru (DTN: LL991110351021.100), and lanthanides (Table 5) (DTN: LL010305312241.022).

Neptunium was identified in a sample of DS from a humid-air test. The Np/U ratio in the DS is estimated to be on the order of 0.003 - 0.006, estimated from EELS (Buck et al. 1998), which is comparable to the Np/U ratio in the fuel (0.0004) (Guenther et al. 1988). On the other hand, Np is not found in substantial amounts in solids from drip tests. For example, combined TEM-EELS (DTNs: LL010305512241.024; LL991110351021.100; LL010305312241.022) and ICPMS analyses (duplicate analyses, DTN: LL010109312241.021) were performed on U(VI) corrosion products obtained from the surface of spent fuel (ATM-106) that had reacted for 5.1 years in the unsaturated drip tests (high drip rate). The predominant solid corrosion product analyzed from the HDR tests is the uranyl silicate Na-boltwoodite, although β-uranophane and minor unidentified solids are also present (the solids were identified by X-ray powder diffraction and electron diffraction) (Finch et al. 1999). These analyses demonstrated that the Np/U ratio in the bulk solids is less than approximately 5% of the Np/U ratio in unaltered fuel (DTN: LL010109312241.021). ICP-MS analyses were also performed on a sample containing $Cs_{2x}Ba_{1-z}(UO_2)_5MoO_6(OH)_6(H_2O)_n$ and minor DS that had been removed during the 0.8-yr sampling of the HDR test on ATM-106. The Np/U ratio in this sample was also far below that in the fuel. These admittedly limited results indicate that solids formed in HDR experiments on ATM-106 do not incorporate Np congruently with U under the test conditions. To date, no Np-rich solid has been identified in the drip tests (HDR or LDR) that might account for Np from the reacted spent-fuel matrix that has not been recovered in solution (DTN: LL991001251021.090).

Table 5. Uranium Corrosion Products Identified in Tests on Spent UO_2 Fuel Reacted in Groundwater and Humid Air

Phase	Formula	Experiment [a]	Interval [b] (yr)	Radionuclide
Metaschoepite	$(UO_2)_4O_4(OH)_6(H_2O)_5$	LDR 103 & 106 Vapor 103 & 106	4.1 4.1	
DS	$(UO_2)O_{0.25-xz}(OH)_{1.5+2x}$ $(0 \le xz \le 0.15)$	HDR 106 LDR 103 Vapor 103 & 106	0.8 4.1 (?) 4.1	Np [d]
Na-UOH[c]	$(Na,K)_2[(UO_2)_3O_2(OH)_3]_2(H_2O)_7$	LDR 103 & 106	4.1, 5.2	
Soddyite	$(UO_2)_2SiO_4(H_2O)_2$	LDR 103 & 106	4.1, 5.2	
β-uranophane	$Ca(UO_2)_2(SiO_3OH)_2(H_2O)_5$	HDR 103 & 106	3.7, 5.2(?)	Ba, Sr
Na-boltwoodite	$(Na,K)(UO_2)(SiO_3OH)(H_2O)_{1.5}$	LDR 103 HDR 103 & 106	4.1, 5.2 3.7, 5.2	
Cs-Ba-Mo-uranate	$(Cs,Ba)(UO_2)_5(MoO_6)(OH)_6(H_2O)_n$	HDR 106 LDR 103 Vapor 106 & 103	0.8 4.1 4.1	Cs, Ba, Mo, U
Zr-U oxide	Uncertain	LDR 103	5.2	U, Zr
Zr-U-Pu oxide	Uncertain	HDR 103	4.1	Zr, U, Pu, Am, Ru, lanthanides

NOTES: [a]103 = ATM-103 PWR fuel; 106 = ATM-106 PWR fuel; LDR = low drip-rate experiment; HDR = high drip-rate experiment.
[b]INTERVAL refers to sampling interval and indicates the total reaction time.
[c]Possibly the Na analogue of compreignacite, $K_2[(UO_2)_3O_2(OH)_3]_2(H_2O)_7$.
[d]Np detected in DS from humid-air tests only.
(?) tentative phase identification for the interval indicated.

Source: Finch et al. (1999)

6.4.2 Nevada Nuclear Waste Storage Investigations (NNWSI) Series 2 and 3 Fuel Dissolution Tests (Wilson 1990a, 1990b)

LWR declad fuel-rod segments (two fuels: burnup = 27.5 and 30.2 MWd/kg-U, 26 g and 82 g, respectively) were immersed in 250 mL J-13 well water (Si-saturated carbonate) water, and solutions were sampled with replenishment (50 mL at each sampling). Series 2 tests were conducted in unsealed fused silica vessels in an ambient hot-cell atmosphere (25°C). Five sampling cycles were done over a total of 34 months. The series 3 tests used sealed stainless-steel vessels and were conducted at 25 and 85°C for three cycles over 15 months.

Actinides–Actinide concentrations in solution tended to reach an upper limit, then decrease during test cycles. Uranium concentrations were higher at 25°C than at 85°C and decreased very slightly over time (up to ~1,000 days). Am and Pu concentrations from (filtered aliquots) decreased over time in the 85°C tests. Np concentrations were commonly near the detection limit and were only measurable in tests on bare fuel (series 2). Solution concentrations of Am, Pu, and Np were all similar (10^{-8} to 10^{-9} M). The actinides (U, Am, Pu, Np) were released congruently (provided sorbed fractions were included for Pu and Am) with all concentrations decreasing very slightly over time. Most Am was filterable, suggesting either the presence of Am-bearing colloids or sorption of Am during filtering. No data are available for Pa.

Fission Products–Cs, I, Sr, and Tc and C-14 were released preferentially with respect to all actinides. Tc and Cs concentrations increased linearly with time (i.e., constant release rates), with the rates of increase greater at higher temperature. Continuous preferential releases of soluble fission products are attributed to dissolution of fine particles of FP-bearing phases located along grain boundaries. No data are reported for Se.

Solids–The Ca-uranyl silicate *uranophane* was identified in the series 2 tests at 85°C and is suspected to be the U-limiting solid. The Si-rich Ca-uranyl silicate haiweeite was identified in both series 2 and 3 tests, commonly as a filtered residue. Amorphous silica was also found in the filter residue. An amorphous-appearing K-Na-Mg Si-rich layer was found on some fuel fragments and in some vessel rinse residues. This layer appeared cracked and spalled when dried solid fuel grains were examined. The estimated volume of amorphous silica plus the relatively high dissolved Si concentrations exceeded the available Si in J-13 well water, suggesting that additional Si was leached from the fused-silica vessel.

6.4.3 Swedish Nuclear Fuel and Waste Management Company (SKB) Series 11, Clad-Fuel Experiments (Forsyth and Werme 1992)

Clad LWR fuel segments with approximately 16g UO_2 (burnup = 21 - 49 MWd/kg-U) were immersed in 200 mL of either low ionic strength Si-bearing, Na-bicarbonate groundwater (i.e., synthetic granite groundwater) or de-ionized water (DIW); experiments were conducted in open Pyrex flasks at 20 to 25°C in either air or Ar-5%H_2 atmosphere. Each sampling cycle consisted of removing the solution and filtering it for analysis, then placing the fuel segments into a new flask with fresh solution.

Actinides–After ~200 days, dissolved uranium concentrations reached nearly constant values, decreasing very slightly over time. Uranium concentrations in solution showed no dependence on fuel burnup. Uranium concentrations in experiments in DIW were three to four orders of magnitude lower than those in granite groundwater, with uranium concentrations being approximately equal to those of Pu and Np within approximately 800 days (10^{-8} to 10^{-9} M). Uranium and Pu concentrations rapidly reached constant values. At longer contact times, Pu concentrations decreased slightly from approximately 10^{-8} mol L^{-1}, leveling off at about 10^{-9} mol L^{-1}. Actinide concentrations were independent of total contact time. Experiments in Ar-5%H_2 atmosphere lost some CO_2 and precipitated calcite, $CaCO_3$, which is known to incorporate U(IV) in nature (Sturchio et al. 1998); calcite is, therefore, a potential host for Pu(IV) and Np(IV). However, Np and Pu concentrations were only marginally higher in DIW than in the groundwater. No data are reported for Am or Pa.

Fission Products–Cs and I displayed early rapid releases (the instant release fraction), presumably from along grain boundaries and the gap exposed to water. Cs release rates decreased by several orders of magnitude over time, achieving a nearly constant rate of ~10^{-6} frac/day after about two years. As for Cs, initially high release rates for Sr began to decrease after the first ~20 days and continued to decrease even after more than 1,000 days. Technetium releases remained constant for the duration of the tests, spanning a range from approximately 4 x 10^{-7} to 6 x 10^{-6} frac/day.

Solids–DS was identified on the surfaces of fuel fragments from tests conducted in DIW. The DS may have originally precipitated as schoepite, which dehydrated during exposure of the samples to heat lamps during examination. The release of uranium to solution increased when fuel that had reacted in DIW was re-exposed to carbonate groundwater. This is consistent with dissolution of a U(VI) solid; however, no similar increase was observed for Pu or Np. No chemical analyses of DS were performed. As noted, calcite precipitated in anaerobic experiments, but no analyses of calcite were performed.

6.4.4 CANDU Dissolution Experiments (Stroes-Gascoyne et al. 1997)

Batch experiments on CANDU fuel segments were immersed in DIW and tap water (50 mg L^{-1} carbonate) and allowed to react for 19 years at room temperature. There are two duplicates for each test configuration.

Actinides–Initial fractional releases of uranium in experiments in DIW were relatively high in one experiment (DA), but dropped by about two orders of magnitude within the first two years to be comparable with that of the second experiment in DIW (DB). After 19 years, test DA released ~0.05% of uranium, whereas test DB has released about twice that much. Release rates and cumulative releases of U are approximately one order of magnitude higher in the experiments in tap water (TA, TB). No data are reported for Pu, Np, Am, or Pa.

Fission Products–Cs-137 and Sr-90 show early rapid releases, but both decrease by several orders of magnitude within the first two years. Sr and uranium releases are congruent except for initial releases, where Sr release exceeded uranium by about a factor of 10. The fractional release rate of Cs rapidly declined, reaching about 10^{-5} d^{-1} within a few months in tap water and 10^{-6} d^{-1} in DIW. After 19 years, approximately 7-8% of the Cs inventory has been released, and Sr-90, Cs-137, and U-238 releases are approaching congruency.

Solids–The surface of fragments reacted in DIW were covered by unidentified acicular (needle-shaped) to thinly bladed crystals. No data are provided on the composition of these crystals, but their appearance (Stroes-Gascoyne et al. 1997, Fig. 3) suggests a uranyl oxyhydroxide such as DS or possibly ianthinite. The habit of the thinnest needles is also consistent with the habit of the uranyl peroxide, studtite. No surface precipitates were observed on fuel specimens reacted in tap water, explained by the higher carbonate concentrations in tap water. Grain boundary-enhanced corrosion of the fuel is noted to be minimal.

6.5 THERMODYNAMIC PARAMETERS FOR U(VI) SOLIDS

In the oxidizing environment that currently exists in the unsaturated zone at Yucca Mountain, the UO_2 matrix of spent UO_2 fuel is unstable. The rate at which the UO_2 matrix oxidizes and dissolves depends on many factors, but given sufficient time, the matrix will be converted to thermodynamically more stable phases. The minimization of energy of a system that is far from thermodynamic equilibrium is what drives the corrosion process, and U(VI) corrosion products represent phases that are stable relative to spent fuel under repository conditions. Under conditions where equilibrium thermodynamics can be realistically applied, the rate at which a thermodynamically stable solid dissolves in an aqueous phase depends on the dissolution rate of

the solid as a function of the saturation index, Q/K, according to the following relation (Aagaard and Helgeson 1982; Alekseyev et al. 1997):

$$rate = \pm kS|1 - (Q/K)^p|^q \quad \text{(Eq. 1)}$$

where K is the thermodynamic equilibrium constant and Q is the activity coefficient; k is the rate constant (sometimes referred to as the "intrinsic" dissolution rate; i.e., the dissolution rate when Q/K = 0), S is the surface area of the reacting solid, and p and q are fitted parameters that depend on the compound and the system of interest (experimental or geological). The sign on the right hand side of Equation 1 depends on whether the compound of interest is dissolving or precipitating, with a positive sign indicating dissolution; however, experimental verification of whether precipitation kinetics obey Equation 1 is not readily obtained (Alekseyev et al. 1997). The sign convention is required because the absolute value of the quantity (1-Q/K) is used, which assures that *rate* has the correct sign when $q \neq 1$ (Alekseyev et al. 1997). In a dynamically flowing system, radionuclide releases will also depend on the rate of groundwater flow as it contacts the dissolving (or precipitating) solids, although a discussion of this would be beyond the scope of this analysis report. In order to properly model Equation 1 we must know K, the equilibrium solubility constant. Thus, thermodynamic parameters for relevant radionuclide-bearing corrosion products are required in order to calculate solution concentrations under dynamic flow conditions. Compilations of thermodynamic data are available from a number of sources, notably the Nuclear Energy Agency compendia such as *Thermodynamics of Uranium* by Grenthe et al. (1992). In order to analyze the potential roles of U(VI) corrosion products on solution concentrations of radionuclides contained within them–the goal of this analysis report–the thermodynamics of U(VI) phases are addresses in this Section.

Two geochemical systems, SiO_2-UO_3-CaO-H_2O and CO_2-UO_3-CaO-H_2O, important for uranyl-phase formation and alteration in environments such as Yucca Mountain and the natural analogue study site, the Nopal I U mine near Peña Blanca, Mexico, will be analyzed. The SiO_2- and CO_2-bearing system are especially important in nature, and the uranyl silicates and uranyl carbonates have been identified as potentially important U(VI) alteration phases of U-bearing waste forms (Finch and Ewing 1992; Wronkiewicz et al. 1992; 1996). The mobility of U(VI) in carbonate-bearing groundwaters is potentially high, as uranyl-carbonate complexes can be quite stable in aqueous solution (Grenthe et al. 1992). The concentration of dissolved uranium required to precipitate many uranyl-carbonate minerals tends to be greater than that required to precipitate most other uranyl minerals, and the geochemical conditions under which solid uranyl carbonates precipitate are of interest for understanding the geochemical controls on U transport (Alwan and Williams 1980). Dissolved silica is another important constituent of natural groundwaters, where it occurs predominantly as orthosilicic acid, H_4SiO_4, below approximately pH = 9 (Stumm and Morgan 1981). Concentrations of H_4SiO_4 in most groundwaters are limited by the precipitation of amorphous silica, which occurs where $\{H_4SiO_4\} = 10^{-2.7}$ mol·liter^{-1} (Stumm and Morgan 1981). Ca-bearing groundwaters are considered because Ca is virtually ubiquitous in near-surface groundwaters, and many Ca-bearing uranyl minerals are known, representing a variety of near-surface environments. In addition, we will examine the SiO_2-UO_3-NaO-H_2O system as well, because of the importance of Na uranyl phases in experiments on spent fuel; however, few Na-rich uranyl minerals are known in nature. Thermodynamic data are available for several of these minerals, although data are lacking especially for uranyl carbonates.

Although uranyl phosphates are important in many natural waters (Finch and Ewing 1992; Sandino and Bruno 1992; Murakami et al. 1997), uranyl phosphates have not been identified from experimental studies of spent UO_2 fuel corrosion.

Due to the paucity of empirical thermodynamic data for many U(VI) compounds, Finch (1997) described a method for estimating the Gibbs free energies of formation for uranyl minerals. This method will be used to aid the following discussion, but the results should not be construed as quantitative. The method is summarized as follows. The ΔG_f° value of the mineral is the arithmetic sum of the oxide contributions, where ΔG_f^* is the free-energy contribution of each oxide *in the mineral structure.*

$$\Delta G_f^\circ = \Sigma \Delta G_f^*{}_i \,. \qquad \text{(Eq. 2)}$$

The values for the hypothetical oxides are used to estimate ΔG_f° for various uranyl compounds by adding contributions from the constituent oxides in their stoichiometric proportions in the compound of interest, and estimated values are used to augment existing empirical data. Chen et al. (1999a) have compiled additional data for oxide constituents in uranyl minerals and inorganic compounds and report on revised free energies and enthalpies derived according to the method described by Finch (1997). Some of the $\Delta G_f^*{}_i$, and $\Delta H_f^*{}_i$ values calculated by Chen et al. (1999a) are listed in Table 6; calculated ΔG_f° and ΔH_f° values for some uranyl compounds of particular relevance for Yucca Mountain groundwaters are given in Table 7. Activity-activity diagrams are used to illustrate the stability fields occupied by solid phases in equilibrium with U-rich waters. The underlying assumption of these diagrams is that the concentration of dissolved U is sufficient to stabilize the solids. It should also be noted that these diagrams are very sensitive to small (potentially insignificant) differences in ΔG_f° values; that is, differences within the uncertainties of thermodynamic measurements can give rise to apparently large differences in the sizes of the stability fields illustrated. This simply reflects the logarithmic relationship between free-energy values and solution concentrations expressed in the equilibrium constants ($\Delta G = -RT\ln K_{eq}$).

Table 6. Molar Contributions of Structural Components to $\Delta G^0_{f,298}$ and $\Delta H^0_{f,298}$ of U(VI) (kJ.mol^{-1})

	UO_3	$Na_2O_{(l)}$	$K_2O_{(l)}$	$CaO_{(l)}$	$SiO_{2(IV)}$	$SO_{3(IV)}$	$CO_{2(III)}$	$H_2O_{(s)}$	$H_2O_{(H)}$
$\Delta G_f^*{}_i$	-1161.05	-686.54	-637.45	-715.77	-853.96	-538.87	-400.61	-237.94	-241.1
$\Delta H_f^*{}_i$	-1233.75	-736.3	-686.95	-726.57		-624.17	-455.59	-299.93	-295.58

Source: Values reported by Chen et al. (1999a)

Table 7. $\Delta G^0_{f,298}$ and $\Delta H^0_{f,298}$ for U(VI) Minerals Indicated in Figures 3 and 4 ($kJ.mol^{-1}$)

Mineral	$\Delta G^0_{f,298}$	$\Delta H^0_{f,298}$	M/C	Reference
schoepite	-13299.4	-14908.7	C	Chen et al. (1999a)
metaschoepite	-13092.0	-14608.8	M	O'Hare et al. (1988)
becquerelite	-10324.7		C	Chen et al. (1999a)
rutherfordine	-1563.0	1689.6	M	Sergeyeva et al. (1972)
urancalcarite	-6036.7		C	Chen et al. (1999a)
sharpite	-11607.6		C	Chen et al. (1999a)
fontanite	-6524.7		C	Chen et al. (1999a)
zellerite	-3879.9		C	Chen et al. (1999a)
liebigite	-6226.0	-7301.6	M	Alwan and Williams (1980)
uranosilite	-7126.1		C	Chen et al. (1999a)
haiweeite	-9367.2		C	Chen et al. (1999a)
ursilite	-20377.4		C	Chen et al. (1999a)
soddyite	-3658.0		M	Nguyen et al. (1992)
uranophane	-6210.6		M	Nguyen et al. (1992)
Na-boltwoodite	-2995		M	Nguyen et al. (1992)

NOTE: M/C designates measured or calculated values.

Source: Chen et al. (1999a) re-evaluated the data of Nguyen et al. (1992) and determined Gibbs free energies of formation of -3655.7, -6192.3, and -2844.8 kJ/mol for soddyite, uranophane, and Na-boltwoodite, respectively. The $\Delta G_f°$ values of dissolved species, calcite and CO_2, used for constructing Figures 3, 4, and 5 are from Grenthe et al. (1992).

6.5.1 System CO_2-CaO-UO_3-H_2O

Virtually all groundwaters contain dissolved carbonate due to interaction with the atmosphere and carbonate minerals and because of organic respiration and decomposition. Clark et al. (1995) calculated the speciation of U(VI) in Yucca Mountain groundwaters and shows that uranyl carbonate complexes predominate above about a pH of 5. The partial pressure of CO_2 in equilibrium with groundwaters open to the atmosphere is approximately $10^{-3.5}$ atm (Stumm and Morgan 1981). Sergeyeva et al. (1972) found that rutherfordine, UO_2CO_3, is the stable phase in solution with respect to DS where $pCO_2 > 10^{-2.2}$ atm. The equilibrium between schoepite and rutherfordine indicates that CO_2 partial pressure must increase to greater than $10^{-1.9}$ atm before schoepite becomes unstable with respect to rutherfordine, according to the reaction (Sergeyeva et al. 1972):

$$[(UO_2)_8O_2(OH)_{12}](H_2O)_{12}+8CO_{2\,(g)} \rightarrow 8UO_2CO_3 + 16H_2O_{(l)} \qquad K = 10^{1.9}$$

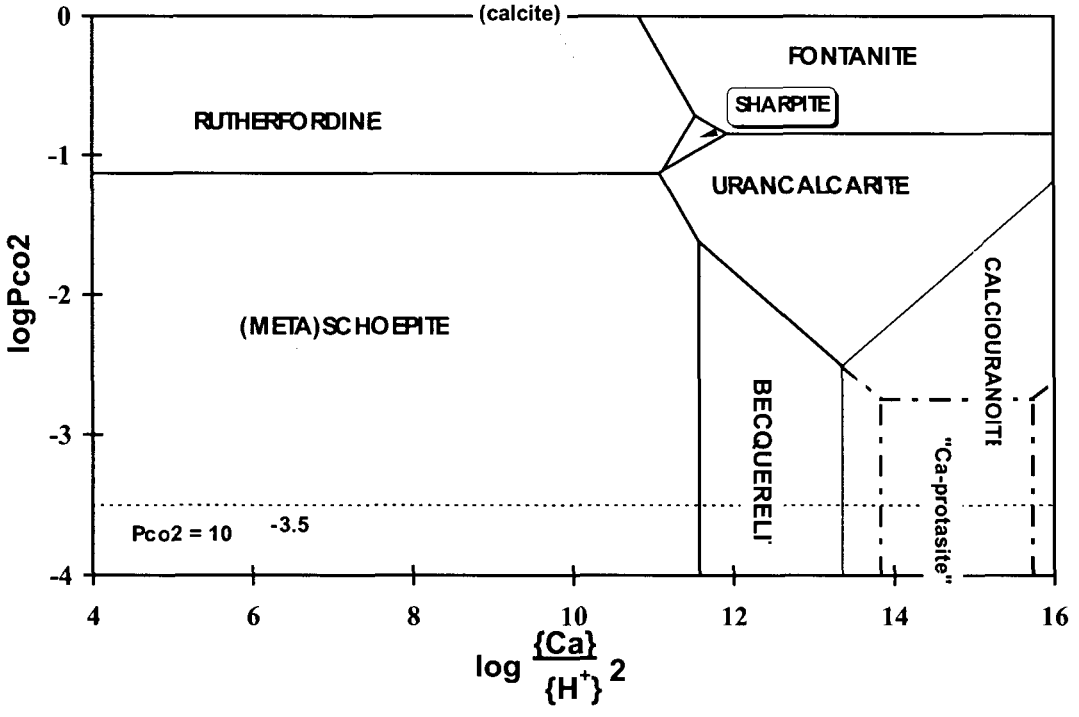
Schoepite is, therefore, the expected uranyl phase precipitated from low ionic strength water open to the atmosphere, in agreement with observation. This explains the formation of schoepite as an initial corrosion product of uraninite in fresh meteoric waters. Also, an important potential consequence of the dehydration of schoepite is that rutherfordine replaces DS at lower pCO_2 values than are required the replacement of schoepite. Schoepite is commonly replaced by

rutherfordine in many U deposits (Finch and Ewing 1992), and rutherfordine may precipitate along grain boundaries within corrosion rinds or directly on the surface of corroded uraninite (Finch and Ewing 1992). Complete replacement of corrosion rinds by rutherfordine is reported from several localities, where the only remnant of the original rind may be residual Pb-rich phases (Finch and Ewing 1992).

Figure 3 illustrates the stability fields for several uranyl carbonate compounds. The concentration of Ca in many groundwaters is controlled by equilibrium with calcite, $CaCO_3$, and dissolved $CO_{2(g)}$:

$$CaCO_3 + 2H^+ \Leftrightarrow Ca^{2+} + H_2O + CO_{2\,(g)}$$

This equilibrium is indicated as a diagonal dotted line in Figure 3. The composition of water in equilibrium with calcite will plot on this line. Also shown in Figure 3 is the partial pressure of CO_2 for waters open to the atmosphere (horizontal dotted line: $pCO_2 = 10^{-3.5}$ atm). The composition of a groundwater, open to the atmosphere and in equilibrium with calcite, will plot at the intersection of the two dotted lines in Figure 3. Notably, this falls within the stability field of becquerelite, the most common uranyl oxyhydroxide mineral in nature (Frondel 1958).



NOTE: Calculated using estimated G°f values from the mineral formulas in Table 7 (empirical $\Delta G°_f$ values used for metaschoepite and rutherfordine). Lines dashed where metastable. Diagonal dotted line is calcite equilibrium. The partial pressure of CO_2 for water open to the atmosphere is shown by horizontal dotted line ($pCO_2 = 10^{-3.5}$ atm).

Figure 3. Activity-Activity Diagram for the System CO2-CaO-UO3-H_2O

The calcite equilibrium line passes through the fields for becquerelite, schoepite, and rutherfordine, the most common minerals among those represented in Figure 3, and rutherfordine is by far the most common uranyl carbonate (Frondel 1958). The other carbonates, fontanite, sharpite, and urancalcarite are relatively rare. These occur where pCO_2 values may reach elevated values, such as where calcite equilibrium does not control groundwater chemistries. In fact, of the three uranyl carbonates that lie above the calcite line in Figure 3, sharpite and urancalcarite are rare and occur in deposits where the predominant carbonate mineral in the host rocks is magnesian calcite or dolomite (Finch and Murakami 1999). Fontanite, which coexists with becquerelite and uranophane, occurs in pelitic silts and shales (Deliens and Piret 1992).

Two uranyl carbonates are not shown in Figure 3: liebigite and zellerite. The stability fields calculated for these two minerals would replace much of the area shown in Figure 3, contrary to observation (Finch 1997). Liebigite and zellerite are commonly found as efflorescences on mine walls, surface outcrops, and elsewhere that evaporation is high. These minerals tend to be extremely fine grained, which will contribute to surface free energy and higher solubilities. A similar argument may explain the lack of agreement between the estimated stability range of zellerite and known natural occurrences.

Comparing UO_3:CO_3 ratios of uranyl carbonate minerals with those of known uranyl carbonate solution complexes may provide some insight into conditions of mineral formation. The relative abundance of complexes depends on pH, total dissolved U, and total carbonate. Structural details of most minerals with UO_2:CO_3 ratios of 1:3 (the liebigite group and schröckingerite subgroup) are well known, and the $(UO_2)(CO_3)_3^{4-}$ (uranyl tri-carbonate or UTC) ion in these minerals is well established. The UTC complex is the dominant uranyl carbonate complex above a pH of 7 over a wide range of total dissolved U in most in natural waters, including Yucca Mountain groundwaters (Langmuir 1978; Clark et al. 1995). The liebigite group minerals commonly form where evaporation is high and ionic strengths can become quite elevated.

The 1:2 uranyl carbonate complex (uranyl di-carbonate or UDC) is predicted to be the predominant complex in Yucca Mountain groundwaters over a narrow range of pH between about 5.5 and 6.5 (Clark et al. 1995). Only two 1:2 uranyl carbonate minerals are known, zellerite and meta-zellerite, $Ca(UO_2)(CO_3)_2 \cdot 3\text{-}5H_2O$, and they are rare in nature (Finch 1997), an observation that is consistent with the predicted narrow range of UDC predominance in most groundwaters (Clark et al. 1995). Also, the UDC complex probably becomes less important where evaporation and precipitation of carbonate minerals occurs, under which conditions the UTC complex may predominate (e.g., high ionic strengths and pH > 7).

The neutral $(UO_2)CO_3^0$ complex predominates between a pH of approximately 4.5 and 5, although it becomes increasingly important at pCO_2 values exceeding atmospheric. Sergeyeva et al. (1972) found that this is the uranyl complex predominating in pure water equilibrated with rutherfordine ($\Sigma U = 10^{-4.4}$ M) and a pCO_2 of 1 atm and a pH between 4.5 and 5.5. Rutherfordine is quite common in many weathered uranium deposits. Two additional, structurally distinct 1:1 uranyl carbonates are known: blatonite, $(UO_2)CO_3 \cdot H_2O$, and joliotite, $(UO_2)CO_3 \cdot nH_2O$ ($n \leq 2$), although they may be rare. All three 1:1 uranyl carbonates probably reflect elevated pCO_2 such as might occur in saturated soils and where organic decomposition and respiration are high.

Several uranyl hydroxy-carbonates are known, suggesting that uranyl hydroxyl-carbonate complexes may be important in some natural waters (Clark et al. 1995). Although the uranyl hydroxy-carbonates are not so abundant as either 1:1 or 1:3 carbonates, they are the most important REE-bearing uranyl minerals and may be important for understanding the potential behavior of REE and certain actinides in U(VI)-saturated carbonate waters, such as might be expected at Yucca Mountain. No lanthanide- or actinide-bearing uranyl carbonates have been identified in corrosion experiments on spent fuel; however, they would not be expected to be abundant, nor readily identified, if they occur intimately mixed with other uranyl compounds.

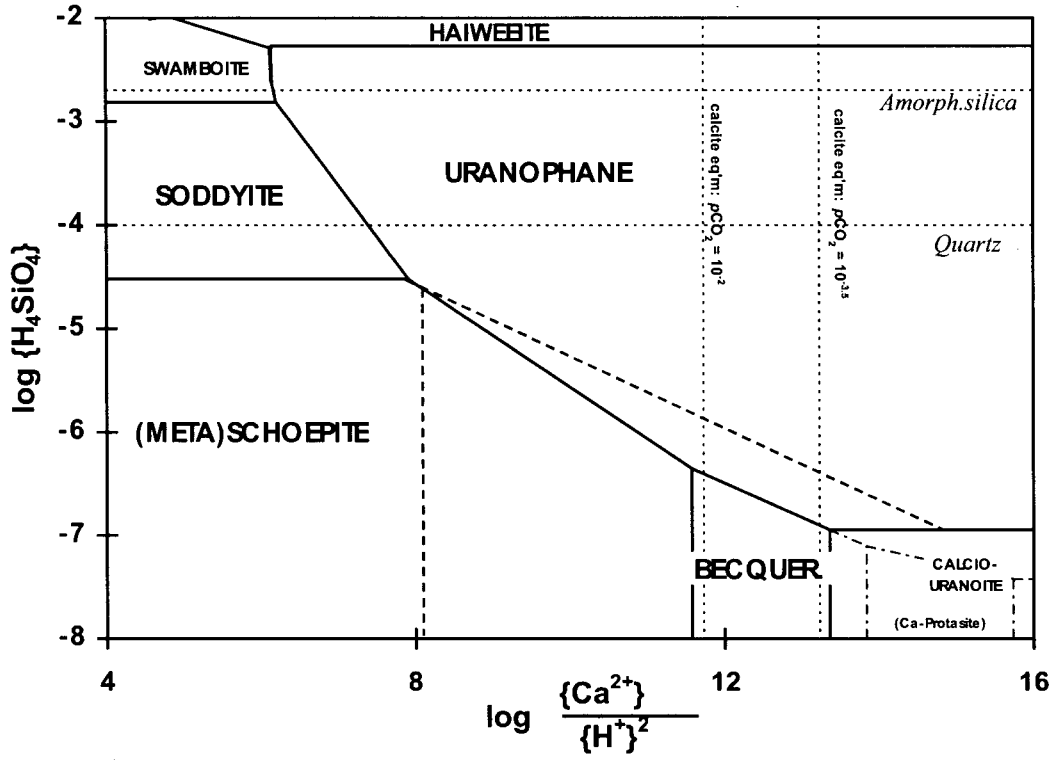
Several uranyl carbonate minerals suggest a complex solution chemistry of uranium in some natural waters, especially at high ionic strengths. Schröckingerite, $NaCa_3(UO_2)(CO_3)_3(SO_4)F{\cdot}10H_2O$, is a complex UTC-based carbonate formed by evaporation of UO_2-CO_3-SO_4-F containing waters. Lepersonite, $Ca(REE)_2(UO_2)_{24}(CO_3)_8(SiO_4)_4O_{12}{\cdot}60H_2O$, is a REE uranyl carbonate-silicate that may precipitate from solutions transitional between being dominated by uranyl carbonate complexes and uranyl-silicate complexes. Lepersonite may be rare, but it has often been confused with studtite and finely acicular uranyl carbonates. Lepersonite is especially intriguing as a potential host for REE, Am, and Pu in Yucca Mountain-type groundwaters; however, it has not been identified from corrosion tests. There are no thermodynamic data currently available. The apparent lack of REE-bearing carbonates at the analogue study site, Nopal I, does not preclude the potential importance of these compounds at the potential repository at Yucca Mountain because the uraninite and host rocks at Nopal I are low in REE.

6.5.2. Systems SiO_2-CaO-UO_3-H_2O and SiO_2-Na_2O-UO_3-H_2O

The concentration of dissolved silica in most groundwaters is controlled by either quartz solubility ($H_4SiO_{4(aq)} = 10^{-4.0}$; pH < 9) (Grenthe et al. 1992) or by amorphous silica (activity of $H_4SiO_{4(aq)} = 10^{-2.7}$; pH < 9) (Stumm and Morgan 1981). After the Pb-uranyl oxyhydroxides, uranyl silicates are the most abundant minerals in corrosion rinds formed in contact with corroded uraninite in nature (Finch and Ewing 1992). Both uranophane and the polymorph β-uranophane replace early-formed uranyl oxyhydroxides at the Nopal I mine in Peña Blanca (Pearcy et al. 1994). Uranophane is, in fact, the most common U(VI) mineral (Frondel 1958; Smith 1984). Soddyite is less abundant than uranophane, but it is common along grain boundaries and within veins and fractures within many uraninite corrosion rinds (Finch and Ewing 1992).

Figure 4 illustrates the stability fields of minerals common in Si-bearing groundwaters. The most common Pb-free U(VI) minerals are schoepite, becquerelite, soddyite, uranophane, and rutherfordine. Schoepite forms early in the alteration paragenesis of uraninite oxidation products. Though common, schoepite is not usually abundant at most oxidized uranium deposits (Finch and Ewing 1992). This is because schoepite is commonly replaced by uranyl silicates and carbonates, especially uranophane, soddyite, and rutherfordine (Finch and Ewing 1992; Wronkiewicz 1992; 1996). Although the direct replacement of schoepite by becquerelite is not readily confirmed in nature, this reaction has been reported from several experimental studies (Sandino and Grambow 1994; Vochten and Van Haverbeke 1990; Sowder et al. 1996). The stability field shown for schoepite probably represents a maximum. Schoepite commonly forms

fine-grained masses, effectively increasing schoepite solubility. Schoepite dehydrates spontaneously, becoming polycrystalline (Finch et al. 1992; Finch et al. 1998). The lower hydrates also have higher solubilities in water at ~25°C (O'Hare et al. 1988).



NOTE: Calculated using estimated $\Delta G°_f$ values from the mineral formulas in Table 7 (empirical $\Delta G°_f$ values are used for metaschoepite, rutherfordine, uranophane and soddyite).

Source: Dashed lines indicate the approximate field of becquerelite stability estimated by Chen et al. (1999a). Horizontal lines indicate equilibria with silica; vertical dotted lines represent calcite equilibrium for pco2 values for water open to the atmosphere ($Pco2 = 10^{-3.5}$) and for a typical water-saturated soil ($Pco2 \cong 10^{-2}$) (Stumm and Morgan 1981). BECQUER. = becquerelite.

Figure 4. Activity-Activity Diagram for the System SiO2-CaO-UO3-H_2O

Uranophane is the most common U(VI) mineral in nature (Frondel 1958), consistent with the large field of stability indicated in Figure 4, as well as the fact that uranophane is the stable U(VI) mineral in contact with groundwaters whose compositions are controlled by calcite and silica equilibria (Langmuir 1978). Soddyite is another common mineral in oxidized U deposits, where it replaces schoepite and, less commonly, replaces uranophane (due to interaction with low ionic strength meteoric waters) (Casas et al. 1994).

Swamboite is a rare mineral. It commonly occurs with soddyite and uranophane (Finch and Murakami 1999), suggesting a genetic relationship. According to Figure 4, swamboite forms near the upper limit for $\{H_4SiO_4\}$ in natural waters. The extremely rare mineral, calciouranoite

defines a stability field in Si-poor waters at high values of pH and/or dissolved Ca. This is consistent with reports of the occurrences for calciouranoite and metacalciouranoite (Finch and Murakami 1999). The stability field for calciouranoite represents a maximum and assumes coarsely crystalline material. In fact, calciouranoite is always cryptocrystalline, and the small grain size will contribute to the surface free energy, increasing its solubility and decreasing its field of stability. The small grain size of calciouranoite is probably due to strain caused by structural limitations on the ability of the uranyl oxyhydroxide sheets to accommodate a large amount of interlayer Ca atoms; the same effect may explain the apparent lack of the hypothetical mineral, Ca-protasite in nature (known only as a synthetic phase). In practice, becquerelite may well replace most of these fields, as suggested by the formation of synthetic becquerelite in Ca-rich solutions (Sandino and Grambow 1994; Vochten and Van Haverbeke 1990; Sowder et al. 1996).

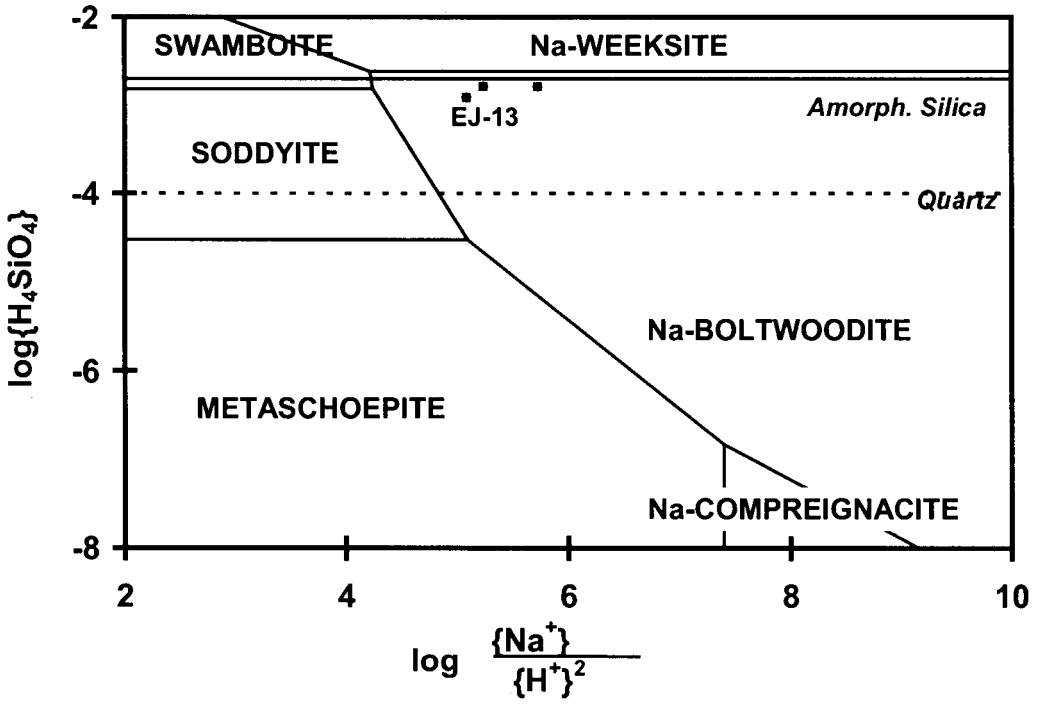
The precipitation of uranyl silicates directly from solution seems to require significant over-saturation (Nguyen et al. 1992; Finch and Ewing 1992), which probably explains early formation of uranyl oxyhydroxides, such as schoepite, which can apparently form metastably from solutions with substantial dissolved Si (Finch and Ewing 1992). The stability fields of schoepite indicated in Figures 2, 4 (and 5) may represent maximum fields of stability (Finch 1997).

Not shown in Figure 4 are the stability fields estimated for the two uranyl silicates, uranosilite and ursilite. The stability fields of these minerals, when estimated using the ΔG_f^* values in Table 6, replace most of the uranophane field, contrary to observation. Uranosilite and ursilite always form as fine-grained masses, and surface-free energy must contribute to the increased solubilities of these minerals.

The uranophane group (U:Si = 1:1) is the most abundant of the uranyl silicates both in number of phases (nine) and in abundance. Uranophane (Ca) and sklodowskite (Mg) are the most common (Frondel 1958). The 1:3 silicates (the "haiweeite group") are only known from Si-rich environments, such as tuffaceous rocks, where weeksite, $K_2[(UO_2)_2Si_5O_{13}](H_2O)$, is common. Uranosilite is indicative of still higher Si activities, but this phase has been reported from only one locality, Menzenschwand, Germany (Walenta 1983). Lepersonite and soddyite are indicative of more U-rich solutions, and both occur in close proximity to corroded uraninite. There are few thermodynamic data available for U-Si solution complexes. Only $UO_2SiO(OH)_3^+$ is known to be important in low ionic strength waters ($\Sigma U = 10^{-8}$ M), where it may predominate in a narrow range of pH near six (Langmuir 1978; Grenthe et al. 1992).

Finally, Figure 5 illustrates the stability diagram relevant to Na-rich groundwaters, such as those used in the ANL drip experiments on unirradiated UO_2 (Wronkiewicz 1992; 1996) and spent fuel (CRWMS M&O 2000b). In those tests (Finch et al. 1999), Na-rich uranyl compounds have been identified including Na-boltwoodite and the Na-analogue of compreignacite (Table 5). The composition of "EJ-13" water (the modified groundwater used in the ANL tests) is shown in Figure 5 as three data points, representing compositions reported from several ANL reports (Wronkiewicz et al. 1992; CRWMS M&O 2000b). Not surprisingly, the most important differences between Figures 4 and 5 are the replacement of uranophane, haiweeite, and becquerelite in the Ca-bearing system by Na-boltwoodite, Na-weeksite, $Na_2[(UO_2)_2Si_5O_{13}](H_2O)$, and Na-compreignacite, respectively. The modified groundwater, EJ-13, plots within the Na-

boltwoodite field but very close to the Na-weeksite field. To date, no Na-weeksite has been identified in any ANL tests on fuel (it is not uncommon in corrosion tests of glass waste forms), although some solids analyses suggest Si in excess of that expected for Na-boltwoodite (Finch et al. 1999).



NOTE: Calculated using estimated $\Delta G°_f$ values from the mineral formulas in Table 7 (empirical $\Delta G°_f$ values are used for metaschoepite, rutherfordine, uranophane and soddyite). Data labeled "EJ-13" shows range of compositions reported for modified groundwater used in ANL unsaturated drip tests (ignoring minor cations, including Ca).

Figure 5. Activity-Activity Diagram for the System SiO_2-Na_2O-UO_3-H_2O

6.6 KINETIC PARAMETERS FOR U(VI) COMPOUNDS

Laboratory experiments on spent fuel address short-term phenomena compared to the thousands of years of regulatory concern for a potential repository. In addition to understanding which compounds might sequester radionuclides during spent fuel corrosion, we need to understand whether those compounds are likely to be long-lived radionuclide hosts. In order to address this issue, we need to know (1) the rates at which corrosion products may crystallize and subsequently dissolve; (2) the rate at which constituents that comprise various secondary and tertiary alteration products are transported to the corroding fuel. The latter factor is addressed by knowing the composition of water that contacts the fuel, along with rates of groundwater infiltration to the waste package. This constrains the limit on uranyl-phase formation and alteration imposed by mass transport. The former factor, dissolution and precipitation rates for various alteration phases, requires knowledge of kinetic rate laws as applicable to repository-

relevant conditions. Kinetic data are available for only a few uranyl compounds; however, dissolution rates for three uranyl compounds relevant to corrosion experiments have been reported.

Casas et al. (1994) examined dissolution kinetics of uranophane and schoepite, both of which were natural samples. They conducted their experiments under oxidizing conditions (open to air, 25°C) within a fairly narrow range of pH (7.9±0.1). Dissolution rates were determined by measuring U concentrations in solution as a function of time and fitting the data by least-squares minimization of a linear regression equation. Due to initial rapid releases, possibly associated with dissolution of fine particles, regression fits do not have zero intercepts but are positive for both experiments. Both experiments were conducted for approximately 580 days (~1.5 yr). Casas et al. (1994) measured the surface area of the uranophane sample by the Brunauer-Emmet-Teller method. Their results are listed in the middle column of Table 8. Because no surface area was measured for the schoepite sample, we have assumed the schoepite to have the same specific surface area as that measured for uranophane (0.3 $m^2 g^{-1}$) in order to calculate the schoepite dissolution rate in terms of surface area. Perez et al. (1997) report the dissolution rate for soddyite. The rates in Table 8 are "intrinsic rates" and are equivalent to k in Equation 1.

Table 8. Intrinsic Dissolution Rates for Uranophane, Schoepite, and Soddyite

Mineral	Reported Dissolution Rate	Mass-Normalized Dissolution Rate* (mg $m^{-2} d^{-1}$)
Uranophane	$rate_{diss}$ = 4.0 x 10^{-9} moles-U h^{-1} m^{-2} (Casas et al. 1994)	k = $rate_{diss}$ = 0.04 mg $m^{-2} d^{-1}$
Schoepite	$rate_{diss}$ = 1.4 x 10^{-9} moles-U h^{-1} (Casas et al. 1994)	k = $rate_{diss}$ = 0.3 mg $m^{-2} d^{-1}$
Soddyite (synthetic)	$rate_{diss}$ = 6.8 x 10^{-14} moles $cm^{-2} s^{-1}$ (Perez et al. 1997)	k = $rate_{diss}$ = 20 mg $m^{-2} d^{-1}$

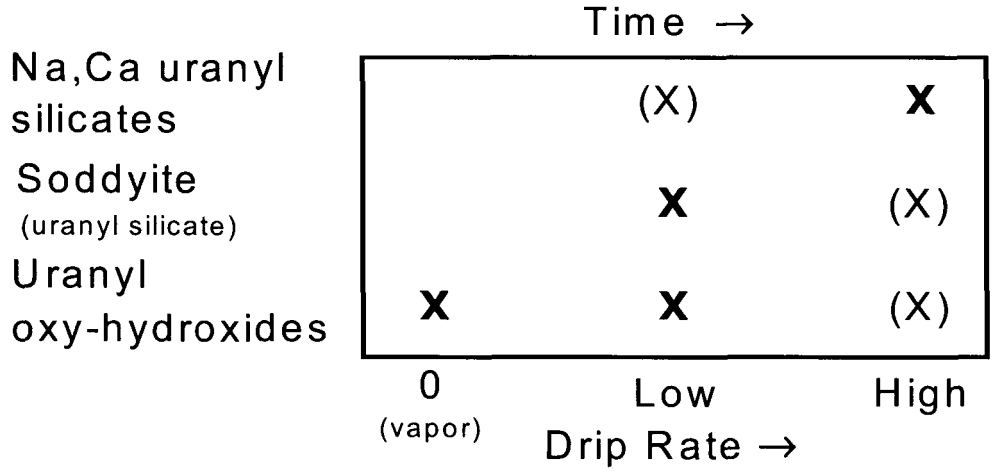
Source: Intrinsic dissolution rates for uranophane and schoepite reported by Casas et al. (1994). Mass-normalized dissolution rates are calculated for the mass of the solid that is dissolved, based on the number of moles of U in the formula (e.g., uranophane, which has 2 moles U per formula unit, has a molar mass of 428.2 g mol^{-1}-U). Mass normalized rate for schoepite is estimated by assuming that the specific surface area of the sample measured by Casas et al. (1994) is identical to uranophane; i.e., ~0.3 $m^2 g^{-1}$. It is further assumed that the surface area did not change significantly over the course of the experiment.

Are U(VI) Solids Long-Term Radionuclide Hosts?–The issue of kinetics raises the question of how long uranyl compounds formed during fuel corrosion might last in a repository environment. Laboratory experiments alone cannot answer this question with much certainty, but studies of natural minerals can help. Despite observations of extensive alteration of schoepite and other uranyl minerals in nature and in some experiments (Wronkiewicz et al. 1996), these minerals are known to persist for many thousands of years. U-series activity ratios for several U(VI) minerals from the Shinkolobwe mine in southern Congo indicate that these minerals did not experience significant preferential loss of U since their formation more than 100,000 years ago (Finch et al. 1996). The minerals studied included rutherfordine, schoepite, becquerelite, and uranophane. Finch et al. (1996) found no correlation between mineral species and mineral age. They concluded that vigorous oxidative dissolution of primary uraninite at the Shinkolobwe mine maintains groundwaters supersaturated with respect to virtually all secondary U(VI) minerals, and, therefore, always provides sufficient dissolved U^{6+}uranium for uranyl-mineral formation and growth. This is supported to some degree by experimental studies on UO_2 corrosion, where schoepite and DS have been identified as forming early (Wronkiewicz et al. 1992). Later-formed

uranyl silicates may directly replace the earliest-formed uranyl oxyhydroxides, but uranyl oxyhydroxides continue to precipitate well after uranyl silicates have become established (Wronkiewicz et al. 1996). Therefore, as long as uncorroded spent UO_2 fuel exists in a repository environment, even metastable uranyl minerals are likely to persist.

6.7 DISCUSSION

U(VI) compounds are likely to be important only after the waste package and fuel cladding are breached, allowing water or water vapor to contact the spent fuel. The unsaturated corrosion experiments at ANL have demonstrated that the degree and rate of general fuel corrosion does not depend on the mode of water contact, as long as water, whether originally as liquid or as condensed water vapor, is in contact with the fuel surface. However, the chemistry of the water in contact with the fuel has a profound effect on the compositions of the corrosion products, as well as their paragenesis (Figure 6) (Finch et al. 1999).



NOTE: Schematic representation of alteration-phase paragenesis in unsaturated experiments with spent fuel. Bold Xs indicate major components of the alteration-phase assemblage; Xs in parentheses indicate minor components. Increased drip rates reproduce paragenetic relationships observed with increased time in experiments and in nature.

Figure 6. Schematic Representation of Alteration-Phase Paragenesis

6.7.1 Water Contact and In-Package Chemistry

An important consideration for understanding potential stabilities of solids that may be important for the long-term performance of a geological repository is the chemistry of the water that will be in contact with radionuclide-bearing solids. The range of water chemistries expected within the waste packages is addressed in the Analysis and Model Report, *Summary of In-Package Chemistry for Waste Forms* (CRWMS M&O 2000c, Table 3) and is reproduced in Table 9 here (a superseded document is cited here and elsewhere in this document because the superseding document does not contain the detail needed). The range of expected water compositions is illustrated by the shaded box in Figure 7, which overlays the U(VI)-mineral stability diagram for the SiO_2-CaO-UO_3-H_2O system (Figure 4). This range of compositions falls largely within the

stability fields of the uranyl oxyhydroxides (meta)schoepite and becquerelite with the upper extremes reaching into the stability fields of the uranyl silicates uranophane and soddyite. Therefore, while the chemistry of the far-field groundwater (treated as being similar to J-13 well water) falls within the stability field of uranophane (or possibly Na-boltwoodite; see Fig. 5), the waters within the waste packages with commercial spent nuclear fuel (CSNF) are likely to contain substantially less dissolved Si and Ca than J-13 water due to reactions with the fuel and other waste-package components (CRWMS M&O 2000c).

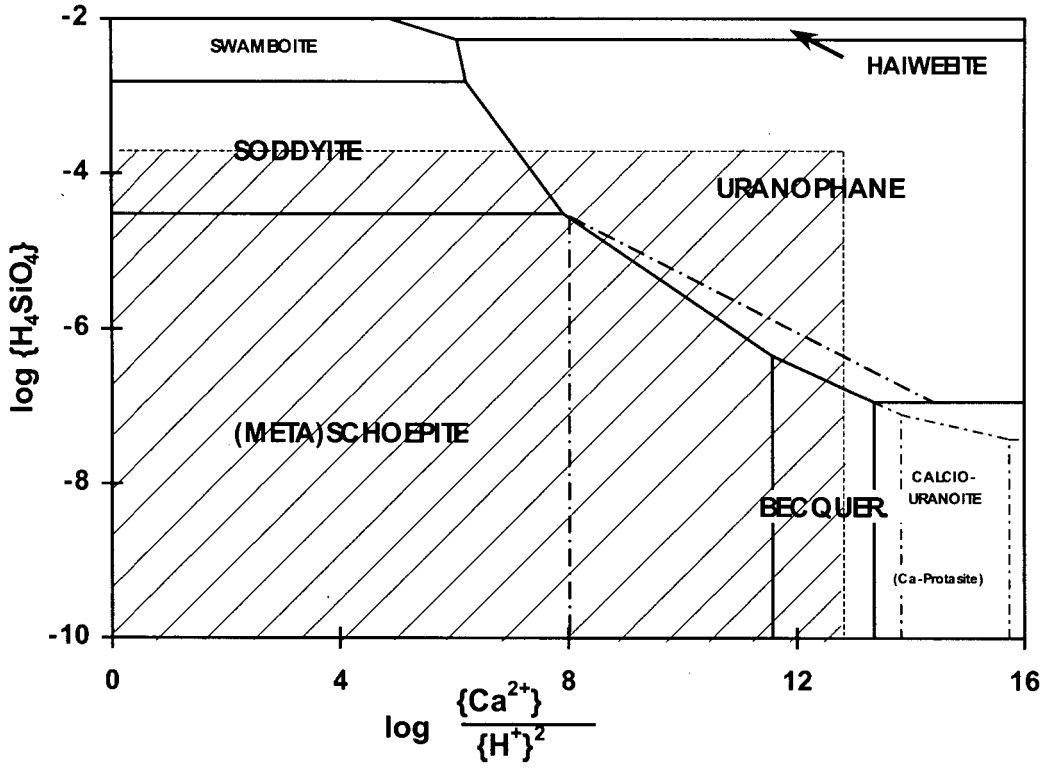
Another issue to consider when evaluating the potential chemistry of water in contact with CSNF within a breached waste package is whether groundwater is dripping into the package and onto the fuel. Another likely condition is that groundwater does not drip onto the fuel, or possibly does not directly enter the waste package at all. Instead, water vapor condenses onto the surface of the fuel. Because condensed water vapor does not contain (significant) dissolved Si, Ca, and similar species, the corrosion of the CSNF in this scenario will not lead to formation of uranyl silicates; the uranyl oxyhydroxides schoepite, metaschoepite, or DS (or some combination) will dominate the alteration-phase assemblage. These solids will persist as long as little or no Si- (and Ca-) bearing groundwater comes in contact with the fuel. Of course, this is the corrosion progress as observed in the ANL humid-air tests on spent fuels.

Only if CSNF is contacted completely by a continuous supply of Si-bearing groundwater will the fuel be replaced by uranyl silicates such as uranophane, Na-boltwoodite, or soddyite. However, the rate at which fuel will alter to uranyl silicates depends on the groundwater flux into the waste package, the dissolution rates of the fuel matrix, and existing corrosion products and the rates at which uranium silicates crystallize. Furthermore, as long as unreacted fuel is dissolving, the supply of dissolved uranium is probably sufficient for formation of newly created uranyl silicates, even if uranyl oxyhydroxides are present. This was concluded from studies of natural uranium deposits where uranyl oxyhydroxides have persisted for hundreds of thousands of years or more (Finch et al. 1996; also see Section 6.6). Only after all the CSNF in a waste package has altered are uranyl silicates likely to begin to replace other more soluble uranyl oxyhydroxides where in contact with Si-rich groundwater.

Table 9. Range of In-Package Fluid Compositions (mol/L, except for pH and Eh)[a]

Variable	CSNF	Codisposal
pH	3.6 - 8.1	4.8 - 10.0
Eh (volts)	0.7 - 1.0	0.6 - 0.9
Ionic Strength	0.003 - 1.7	0.003 - 5.8
Ca	3.9×10^{-6} - 3.2×10^{-4}	3.0×10^{-7} - 0.02
C	2.8×10^{-5} - 0.002	3.5×10^{-5} - 0.5
Pu	0 - 5.610^{-9}	0 - 0.0001
Si	3.7×10^{-10} - 1.9×10^{-4}	5.3×10^{-10} - 1.9×10^{-4}
U	0 - 5×10^{-3}	0 - 1.1×10^{-3}

Source: [a]Reproduced from CRWMS M&O (2000c, Table 3) (a superseded document is cited here and elsewhere in this document because the superseding document does not contain the detail needed).



NOTE: Activity-activity diagram calculated as for Figure 5.

Source: Cross-hatched region shows range of water chemistries considered relevant to in-package chemistry (CRWMS M&O 2000c, Table 3, page 24) (see Table 9). The lower extremes of $\log\{H_4SiO_4\}$ and $\log\{Ca^{2+}\}/\{H^+\}^2$ reported by CRWMS M&O (2000c, Table 3) are not shown here but extend to approximately -10 and 0, respectively. A superseded document (CRWMS M&O 2000c) is cited here and elsewhere in this document because the superseding document does not contain the detail needed.

Figure 7. Activity-Activity Diagram for the System SiO_2-CaO-UO_3-H_2O

6.7.2 Neptunium

Np-237 is a radionuclide of concern because of its potential mobility in Yucca Mountain groundwaters and long half-life (2.14×10^6 yr). The only realistic geochemical analogue for Np(V) is U(V), which is not present in substantial concentrations in most natural groundwaters (Langmuir 1978). However, at least two mixed U(V)-containing minerals are known from nature: wyartite and wyartite II (the second is a dehydration product of wyartite) (Burns and Finch 1999). The mixed-valence uranium oxyhydroxide ianthinite may also contain U(V) (Burns et al. 1997a), but this requires verification through more detailed structure analysis. Ianthinite has been positively identified as an early-formed corrosion product of uraninite at the Nopal I mine near Peña Blanca, Mexico, which is being studied as a natural analogue for fuel corrosion in a repository at Yucca Mountain (Pearcy et al. 1994).

DS that formed during fuel corrosion in humid air contains Np, and the Np/U ratio in DS is comparable to that of the fuel (Buck et al. 1998). In contrast, U(VI) solids from drip tests with high rates of groundwater injection display Np/U ratios significantly below that expected for congruent dissolution and coprecipitation of Np and U. It remains uncertain whether the lack of substantial Np in solids formed in drip tests reflects incompatibility of Np(V) in solids (i.e., the uranyl silicate, Na-boltwoodite, and the Cs-Mo-uranate) or whether differences in the solutions contacting dissolving fuel prevent coprecipitation of U and Np. Current experiments are underway at ANL that inject Np-bearing groundwater onto unirradiated UO_2 that has already formed a suite of U(VI) corrosion products, and data from these experiments may help answer questions about the influence of pre-existing U(VI) solids on the solution behavior of Np.

The fact that not all the Np from the reacted fuel matrix has been recovered in solution taken from the ANL drip experiments with Si-saturated water (see Attachment I, Section A2.2) may reflect one or more of several factors, including:

1. Incomplete oxidation of Np(IV) in the fuel to Np(V) under the experimental conditions in the ANL drip tests

2. Coprecipitation of Np in U(VI) compounds

3. Sorption of Np onto solid corrosion products or components of the fuel holder in the test vessel (or both)

4. Ion exchange of Np species with cations in existing minerals (e.g., NpO_2^+ replacing Na^+ in Na-boltwoodite).

The question of Np oxidation state has not been examined; however, the high radiation field associated with fuel that has been out of the reactor for only 15 to 20 years has been used to argue for strongly oxidizing conditions in those experiments (CRWMS M&O 2000b). That hypothesis remains to be tested. Coprecipitation of Np in corrosion products may be important in the drip tests, although the Np/U ratio measured in solids recovered from the HDR tests to-date is substantially below that expected for congruent precipitation of Np and U. Owing to the high surface area of fine-grained uranyl corrosion products that exist on the surfaces of corroded fuel in the ANL drip tests, sorption may be an important factor for Np retention. Sorption of Np onto the fuel holder in the test vessel may also be important. Although the singly valent NpO_2^+ ion does not sorb strongly on most solids, even a small degree of sorption might account for a significant fraction of Np from the reacted fuel matrix that has not been recovered in solution (also see discussion in Attachment I, Section A2.2). Another process that is potentially enhanced by the high surface area of solids in the drip tests is ion exchange. Ion exchange of dissolved NpO_2^+ into exchangeable sites of, for example, Na-boltwoodite, might sequester some Np in U(VI) solids; however, no firm evidence for this has yet been obtained.

6.7.2.1 Crystal Chemistry of Np and Its Potential Incorporation into U(VI) Compounds

Based on crystal-chemical arguments, Burns et al. (1997b) suggested that minor amounts of NpO_2^+ may replace UO_2^{2+} in uranyl compounds. This is possible only if charge-balance can be

maintained. Congruent coprecipitation is also possible only if NpO_2^+ and UO_2^{2+} occur together in solution such that they can coprecipitate. The discovery of trace Np within DS formed in a humid-air experiment at ANL corroborated the hypothesis of Burns et al (1997b); however, Np has not been found in comparable amounts in uranyl silicates formed in similar experiments where silica-bearing water is introduced. It is notable that Np was found in a uranyl oxyhydroxide from the humid-air experiments but not, as yet, in uranyl silicates in the drip experiments. The NpO_2^+ ion should readily substitute for the uranyl ion (UO_2^{2+}) if *local* charge balance can be maintained (Burns et al. 1997b). (Note that this requirement for *local* charge balance is related to the concept of "bond valence" [Brown 1981], which refers to the strength of the chemical bond received at a particular atomic site, and is not necessarily satisfied by overall charge balance involving cations at more than one structural site.) The coupled substitution, $NpO_2^+ + OH^- = UO_2^{2+} + O^{2-}$, may maintain local charge balance in uranyl oxyhydroxides such as metaschoepite and DS. This substitution mechanism for Np incorporation into DS may operate in other uranyl oxyhydroxides, including becquerelite, $Ca(UO_2)_6O_4(OH)_6(H_2O)_8$, and compreignacite, $K_2(UO_2)_6O_4(OH)_6(H_2O)_7$. However, the same substitution may not be possible in uranyl silicates, such as soddyite, $(UO_2)_2SiO_4(H_2O)_2$, or uranophane-type structures, $M^{m+}[(UO_2)(SiO_3OH)]_m(H_2O)_n$, because O^{2-} ions in those phases form bonds with Si^{4+} ions that have significant covalent character and are also bonded to UO_2^{2+} ions. The only O atom not coordinated to a *Si* site in soddyite is a fully protonated H_2O group. As for uranophane-type silicates, there is but one O atom bonded to Si^{4+} that does not also bond to a UO_2^{2+} ion, and it is a protonated OH^- group coordinated to the Si atom and interlayer constituents. The potential lack of local charge-balancing mechanism for the substitution of Np^{5+} for U^{6+} in uranyl silicates is consistent with a lack of evidence for congruent coprecipitation of Np and U in uranyl silicates examined so far from drip tests.

It has been reported that schoepite and similar uranyl oxyhydroxides are transitory phases in the paragenesis of uraninite alteration in nature (Finch and Ewing 1992; Pearcy et al. 1994; Finch et al. 1992), as well as in experimental studies (Wronkiewicz et al. 1992; 1996). On the other hand, it has also been documented that schoepite can persist for many thousands of years in some natural settings (Finch et al. 1996). If schoepite and similar alteration phases formed in the repository can persist for comparable periods, the incorporation of Np into DS may be a long-term mechanism for Np retention. The durability of DS under conditions expected during the life of the repository at Yucca Mountain remains an important, though poorly understood, issue.

6.7.2.2 Aqueous Chemistry of Np

In addition to possible crystal-chemical arguments, differences in the apparent propensities for Np incorporation exhibited by DS formed in humid-air experiments and Na-boltwoodite formed in the drip experiments may also reflect differences in experimental conditions (see Section 6.4.1 and Attachment 1). The chemical behavior of NpO_2^+ may differ according to test environment. In humid-air experiments, NpO_2^+ and UO_2^{2+} may co-precipitate in DS. In the Si-saturated, Na-carbonate dominated water used in the drip experiments, which is compositionally similar to groundwaters at Yucca Mountain, the two ions may not occur together in solution. This observation may suggest important differences between the complexation behaviors of NpO_2^+ and UO_2^{2+} in J13-like groundwaters. Local redox conditions can also be important for

determining Np behavior, and, although the humid-air and drip experiments at ANL are conducted under nominally identical redox conditions, the accumulation of radiolytically-derived oxidants in the humid-air experiments may exceed that in the drip experiments where replenishment of low ionic strength groundwater can prevent their build-up near the fuel surface. Furthermore, many redox reactions are notoriously slow (for example, see Stumm and Morgan 1981), and the complete oxidation of Np(IV) to Np(V) has not been demonstrated to occur in the ANL tests. If some Np remains in the reduced state, it is not expected to be as mobile as Np(V) but should display release behavior similar to that of Pu(IV).

The incorporation of Np into U(VI) compounds may depend, at least in part, on the way that water contacts the fuel, whether as condensed water vapor or as groundwater. Although we are not currently able to explain why this might be true, estimating the long-term potential for the sequestration of Np during the corrosion of fuel at Yucca Mountain, even from a first approximation, requires that the mode of fuel-water interaction be specified.

6.7.2.3 A Model for Calculating Neptunium Concentrations in a Breached CSNF Waste Package

The uranyl oxyhydroxides are important corrosion products where water flux is limited or sporadic. In addition to the aforementioned kinetic limitations on uranyl silicate formation (Section 6.6), limitations on the availability of the chemical components of potential corrosion products will determine which solids will precipitate. This is demonstrated in part by variations in drip rates among ANL tests of both SNF and unirradiated UO_2. Nearly complete conversion of the U in fuel to uranyl silicates is observed only in tests with the highest drip rates, whereas tests on both unirradiated UO_2 and on SNF with lower drip rates (~1/10 of the HDR tests) display a mixture of uranyl silicates and uranyl oxyhydroxides including schoepite and DS (Wronkiewicz et al. 1992; 1996; Finch et al. 1999). Furthermore, drip tests on unirradiated UO_2 demonstrate that, even after 15 years of reaction in dripping groundwater at an injection rate comparable to that of the ANL LDR tests on SNF, schoepite and DS remain the predominant corrosion products.

DS has been demonstrated to sequester Np. If Np is incorporated into DS during fuel corrosion, the release of Np will not depend solely on the dissolution rate of the fuel but also on the equilibrium solubility of Np-bearing schoepite or DS (or whichever uranyl compounds incorporate Np) and the dissolution rate of Np-bearing schoepite or DS, as well as water flux (Chen et al. 1999c).

Modeling Np concentrations in equilibrium with Np-bearing uranyl oxyhydroxides is probably best accomplished by assuming that Np replaces U as a trace constituent, which is a valid assumption based on both theory (Burns et al. 1997b) and experimental results (Buck et al. 1998; Finch et al. 1999), and by calculating the coprecipitation and codissolution of Np and U according to the method described by Bruno et al. (1998). Bruno et al. (1998) defined a conditional solubility product, K^*_{s0}, for a hypothetical pure phase that is related to the solubility of the pure major phase:

$$K^*_{s0} = x_T \cdot K_{s0} = \gamma_T[T^+] \cdot \gamma_{L^-}[L^-] \qquad \text{(Eq. 3)}$$

Where x is the mole fraction of the pure trace component in the major phase and L is an arbitrary ligand. In applying this method, Bruno et al. (1998) assumed that substitution of a trace element (T) (T < 0.5 mol %) for a major element (M) in the structure of a solid obeys Henry's Law, with an activity coefficient (γ_T) equal to one. Thus, the concentration of the trace component in solution due to the dissolution reaction, $T_xM_{1-x}L_n \Rightarrow xT + (1-x)M + nL$, is given by:

$$[T] = \frac{x}{1-x}[M] \qquad \text{(Eq. 4)}$$

So the solution concentration of the trace element is proportional to the concentration of the major element in the solid. Of course, this assumes that the trace element and the major element dissolve congruently from the solid, which is probably a valid assumption for NpO_2^+ and UO_2^{2+} in DS. It also tacitly assumes that the trace element can occur in a compound that is iso-structural with the major phase. In the case of Np^{5+} substitution for U^{6+} in DS, pure end-members cannot be iso-structural, owing to valence differences. This is readily seen when writing the formulas for the respective ideal hydroxide formulas, $NpO_2(OH)$ and $UO_2(OH)_2$. These two hydroxides can only form a solid solution by creating vacancies and/or interstitials, which could lead to large deviations from Henry's Law behavior. However, this may not be a significant factor for Np substitution in many uranyl oxyhydroxides if Np substitution is small.

Buck et al. (1998) estimated that the ratio of Np to U in DS may be as high as 0.006 (estimated from electron energy-loss spectroscopy). At such low concentrations, Np is considered a trace constituent in DS, so that Np substitution in DS may obey Henry's law. Dissolved neptunium concentration in solution can be calculated by using the method described by Bruno et al. (1998), in which a Henry's law constant of one is assumed for trace elements in a solid that precipitates and dissolves congruently with respect to the major and trace elements (U and Np, respectively). The relationship between the concentrations of Np and U is:

$$[Np] = \frac{x}{1-x}[U] \qquad \text{(Eq. 5)}$$

The proportionality is simply the ratio of Np/U, which, if equal to the molar ratio in both solution and solid, indicates congruent release of Np and U from the solid during dissolution of the corrosion products.

Equation 5 can be used to calculate the total concentration of Np in solution by multiplying the calculated concentration of dissolved U by the ratio $x/(1-x)$; i.e., the Np/U ratio in DS. The Np/U value used here is the highest value reported by Buck et al. (1998): 0.006. The calculated dissolved U concentration, taken from CRWMS M&O (2000d), is a function of temperature, pH, and CO_2 partial pressure and assumes metaschoepite is the solid that limits dissolved U concentrations in solution. Mass balance requires that the net Np/U ratio of all solid corrosion products plus the water that interacts with them must be identical to that of the dissolving fuel; however, by using the highest measured Np/U ratio, the model is founded upon an empirical observation. Furthermore, it is readily seen from Equation 5 that using the highest reported Np/U ratio makes the model more "conservative" (that is, it will tend to overestimate Np concentrations).

The model described by Equation 5 provides a means to calculate dissolved Np concentrations that is an alternative to using Np2O5 (i.e., "pure-phase" solubility) (CRWMS M&O 2000d). The pure-phase solubility model is believed to be "conservative"; however, no evidence for Np2O5 has been reported from any studies of spent-fuel corrosion. Because Np can occur in a U(VI) alteration product, the influence of U(VI) alteration products is considered a more realistic approach for estimating Np concentration limits, as suggested by the *Issue Resolution Status Report Key Technical Issue: Container Life and Source Term* (NRC 1999, Sections 5.3.4.2 and 5.3.4.3) and the *Peer Review of the Total System Performance Assessment-Viability Assessment Final Report* (Budnitz et al. 1999). The identification of Np-bearing schoepite from spent fuel corrosion studies provides the observational basis for the model described here (also see Section 6.7.2.3.1 below), and Equation 5, therefore, provides a basis for implementing and evaluating the potential role of Np-bearing U(VI) corrosion products in controlling Np concentrations in groundwaters associated with a geologic repository.

The formula for Np(V)-substituted DS is $(NpO_2)_y(UO_2)_{1-y}O_{0.25-z-y}(OH)_{1.5+2z+y}$. Substitution of NpO_2^+ into DS may simply require protonation of an O atom, according to the charge-balance mechanism, $NpO_2^+ + H^+ = UO_2^{2+}$. This suggests that the substitution may be sensitive to pH, although this may not be a significant factor for trace substitutions. The number of unprotonated O atoms may limit the maximum number of NpO_2^+ ions that can replace UO_2^{2+}. The maximum value for y in DS is 0.25 (for which z must be zero), and the corresponding limit on Np/U is 0.25/0.75 = 0.33. A similar substitution applies to Np incorporation into schoepite and metaschoepite, $(NpO_2)_y(UO_2)_{4-y}O_{1-y}(OH)_{6+y}(H_2O)_n$, for which the maximum Np/U ratio is the same as for DS with $z = 0$. It is unknown whether this degree of solid solution between a U(VI) oxyhydroxide and a Np(V) oxyhydroxide occurs; however, such extensive substitution would likely lead to significant deviation from Henry's law. Nevertheless, the limit on y imposed by this type of substitution provides an upper bound for the maximum allowable Np/U ratio in these U(VI) oxyhydroxides.

Another U(VI) oxyhydroxide identified from corrosion studies on unirradiated UO_2, and a common U(VI) mineral in nature, is becquerelite. A formula for Np-substituted becquerelite would be $Ca[(NpO_2)_y(UO_2)_{6-y}O_{4-y}(OH)_{6+y}](H_2O)_8$, and the theoretical maximum Np/U ratio could actually exceed one (Np/U $\leq$ 2) in a Np-becquerelite. We do not include Np-substituted becquerelite in our current model, as it has not been identified from corrosion studies on spent fuel; however, becquerelite is a potentially important long-term Np-bearing corrosion product under repository-relevant conditions.

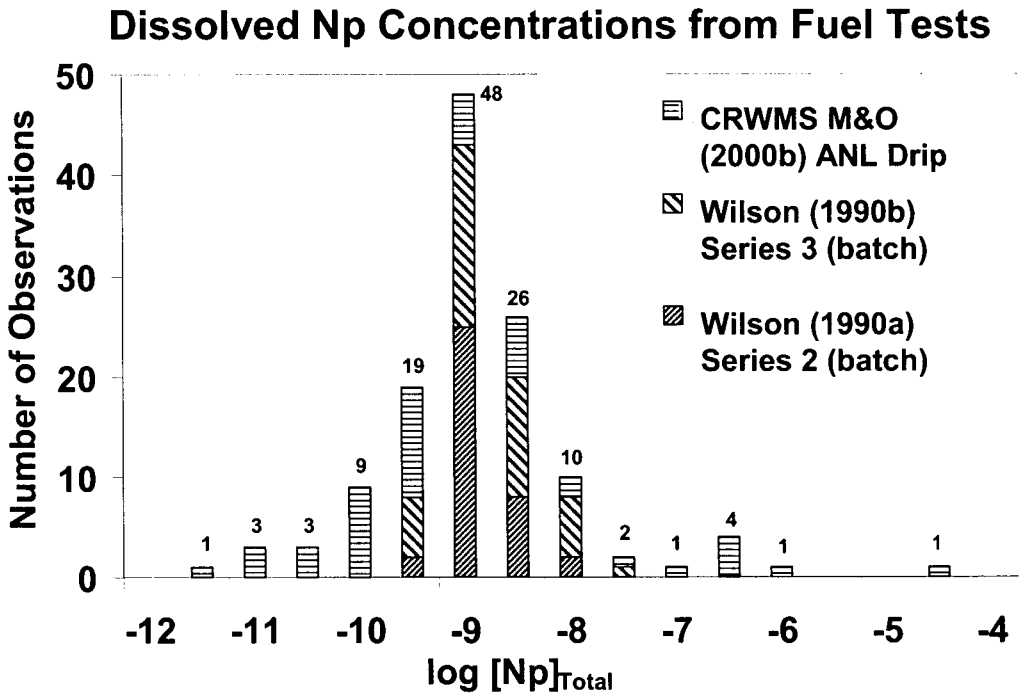
6.7.2.3.1 Comparing Modeled Neptunium Concentrations with Empirical Neptunium Concentrations

Validation of the model described by Equation 5 is performed by comparing the modeled Np concentrations with experimental data reported from corrosion and dissolution experiments on spent-fuel (CRWMS M&O 2000b; Wilson 1990a, 1990b). Figure 8 illustrates the distribution of reported Np concentrations from selected batch experiments (Wilson 1990a, 1990b) and hydrologically unsaturated drip tests (CRWMS M&O 2000b) on spent UO_2 fuels. The concentration of dissolved Np calculated by the model proposed above is shown as a function of pH in Figure 9 (solid line). Figure 9 also shows Np concentration vs. pH calculated by assuming

solid Np_2O_5 limits dissolved Np concentrations (CRWMS M&O 2000d derived with data from Efurd et al. 1998). The Np concentrations calculated with the proposed model are also compared with Np concentrations reported from sequential batch experiments on the dissolution of spent UO_2 fuels (Wilson 1990a, 1990b) and from hydrologically unsaturated drip tests of spent UO_2 fuel (CRWMS M&O 2000b). (Dissolved Np concentrations calculated here use U concentrations calculated for 90°C because data in Figure 7 correspond to experiments at 85°C [batch] or 90°C [drip]; the Np_2O_5 curve applies to 25°C.) Schoepite displays retrograde solubility, with (U) increasing as temperature decreases, so that Np concentrations calculated for 25°C will be higher than those calculated here. The experimental data illustrated in Figure 9 span a wide range; however, the scatter primarily reflects data from the drip tests, which are dynamic flow experiments in which solution concentrations are potentially influenced by multiple processes. Data from sequential batch experiments show a much tighter distribution.

A simple statistical analysis of the experimental data helps quantify uncertainty in experimental Np concentrations. The geometric mean and standard deviation (σ) of 118 reported Np concentrations (Wilson 1990a, 1990b; DTN: LL991001251021.090) were calculated and are listed in Table 10, along with the median value (which is equal to the geometric mean). The geometric mean was calculated (rather than the arithmetic mean) in order to weight all observations more equally, most of which are very small numbers. The 95% confidence interval (CI) calculated for all data ($\pm 2\sigma$) is shown in Table 10, and the 95% CI is indicated in Figure 9 as a double-headed arrow. Visual inspection of Figure 9 illustrates the effectiveness of this model for estimating dissolved Np concentrations reported from experiments on spent UO_2 fuels. Most calculated Np concentrations fall within, although they are somewhat higher than, the range of measured Np concentrations given by a 95% CI (based on a log-normal distribution). Therefore, the model for Np-bearing schoepite proposed here provides a reasonable estimate of dissolved Np concentrations, with some bias towards conservative values.

The uncertainty in the accuracy with which the model predicts measured Np concentrations can also be assessed by calculating the range of Np/U values that will predict Np concentrations spanning the full 95% CI of data reported from experimental studies (Figure 9). Bracketing the 95% CI for empirical Np concentrations with this model requires a Np/U ratio from 6.2×10^{-5} to 0.23 (provided the upper bound is constrained to be the minimum the calculated (Np) curve, which occurs near pH 7). A Np/U ratio of 0.23 corresponds to DS with nearly 20 mol % Np-oxyhydroxide, which is just less than the theoretical maximum of 0.33, or 25 mol % Np-oxyhydroxide in DS. Applying the proposed model to a maximally substituted schoepite (and still assuming Henry's law behavior) produces the dotted curve shown in Figure 1. The minimum Np concentration for Np/U = 0.33 calculated with this model ($(Np)max \cong 1.7 \times 10^{-7}$ mol/L at pH 7 and 90°C) bounds the 95th percentile of the reported empirical Np data from studies of spent-fuel corrosion ($(Np)_{95} \cong 1.1 \times 10^{-7}$; cf. Table 10). The results of this model and its potential range of application is consistent with Np concentrations reported from several studies of spent-fuel dissolution under a variety of conditions (from batch to low water flow) (Figure 9).



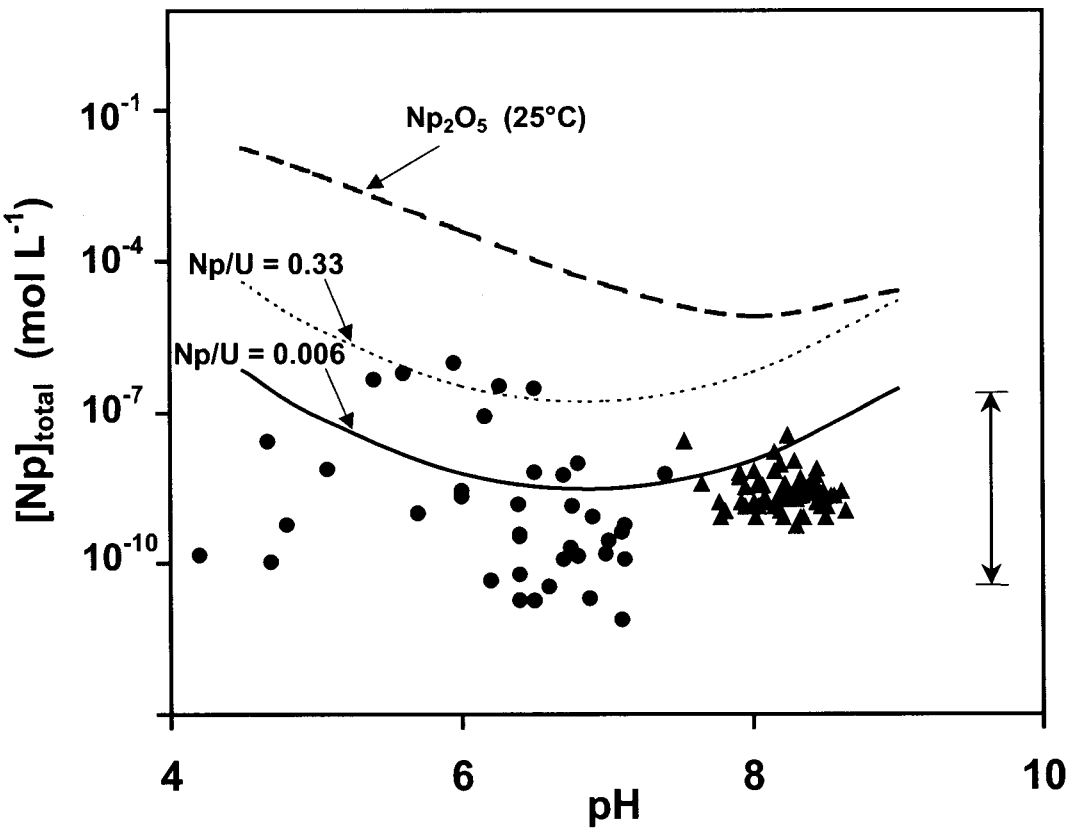
Source: Hydrologically unsaturated drip (CRWMS 2000b) and batch (Wilson 1990a, 1990b) experiments

Figure 8. Distribution of Reported log[Np] Values for Hydrologically Unsaturated and Batch Experiments with Spent Fuel

Table 10. Statistics Calculated from Np Concentrations Reported from Fuel Studies[a]

Statistic	Value
Geometric Mean $[Np]_{Total}$	1.9×10^{-9} mol L^{-1}
Mean of $\log[Np]_{Total}$ (log units)	-8.73
Median (N = 118)	1.9×10^{-9} mol L^{-1}
Standard Deviation (σ) (log units)	0.892
95% CI for $[Np]_{meas}$: $10^{(-8.73 \pm 2\sigma)}$	3.1×10^{-11} to 1.1×10^{-7} mol L^{-1}

Source: [a]Data from Wilson (1990a, 1990b); DTN: LL991001251021.090



NOTE: Solid line shows the total dissolved Np in solution calculated with the model proposed here for Np-bearing schoepite (Np/U = 0.006); light dotted line indicates the Np concentration for the theoretical maximum Np/U in schoepite (see text); calculations are for T = 90°C and log pCO_2 = -3.2. The double-headed arrow indicates the 95% CI calculated for the data (Table 10).

Source: Heavy dashed line shows the concentration of Np calculated by assuming Np_2O_5 is the solubility-limiting solid for Np (Np_2O_5 solubility function from CRWMS M&O 2000d, based on data from Efurd et al. 1998). Solid triangles indicate Np concentrations and pH values measured from batch dissolution studies of spent UO_2 fuel (Wilson 1990a, 1990b). Solid circles indicate Np concentrations reported from hydrologically unsaturated drip studies of spent-fuel corrosion (CRWMS M&O 2000b).

Figure 9. Distributions of Np Concentrations Versus pH Calculated from the Model Proposed Here and Compared with Measured Np Concentrations Reported from Dissolution Studies on Spent Fuel

6.7.2.3.2 Justification of the Conceptual Model

The conceptual model of Np-substituted schoepite proposed here provides a relatively conservative estimate of Np concentrations in J-13-like groundwaters. It is also founded on both theoretical grounds and the empirical observation that Np is incorporated into the structures of U(VI) oxyhydroxides. This conceptual model considers Np-bearing U(VI) oxyhydroxides as long-term Np-controlling solids in a breached waste package. A number of factors support using such a model to calculate dissolved Np concentrations in a breached waste package.

- Np(V) and U(VI) exhibit similar crystal-chemical behaviors (Burns et al. 1997a) providing a sound theoretical foundation for the conceptual model proposed here.

- Np is known to enter the structure of DS where CSNF has corroded in contact with humid air (Buck et al. 1998). This provides empirical verification of Np sequestration by a U(VI) solid.

- DS is structurally similar to schoepite (Finch et al. 1998) so that extending the model to use schoepite or metaschoepite as the Np-bearing phase is reasonable.

- Current estimates of in-package chemistries for water in a waste package that contains CSNF mostly fall within the stability field for schoepite (CRWMS M&O 2000c). This provides a sound basis for treating Np-bearing schoepite as a thermodynamically stable Np-limiting solid under conditions expected in a repository at Yucca Mountain.

- Schoepite and DS are known to be long-lived minerals in nature (Finch et al. 1996). This provides a basis for Np-bearing schoepite as a long-term Np-limiting solid (> 100,000 yr).

- Estimates of Np concentrations from Np-bearing schoepite are independent of empirical measurements of Np concentrations measured in leachates. In fact, the empirical solution data provide a useful independent measure of the model's utility (e.g., Chen et al. 1999c).

6.7.3 Technetium

No evidence exists for the retention of technetium (Tc) in any solid phases, except, perhaps, at trace levels. Essentially all Tc dissolved from ε-Ru particles is released to solution. A potentially large fraction of Tc may be derived from ε-Ru particles along grain boundaries. Uranyl corrosion products are not expected to play any role in the retention of Tc under oxidizing conditions, except as they may limit the penetration of water into fuel rods or grain boundaries. To date there seems little evidence that this is a factor in the ANL drip tests.

6.7.4 Plutonium

Even under relatively oxidizing conditions, there is strong evidence that plutonium (Pu) is retained in a solid phase or sorbed onto cladding or test-vessel components (Finch et al. 1999; Wilson 1988; Werme and Spahiu 1998). Releases are near zero for ANL drip and humid-air tests (fractional releases on the order of parts per million per year), indicating that Pu is nearly quantitatively retained. Wilson (1990a, 1990b) reported an early increase of Pu concentrations in batch experiments, followed by a sharp decrease, which he attributed to precipitation of a secondary phase; however, no Pu-containing phase was identified. Wilson identified two uranyl silicates in his batch experiments, uranophane and haiweeite, but no chemical analyses of these corrosion products were performed. TEM identification of Pu-rich amorphous solids on the surfaces of reacted fuel grains in the ANL tests probably explains apparent Pu deficits in solution, although sorption onto the fuel holder in the test vessel may also be a factor. Although the mixed-valence uranyl phase, ianthinite, has been proposed as a potential host for Pu(IV) under uranium-saturated conditions (Finch and Ewing 1994; Burns et al. 1997a). There is no direct evidence for ianthinite in the ANL tests, nor has ianthinite been identified from other

corrosion experiments with spent fuel. The long-term stability of the Pu-bearing amorphous residue identified in the ANL drip tests is not known, but such amorphous phases commonly recrystallize to more stable (and less soluble) compounds, although radionuclides incorporated in amorphous phases may not be incorporated into the crystalline phases. The potential for the spallation of this residue from the surface of corroded fuel may also be a factor in the generation of Pu-bearing colloids. Little or no spalled material is released to solution in the ANL unsaturated tests due to the intervening Zircaloy holder, which seems to be an effective filter for many particulates.

Geochemical analogues of Pu depend on its oxidation state, and numerous potential oxidation states are known for Pu under the experimental conditions of the ANL drip tests (see Table 2). The most likely Pu oxidation states in the ANL drip tests are probably Pu(IV), for which the analogue is U(IV), and Pu(V), for which the analogue is U(V). The two should behave very differently. Pu(IV) tends to form relatively insoluble solids, whereas Pu(V) (as the PuO_2^+ ion) may form more soluble compounds or Pu(V) may behave like U(VI) (Burns et al. 1997a).

6.7.5 Iodine

Iodine is released essentially quantitatively from corroded fuel. There is no evidence for retention in any solids under any experimental conditions.

6.7.6 Selenium

No experimental data are available for the release of selenium (Se) from spent UO_2 fuels during corrosion tests. Trace levels Se-79, with a long (though uncertain) half life (> 650 000 yr), can be difficult to measure due to isobaric interference by Br-79. Se has not been detected in any uranyl corrosion products analyzed to date. Concentrations of Se in groundwater due to the release of Se from fuel are likely to be too low to stabilize pure uranyl selenites at Yucca Mountain. Chen et al. (1999b) have speculated about the potential for uranyl silicates formed during fuel corrosion to scavenge dissolved Se from solution through the substitution of Si^{4+} by Se^{4+}; however, no evidence is available to support this contention. Chemical similarities between S and Se at oxidation potentials above approximately 600 mV at pH near 8 suggests that Se may behave geochemically like S(VI) at Yucca Mountain, that is, as the SeO_4^{2-} ion. This ion is likely to be mobile, although if U-bearing groundwaters migrate to regions where evaporation can become important, Se may precipitate if uranyl sulfates can form; however, uranyl sulfates are highly soluble in most waters and precipitate during evaporation of fairly low pH solutions (pH < 6) (see Attachment II, Section B3.1).

6.7.7 Americium

The chemical behavior of americium (Am) is analogous to that of the trivalent lanthanides. Like the lanthanides, Am is relatively immobile in most groundwater, except where Am-carbonate complexes may solubilize and mobilize Am. The most important Am-carbonate complex in J-13 well waters is probably $AmCO_3^+$ or $Am(CO_3)_2^{2-}$ (Clark et al. 1995).

Under the conditions of the ANL unsaturated tests, Am appears to be relatively immobile, and Am has been detected in a solid residue precipitated on the surface of corroded fuel grains (Finch et al. 1999). The composition of this residue may vary and it is electron-diffraction amorphous. The long-term durability of this residue is unknown but such amorphous phases tend to recrystallize over time (Ostwald ripening), and the fate of entrained radionuclides during re-crystallization is unclear. If mobilized as a carbonate complex, Am may migrate to coprecipitate with uranyl carbonates if pCO_2 levels become elevated or evaporation becomes important. Experimental evidence indicates that Am is not incorporated into secondary uranyl phases formed during the corrosion process.

6.7.8 Protactinium

There are no data available for the release of protactinium (Pa) from corroded spent UO_2 fuel. Pa is chemically analogous to Ta, Nb, and Zr and insoluble. It exhibits long-term retention in uranyl minerals, where it occurs as a product of U decay, but there is no evidence for the coprecipitation of Pa with U(VI) in naturally occurring uranyl compounds. Based on analogy with chemically similar elements, Pa is probably retained in residues formed during fuel corrosion, along with Am, Pu, REE, and Zr.

6.7.9 Carbon

No information is available on the potential incorporation of carbon-14 (C) into solid uranyl compounds during fuel corrosion. Carbon is likely soluble as the bicarbonate ion, and those studies of fuel dissolution that monitor C-14 releases to solution generally report preferential release relative to the actinides (Wilson 1990a, 1990b). Precipitation of C-14 in solid carbonates (uranyl carbonates or calcite/aragonite) seems possible if pCO_2 is sufficiently high or during evaporation of alkaline waters. Solid carbonates may not sequester a significant fraction of the released C-14 inventory due to dilution by atmospheric C.

6.7.10 Codisposal Waste Packages (Defense Spent Nuclear Fuel and High-Level Waste Glasses)

The range of water chemistries expected to develop within codisposal waste packages is summarized in Table 9 (from Table 3 of CRWMS M&O 2000c; a superseded document is cited here and elsewhere in this document because the superseding document does not contain the detail needed). Major differences between water chemistries expected for codisposal packages and those expected for CSNF packages are that codisposal packages may develop higher pH, higher ionic strengths, higher upper limits on dissolved C and Pu, and a wider range of dissolved Ca (CRWMS M&O 2000c). Importantly, the range of total dissolved Si is not dramatically different for the two types of waste packages. This is because the concentration of dissolved Si is limited by precipitation of amorphous silica, and the saturation concentration of Si is independent of pH below pH of approximately 9 or so. Furthermore, the Si concentration in J-13 water is near silica saturation already. What is probably most important is that, because of the large volume of Si-based high-level waste glass in a codisposal waste package, the concentration of dissolved Si may be less likely to become depleted to the same extent as might happen in a

CSNF waste package; however, this depends to a large degree on the dissolution rate of glass (CRWMS M&O 2000c).

The concentration of dissolved Si in water contacting the waste form is an important factor when considering what U(VI) solid or solids will limit dissolved U concentrations. Alkali- and alkaline-earth uranyl silicates are expected to be stable in most near-neutral to basic groundwaters (Figures 4 and 5); the uranyl silicate soddyite is stable in more acidic groundwaters (or those lower in dissolved alkalis and alkaline-earth elements) if there is sufficient dissolved silica (Figures 4 and 5). To date, no evidence has been found for the incorporation of significant amounts of actinides into uranyl silicates that have been examined from the ANL drip tests with spent fuel (uranyl silicates do not form in the humid-air tests); however, Np was found to be incorporated into the uranyl silicate weeksite from a vapor-hydrated waste glass that was also exposed to dripping water (Buck and Fortner 1997). The pH of the water in that experiment was reportedly as high as 11 or 12, and Np may be stable as Np(VI) under those conditions. Hexavalent Np can be expected to substitute freely for U(VI) in uranyl silicates, as there is no charge-compensation requirements. The concentration of Np in weeksite reported by Buck and Fortner (1997) is 325 (± 50) ppm. Whether Np-bearing weeksite would be an important Np-bearing solid in a breached codisposal waste package is unknown because the conditions necessary for its formation are not well understood. One potentially important factor might be solution pH, with more alkaline pH favoring Np incorporation into uranyl silicates. The current upper range of pH values calculated for the codisposal packages is 10 (Table 9) (cf. Table 3 of CRWMS M&O 2000c), which may well stabilize Np(VI) and allow sequestration of Np by uranyl silicates such as weeksite.

6.7.11 Estimating RN Concentrations Over the Very Long Term (to ~10^6 years)

Will Np-bearing schoepite remain stable over very long times, beyond 10,000 years or so (and as long as 1,000,000 years after closure of the repository)? If so, the model to calculate dissolved Np concentrations discussed in Section 6.7.2.3 can be used without reservation. The longevity of naturally-occurring schoepite and related U(VI) oxyhydroxides was discussed in Section 6.6, where it was shown that schoepite may persist for hundreds of thousands to millions of years. Such time spans are of the length necessary to justify accepting schoepite as the long-term, U-limiting solid and, therefore, as the long-term Np-limiting solid according to the model proposed here. However, the reasons for such remarkable U(VI) mineral persistence are not fully understood. Finch et al. (1996) proposed that schoepite will persist as long as undissolved uraninite persists. Once essentially all the spent fuel in a CSNF waste package has dissolved, and Si-bearing groundwater continues to enter the waste package, the U(VI) oxyhydroxides will probably alter to uranyl silicates. The rate at which this may occur is uncertain but is estimable with the aid of kinetic dissolution (and precipitation) parameters (see Section 6.6) and a knowledge of likely infiltration rates of groundwater into a breached waste package over very long times. Nevertheless, assuming that all Np-bearing schoepite eventually converts to U(VI) silicates (within ~1,000,000 years), the question becomes: What solid, if any, will control dissolved Np concentrations once schoepite no longer plays that role?

Based on current thermodynamic data, NpO_2 is considered the most stable Np-bearing solid in *J-13-like* waters. Although crystalline NpO_2 has not been observed to form from

Np(V)-containing waters (including J-13 and similar water chemistries) in laboratory experiments, it has been argued that this reflects a kinetic barrier to NpO_2 nucleation. At very long times, it is reasonable to expect the more thermodynamically stable solid, NpO_2, to form. Also, the presumed kinetic barrier to nucleation of crystalline NpO_2 from homogeneous solutions may not be relevant to heterogeneous nucleation of NpO_2 in the presence of solid fuel, especially over long time scales. In fact, Np concentrations reported from experimental studies of spent fuel dissolution are not inconsistent with Np concentrations that might be expected if NpO_2 were the solid helping to limit Np concentrations in those experiments. Although NpO_2 has not been observed in those studies, such an observation would be difficult to make owing to the extremely small mass of Np in the fuel specimens used in those studies.

7. CONCLUSIONS

The following conclusions are drawn from our analysis of the seven radionuclides addressed in this report. The results of this AMR are primarily intended for use in sensitivity analyses in performance assessment. This document draws upon information that may be superseded in the future, and the potential impact any superseded documents have on this AMR will be evaluated as needed.

Pa-231, Pu-239, Am-241–Plutonium, Am, Zr, Ru, lanthanides, and U have been found within a residual solid on surfaces of corroded fuel grains in the ANL drip and humid-air tests. Based on our understanding of Pa chemistry, Pa may also be incorporated into this compound. However, poorly crystalline solids, such as this residue, are not expected to be long-term solubility limiting phases, because of Ostwald ripening, a process likely to release some or all elements from a metastable solid. Although aging of solids may attenuate radionuclide release compared with congruent releases from dissolving spent fuel, rates at which metastable solids might release entrained radionuclides through aging is difficult or impossible to predict. Therefore, until a more complete understanding of the potential long-term process(es) that might control the release of transuranium actinides, modeling the long-term geochemical behaviors of Pu, Pa, and Am may need to rely on the pure-phase solubilities of these elements.

Tc-99 and I-129–During the 10,000-year period of immediate regulatory concern for the proposed Yucca Mountain Repository, Tc-99 and I-129 are estimated to contribute more than 95% of the potential dose (CRWMS M&O 1998). Chemical behaviors of these two elements from a wide range of experiments indicate that their releases will not be significantly reduced by Tc- or I-bearing solids, as all known Tc(VII) and I compounds are highly soluble in water (e.g., Neck et al. 1998). Releases of Tc and I to solution are consistent with the concentrations of these two elements being limited by the convolution of rates of reaction of Tc- and I-bearing solids with fuel dissolution, grain-boundary penetration, and water flux. No Tc- or I-bearing corrosion products have been identified in any dissolution experiments on fuel, and, based on purely crystal-chemical argument, neither of these elements is considered likely substituents in any known uranyl compound. Modeling the rates at which these fission products are released from the fuel must rely on accurately modeling the dissolution of the solids in which they occur (e.g., ε-Ru).

C-14–Like I and Tc, C-14 is released in dissolution experiments preferentially to all actinides, although C-14 concentrations of fuel may be poorly known. Calculated release fractions for C-14 are comparable to those of I-129 (Wilson 1988), so that, as for I-129, the rate of release for C-14 may require that the chemical form of C-14, and its location in the fuel, be ascertained. U(VI) solids are unlikely to play an important role in sequestering a significant amount of C-14; however, the identification of calcite in the SKB series 11 and in ANL drip tests suggest that both calcite and uranyl carbonate near equilibrium with calcite may be important.

Se-79–No data are currently available for the release behavior of Se. Under the conditions of the repository, Se will probably form selenite or selenate ions, which are potentially mobile. Pure selenate or selenite solids are unlikely to form, and the release rate for Se will depend on the

dissolution rate of, presumably, the spent fuel matrix; however, it is not well understood how Se is distributed in the spent fuel matrix.

Np-237–The dose contribution from Np-237 becomes a significant concern only beyond 10,000 years (CRWMS M&O 1998). The behavior of Np in many dissolution experiments resembles that of the other actinides, U, Am, and Pu, but the reason for this is not yet understood. The underlying cause of the observed Np behavior in the ANL drip tests remains unexplained, but preliminary results suggest that uranyl silicates do not retain Np in sufficient quantities to explain its release behavior. One hypothesis is that Np(IV) in the fuel matrix does not fully oxidize to Np(V) in experiments conducted under nominally oxidizing conditions. On the other hand, DS in humid-air tests has been shown to sequester Np. In humid-air experiments at ANL, radiolytically produced oxidants may accumulate in a thin water film at the surface of the dissolving fuel, effectively increasing the oxidation potential. Schoepite and DS have been identified in other dissolution experiments (see Section 6.4) but were not analyzed for Np.

If fresh (or constantly replenished) groundwater continuously contacts the fuel over its entire surface—as is the case for the fuel fragments in the ANL HDR tests—then we can expect that all the fuel will be *eventually* converted to uranyl silicates. However, the time required to convert all exposed fuel to uranyl silicates depends in part on the availability of components such as Ca, Na and Si, and the rate at which the groundwater carrying these elements enters the waste package (Chen et al. 1999c). Furthermore, Np appears to be sequestered even in those experiments where silicates are the predominant uranyl corrosion product (Wilson 1988; CRWMS M&O 2000b; Finch et al. 1999). This indicates that an as yet undetermined process is responsible for Np retention in the ANL drip tests, a process with potentially important consequences for understanding future Np release in a geological repository.

7.1 RECOMMENDATIONS

Current data from fuel-corrosion studies suggest that the two fission products, Tc and I, be considered as being released from the fuel as it dissolves and as fuel-grain boundaries open and are exposed to humid air or groundwater. A combination of the dissolution rate of the fuel matrix, combined with the water-flow rate, appears to control the releases of Tc and I during fuel corrosion. Technetium release may depend on the corrosion rate of ε-Ru metal particles rather than the dissolution rate of the fuel matrix, which was suggested by Forsyth and Werme (1992). A conservative approach to modeling the releases of the two radionuclides Se and C is the only reasonable option at this time due to a lack of sufficient data. The conservative approaches identified in *Summary of Dissolved Concentration Limits* (CRWMS M&O 2000d) define upper limits on the solubilities of Tc, I, and C-14, and conservative assumptions (CRWMS M&O 2000d) for the releases of Tc, I, and C-14 are probably reasonably realistic, as these three elements seem unlikely to precipitate under repository-relevant conditions. A conservative assumption for the upper limit on Se concentrations (e.g., 1 molar total dissolved Se) is also recommended at this time because of the potentially high solubility of Se compounds under repository conditions (Chen et al. 1999b). Based on theoretical considerations, only Se and C might become incorporated into corrosion products; however, no experimental evidence for this is available at this time.

Of the eight radionuclides identified in this report as being most important for Performance Assessment (Table 2), only the three actinides, Np, Pu, and Am, are known to occur in solid alteration products. The fate of Pa during fuel corrosion is not currently known from any fuel dissolution experiments, due in part to its low concentration in the fuel. However, based on crystal-chemical considerations and aqueous chemistry, Pa seems likely to be retained with similar elements, such as Pu, Am, Zr, and REE. The long-term behavior of the solid(s) in which Pu and Am (and possibly Pa) are retained during the short-term corrosion of fuel is unknown. The compound in which these radionuclides occur (or might occur) is a chemically inhomogeneous amorphous to cryptocrystalline solid of uncertain composition and structure (Finch et al. 1999). Empirical evidence indicates that uranium(VI) compounds formed during fuel corrosion (i.e., uranium secondary phases) may play a significant role in controlling dissolved concentrations of transuranic actinides (and certain fission products); however, a firm scientific basis for applying this evidence to predicting long-term geochemical behaviors is not yet established. On the other hand, the thermodynamic basis for pure-phase solubility control is well accepted and may be used in long-term predictive geochemical models, at least until a stronger scientific basis (mechanistic and thermodynamic) is established for modeling how uranium secondary phases, or other alternative solubility-control mechanisms, may influence geochemical behaviors of some radionuclides over the long term.

Of the actinides discussed in this report, only Np has been demonstrated to be incorporated into a U(VI) compound: DS formed in humid-air tests on spent fuel (Buck et al. 1998). This latter empirical observation combined with theoretically founded crystal-chemical arguments (Burns et al. 1997a) strongly suggests that DS is a potentially important radionuclide-bearing solid formed during the oxidative corrosion of spent UO_2 fuel. Furthermore, the corrosion of fuel that is contacted with humid air can only lead to formation of DS and related uranyl oxyhydroxides. Uranyl oxyhydroxides can continue to form even after uranyl silicates have precipitated (Finch and Ewing 1992; Wronkiewicz et al. 1992; 1996; Finch et al. 1999). The continuous formation of uranyl oxyhydroxides reflects depletion of Si from groundwater during the corrosion process because U continues to oxidize and dissolve as long as O_2 (or other oxidants) and H_2O are available.

Such considerations strongly indicate that uranyl oxyhydroxides will be important long-term solids. Because uranyl oxyhydroxides are known to incorporate Np, the concentration of Np in a breached CSNF waste package may be modeled by using a conditional solubility product and assuming congruent release of U and Np from uranyl oxyhydroxides, such as schoepite. The details of this model, and its efficacy in predicting dissolved Np concentrations from experimental studies of fuel dissolution, are described in Section 6.7.2.3. Over very long times (approaching ~10^6 years), NpO_2 seems the most likely Np-limiting solid in a geologic repository.

The analyses and results of this AMR are recommended primarily for use in sensitivity studies.

7.2 EFFECTS OF UNCERTAINTIES

The potential for uranyl compounds to exert long-term controls on radionuclide releases remains a subject of considerable interest, but a more detailed understanding is still needed. Several uranyl corrosion products are known to incorporate radionuclides into their structures, including

the two predominant uranyl silicates uranophane and Na-boltwoodite (Buck et al. 1997; Finn et al. 1998; CRWMS M&O 2000b; Burns 1999), demonstrating the abilities of these compounds to incorporate additional elements. To date, only one series of six tests on fewer than 50 g of fuel (the ANL drip tests) form the basis of our knowledge of how uranyl compounds might affect radionuclide releases during spent fuel corrosion. Laboratory-based fuel-corrosion studies are necessarily conducted on spent fuels that are recently out of the reactor; however, radionuclide inventories in such fuels are not the same as those of spent fuel after many hundreds or thousands of years. Because of this and other differences (e.g., radiation fields) between "young" and "old" fuels, mechanisms of radionuclide retention in laboratory experiments may obfuscate substitutional mechanisms of many radionuclides considered important for performance assessment (PA); for example, short-lived radionuclides may dominate radionuclide substitutions in corrosion products formed on young spent fuels. Understanding of many processes operating during the corrosion of spent fuel in laboratory experiments is limited, and can make it difficult to distinguish between processes that may occur only under the experimental conditions (artifacts) and potential long-term, repository-relevant behavior.

If the PA of the potential repository at Yucca Mountain is to accurately consider retardation by solid corrosion products, then additional data are needed about the degree to which these compounds can mitigate RN migration. If further studies can reduce uncertainties related to releases at the source (i.e., the corroded fuel), then uncertainties that accumulate through the complex systems of models related to the geologic repository can be reduced, helping to make related compliance arguments more convincing. The ability to defensibly reduce calculated radionuclide releases at their source should significantly enhance acceptance of PA results by reducing their uncertainties.

The discovery that DS from humid-air experiments can sequester Np in its structure redoubled efforts at ANL to locate and identify Np-bearing solids in ANL drip experiments that use Si-saturated waters. Despite intensive and concerted efforts to locate a Np-bearing compound that would help explain the observed Np release behaviors in the ANL drip experiments, none has been found to date. The most important limitations on identifying such a compound are: (1) the extremely low concentrations of Np in the unreacted fuel (~0.05 wt.%); and (2) uncertainty in the mass of Np that has dissolved from the fuel relative to the mass that has been released to solution (i.e., the mass of "missing" Np), which reflects the combined uncertainties in knowing the total mass of fuel that has dissolved in the experiments (estimated to be ~3 %), as well as the actual concentration of Np in the unreacted fuel fragments used in the corrosion experiments (estimates are based on burnup and decay calculations for an average fuel rod of specified burnup and age). Whatever the actual mass of Np retained in the ANL drip tests, it is certainly very small. Although efforts to isolate a Np-rich solid from the ANL drip tests continue, additional experiments on the behavior of Np during fuel corrosion could significantly enhance those efforts. Examples of such experiments might include reacting Np-doped U oxide(s) under experimental conditions similar to those of the drip tests and analyzing the resulting solids for Np-bearing compounds. This could help determine which phases are most likely to contain Np in drip tests on spent fuel. Experiments are currently underway at ANL that inject Np-bearing water (EJ-13 water with 65 parts per billion Np(V)) onto corroded UO_2 under experimental conditions closely similar to those of the LDR tests on spent fuel. These latter experiments may help identify the roles that existing uranyl corrosion products might have on Np release.

Preliminary data from those experiments suggest that Np is nearly quantitatively removed from solution, although detailed analyses of the solids have not yet been performed.

Identifying solids (and related processes) responsible for the retention of radionuclides in corrosion experiments on spent fuel is a critical first step in using such information in PA models of radionuclide releases, as these solids will form the basis of geochemical models for radionuclide releases from corroded fuel. However, using such empirical observations in PA will require additional fundamental data (see Section 6.1). Partition coefficients between U(VI)-bearing corrosion products and radionuclide-bearing solutions–especially under U-saturated conditions–are necessary for predicting whether and to what extent radionuclides might become incorporated into solids. Thermodynamic parameters remain unknown for many uranyl compounds, and estimated parameters (Section 6.5) cannot replace accurate experimental data, which are needed to model radionuclide releases to groundwater. Kinetic rate laws for the crystallization and dissolution of most uranyl corrosion products are still unknown, with dissolution rates being reported for only three uranyl compounds: uranophane and schoepite (Casas et al. 1994) and soddyite (Perez et al. 1997). These data would need to be confirmed, and additional data may be needed for other solids (e.g., becquerelite and Na-boltwoodite) that might affect radionuclide releases. Kinetic rate laws are required input to geochemical transport models involving formation and alteration of radionuclide-bearing solids. Acquisition of data such as those listed in Table 11 can improve our understanding of the roles of uranyl compounds in limiting radionuclide releases under repository-relevant conditions, helping to improve confidence in potential repository performance.

Table 11. Data Required for Understanding the Role of Corrosion Products in Radionuclide Release

Issue	Status
Identity of solids that incorporate Np and other Radionuclides.	Incomplete data
Radionuclide partition coefficients between U(VI) solids and aqueous solutions as a function of solid and solution compositions.	No data
Thermodynamic solubilities and stabilities of relevant U(VI) solids.	Incomplete data
Kinetic rate laws for precipitation and dissolution for relevant U(VI) solids.	Data for three minerals (Table 8)

8. INPUTS AND REFERENCES

8.1 DOCUMENTS CITED

Aagaard, P. and Helgeson, H.C. 1982. "Thermodynamic and Kinetic Constraints on Reaction Rates Among Minerals and Aqueous Solutions. I. Theoretical Considerations." *American Journal of Science, 282,* (3), 237-285. New Haven, Connecticut: Yale University. TIC: 225516.

Alekseyev, V.A.; Medvedeva, L.S.; Prisyagina, N.I.; Meshalkin, S.S.; and Balabin, A.I. 1997. "Change in the Dissolution Rates of Alkali Feldspars as a Result of Secondary Mineral Precipitation and Approach to Equilibrium." *Geochimica et Cosmochimica Acta, 61,* (6), 1125-1142. New York, New York: Elsevier Science. TIC: 235778.

Alwan, A.K. and Williams, P.A. 1980. "The Aqueous Chemistry of Uranium Minerals. Part 2. Minerals of the Liebigite Group." *Mineralogical Magazine, 43,* 665-667. London, England: Mineralogical Society of Great Britain. TIC: 246767.

Brown, I.D. 1981. "The Bond-Valence Method: An Empirical Approach to Chemical Structure and Bonding." *Structure and Bonding in Crystals.* Volume II. O'Keeffe, M. and Navrotsky, A., eds. Pages 1-30. New York, New York: Academic Press. TIC: 249443

Bruno, J.; Casas, I.; and Sandino A. 1992. "Static and Dynamic SIMFUEL Dissolution Studies Under Oxic Conditions." *Journal of Nuclear Materials, 190,* 61-69. Amsterdam, The Netherlands: Elsevier Science. TIC: 246436.

Bruno, J.; De Pablo, J.; Duro, L.; and Figuerola, E. 1995. "Experimental Study and Modeling of the U(VI)-Fe(OH)3 Surface Precipitation/Coprecipitation Equilibria." *Geochimica et Cosmochimica Acta, 59,* (20), 4113-4123. New York, New York: Elsevier Science. TIC: 239820.

Bruno, J.; Duro, L.; de Pablo, J.; Casas, I.; Ayora, C.; Delgado, J.; Gimeno, M.J.; Peña, J.; Linklater, C.; Pérez del Villar, L.; and Gómez, P. 1998. "Estimation of the Concentrations of Trace Metals in Natural Systems. The Application of Codissolution and Coprecipitation Approaches to El Berrocal (Spain) and Poços de Caldas (Brazil)." *Chemical Geology, 151,* 277-291. Amsterdam, The Netherlands: Elsevier Science B.V. TIC: 246492.

Buck, E.C. and Fortner, J.A. 1997. "Detecting Low Levels of Transuranics with Electron Energy Loss Spectroscopy." *Ultramicroscopy, 67,* 69-75. Amsterdam, The Netherlands: Elsevier Science. TIC: 246495.

Buck, E.C.; Finch, R.J.; Finn, P.A.; and Bates, J.K. 1998. "Retention of Neptunium in Uranyl Alteration Phases Formed During Spent Fuel Corrosion." *Scientific Basis for Nuclear Waste Management XXI, Symposium held September 28-October 3, 1997, Davos, Switzerland.* McKinley, I.G. and McCombie, C., eds. *506,* 87-94. Warrendale, Pennsylvania: Materials Research Society. TIC: 240702.

Buck, E.C.; Wronkiewicz, D.J.; Finn, P.A.; and Bates, J.K. 1997. "A New Uranyl Oxide Hydrate Phase Derived from Spent Fuel Alteration." *Journal of Nuclear Materials, 249,* (1), 70-76. Amsterdam, The Netherlands: Elsevier Science. TIC: 234844.

Budnitz, B.; Ewing, R.C.; Moeller, D.W.; Payer, J.; Whipple, C.; and Witherspoon, P.A. 1999. *Peer Review of the Total System Performance Assessment-Viability Assessment Final Report.* Las Vegas, Nevada: Total System Performance Assessment Peer Review Panel. ACC: MOL.19990317.0328.

Burns P.C. 1999. "Cs Boltwoodite Obtained by Ion Exchange from Single Crystals: Implications for Radionuclide Release in a Nuclear Repository." *Journal of Nuclear Materials, 265,* 218-223. Amsterdam, The Netherlands: Elsevier Science. TIC: 246432.

Burns, P.C. and Finch, R.J. 1999. "Wyartite: Crystallographic Evidence for the First Pentavalent-Uranium Mineral." *American Mineralogist, 84,* p. 1456-1460. Washington, D.C.: Mineralogical Society of America. TIC: 246818.

Burns, P.C.; Ewing, R.C.; and Miller, M.L. 1997b. "Incorporation Mechanisms of Actinide Elements into the Structures of U(6+) Phases Formed During the Oxidation of Spent Nuclear Fuel." *Journal of Nuclear Materials, 245,* (1), 1-9. Amsterdam, The Netherlands: Elsevier Science B.V. TIC: 235501.

Burns, P.C.; Finch, R.J.; Hawthorne, F.C.; Miller, M.L.; and Ewing, R.C. 1997a. "The Crystal Structure of Ianthinite, [U24+(UO2)4O6(OH)4(H2O)4](H2O)5: A Possible Phase for Pu4+ Incorporation During the Oxidation of Spent Nuclear Fuel." *Journal of Nuclear Materials, 249,* 199-206. Amsterdam, The Netherlands: Elsevier Science Publishers. TIC: 246370.

Casas, I.; Bruno, J.; Cera, E.; Finch, R.J.; and Ewing, R.C. 1994. *Kinetic and Thermodynamic Studies of Uranium Minerals - Assessment of the Long-Term Evolution of Spent Nuclear Fuel.* SKB Technical Report 94-16. Stockholm, Sweden: Swedish Nuclear Fuel and Waste Management Company. TIC: 213723.

Casas, I.; Cera, E.; and Bruno, J. 1993a. "Kinetic Studies of Natural Uranium Minerals for the Long-Term Evolution of Spent Nuclear Fuel Under Oxidizing Conditions." *Scientific Basis for Nuclear Waste Management XVI, Symposium held November 30-December 4, 1992, Boston, Massachusetts.* Interrante, C.G. and Pabalan, R.T., eds. *294,* 521-526. Pittsburgh, Pennsylvania: Materials Research Society. TIC: 208880.

Casas, I.; Gimenez, J.; De Pablo, J.; and Torrero, M.E. 1993b. "Dissolution of UO2(s) in MgCl2-Brines Under Different Redox Conditions." *Scientific Basis for Nuclear Waste Management XVI, Symposium held November 30-December 4, 1992, Boston, Massachusetts.* Interrante, C.G. and Pabalan, R.T., eds. *294,* 67-72. Pittsburgh, Pennsylvania: Materials Research Society . TIC: 208880.

Casas, I.; Gimenez, J.; Marti, V.; Torrero, M.E.; and De Pablo J. 1993c. "Kinetically Controlled Dissolution of UO2(s) Under Oxidizing Conditions. A Combined Dissolution-Oxidation Model." *Scientific Basis for Nuclear Waste Management XVI, Symposium held November 30-December 4,*

1992, Boston, Massachusetts. Interrante, C.G. and Pabalan, R.T., eds. *294,* 61-66. Pittsburgh, Pennsylvania: Materials Research Society. TIC: 208880.

Cejka, J. 1999. "Infrared Spectroscopy and Thermal Analysis of the Uranyl Minerals." Chaper 12 of *Uranium: Mineralogy, Geochemistry and the Environment.* Burns, P.C. and Finch, R., eds. Reviews in Mineralogy, Volume 38. Washington, D.C.: Mineralogical Society of America. TIC: 247121.

Chen, F.; Ewing R.C.; and Clark S.B. 1999a. "The Gibbs Free Energies and Enthalpies of Formation of U6+ Phases: An Empirical Method of Prediction." *American Mineralogist, 84,* (4), 650-664. Washington, D.C.: American Mineralogist. TIC: 245800.

Chen, F.; Burns, P.C.; and Ewing R.C. 1999b. "79Se: Geochemical and Crystallo-Chemical Retardation Mechanisms." *Journal of Nuclear Materials, 275,* 81-94. Amsterdam, The Netherlands: Elsevier Science. TIC: 247104.

Chen, Y.; Siegmann, E.; Mattie, P.; NcNeish, J.; Sevougian, S.D.; and Andrews, R. 1999c. "A Mechanistic Model of Spent Fuel Dissolution, Secondary Mineral Precipitation, and Np Release." *Scientific Basis for Nuclear Waste Management XXII, Symposium held November 30-December 4, 1998, Boston, Massachusetts, U.S.A.* Wronkiewicz, D.J. and Lee, J.H., eds. *556,* 471-478. Warrendale, Pennsylvania: Materials Research Society. TIC: 246426.

Clark, D.L.; Hobart, D.E.; and Neu, M.P. 1995. "Actinide Carbonate Complexes and Their Importance in Actinide Environmental Chemistry." *Chemical Reviews, 95,* (1), 25-48. Washington, D.C.: American Chemical Society. TIC: 236729.

CRWMS M&O 1998. "Near-Field Geochemical Environment." Chapter 4 of *Total System Performance Assessment-Viability Assessment (TSPA-VA) Analyses Technical Basis Document.* B00000000-01717-4301-00004 REV 01. Las Vegas, Nevada: CRWMS M&O. ACC: MOL.19981008.0004.

CRWMS M&O 2000a. *Technical Work Plan for Waste Form Degradation Process Model Report for SR.* TWP-EBS-MD-000006 REV 00. Las Vegas, Nevada: CRWMS M&O. ACC: MOL.20001204.0036.

CRWMS M&O 2000b. *Commercial Spent Nuclear Fuel Degradation in Unsaturated Drip Tests.* Input Transmittal WP-WP-99432.T. Las Vegas, Nevada: CRWMS M&O. ACC: MOL.20000107.0209.

CRWMS M&O 2000c. *Summary of In-Package Chemistry for Waste Forms.* ANL-EBS-MD-000050 REV 00. Las Vegas, Nevada: CRWMS M&O. ACC: MOL.20000217.0217.

CRWMS M&O 2000d. *Summary of Dissolved Concentration Limits.* ANL-WIS-MD-000010 REV 00. Las Vegas, Nevada: CRWMS M&O. ACC: MOL.20000525.0372.

CRWMS M&O 2001a. *Colloid-Associated Radionuclide Concentration Limits: ANL.* ANL-EBS-MD-000020 REV 00 ICN 01. Las Vegas, Nevada: CRWMS M&O. ACC: MOL.20010216.0003.

CRWMS M&O 2001b. *Waste Form Colloid-Associated Concentrations Limits: Abstraction and Summary.* ANL-WIS-MD-000012 REV 00 ICN 01. Las Vegas, Nevada: CRWMS M&O. ACC: MOL.20010130.0002

Curtis, D.; Fabryka-Martin, J.; Dixon, P.; and Cramer, J. 1999. "Nature's Uncommon Elements: Plutonium and Technetium." *Geochimica et Cosmochimica Acta, 63,* (2), 275-285. [New York, New York]: Pergamon. TIC: 246120.

Dall'aglio, M.; Gragnani, R.; and Locardi, E. 1974. "Geochemical Factors Controlling the Formation of the Secondary Minerals of Uranium." *Formation of Uranium Ore Deposits, Proceedings of a Symposium on the Formation of Uranium Ore Deposits Organized by the International Atomic Energy Agency and held in Athens, Greece, 6-10 May 1974. IAEA-SM-183/21,* 33-48. Vienna, Austria: International Atomic Energy Agency. TIC: 247089.

Deliens M. and Piret, P. 1992. "La Fontanite, Carbonate Hydraté d'Uranyle et de Calcium, Nouvelle Espèce Minérale de Rabejac, Hérault, France." *European Journal of Mineralogy, 4,* 1271-1274. Stuttgart, Germany: E. Schweizerbart'sche Verlagsbuchhandlung. TIC: 246141.

Deliens, M. 1977. "Associations de Minéraux Secondaires d'Uranium à Shinkolobwe (Région du Shaba, Zaïre)." *Bulletin de la Société Française de Minéralogie et la Cristallographie, 100,* (1), 32-38. Paris, France: Masson. TIC: 246947.

Dent, A.J.; Ramsay, J.D.F.; and Swanton, S.W. 1992. "An EXAFS Study of Uranyl Ion in Solution and Sorbed onto Silica and Montmorillonite Clay Colloids." *Journal of Colloid and Interface Science, 150,* (1), 45-60. New York, New York: Academic Press. TIC: 246166.

DOE (U.S. Department of Energy) 1998. *Total System Performance Assessment.* Volume 3 of *Viability Assessment of a Repository at Yucca Mountain.* DOE/RW-0508. Washington, D.C.: U.S. Department of Energy, Office of Civilian Radioactive Waste Management. ACC: MOL.19981007.0030.

DOE (U.S. Department of Energy) 2000. *Quality Assurance Requirements and Description.* DOE/RW-0333P, Rev. 10. Washington, D.C.: U.S. Department of Energy, Office of Civilian Radioactive Waste Management. ACC: MOL.20000427.0422.

Efurd, D.W.; Runde, W.; Banar, J.C.; Janecky, D.R.; Kaszuba, J.P.; Palmer, P.D.; Roensch, F.R.; and Tait, C.D. 1998. "Neptunium and Plutonium Solubilities in a Yucca Mountain Groundwater." *Environmental Science & Technology, 32,* (24), 3893-3900. [Easton, Pennsylvania]: American Chemical Society. TIC: 243857.

Einziger, R.E.; Thomas, L.E.; Buchanan, H.C.; and Stout, R.B. 1992. "Oxidation of Spent Fuel in Air at 175 to 195°C." *Journal of Nuclear Materials, 190,* 53-60. Amsterdam, The Netherlands: North-Holland Publishing Company. TIC: 238511.

Finch R.J. 1997. "Thermodynamic Stabilities of U(VI) Minerals: Estimated and Observed Relationships." *Scientific Basis for Nuclear Waste Management XX, Symposium held December 2-6, 1996, Boston, Massachusetts.* Gray, W.J. and Triay, I.R., eds. *465,* 1185-1192. Pittsburgh, Pennsylvania: Materials Research Society. TIC: 238884.

Finch, R. and Ewing, R. 1990. *Uraninite Alteration in an Oxidizing Environment and Its Relevance to the Disposal of Spent Nuclear Fuel.* SKB Technical Report 91-15. Stockholm, Sweden: Swedish Nuclear Fuel and Waste Management Company. TIC: 208641.

Finch, R.J. and Ewing, R.C. 1992. "The Corrosion of Uraninite Under Oxidizing Conditions." *Journal of Nuclear Materials, 190,* 133-156. Amsterdam, The Netherlands: Elsevier Science Publishers. TIC: 246369.

Finch, R.J. and Ewing, R.C. 1994. "Formation, Oxidation and Alteration of Ianthinite." *Scientific Basis for Nuclear Waste Management XVII, Symposium held November 29-December 3, 1993, Boston, Massachusetts.* Barkatt, A. and Van Konynenburg, R.A., eds. *333,* 625-630. Pittsburgh, Pennsylvania: Materials Research Society. TIC: 213541.

Finch, R.J. and Murakami, T. 1999. "Systematics and Paragenesis of Uranium Minerals." Chapter 3 of *Uranium: Mineralogy, Geochemistry and the Environment.* Burns, P.C. and Finch, R.J., eds. Reviews in Mineralogy, Volume 38. Washington, D.C.: Mineralogical Society of America. TIC: 247121.

Finch, R.J.; Buck, E.C.; Finn, P.A.; and Bates, J.K. 1999. "Oxidative Corrosion of Spent UO2 Fuel in Vapor and Dripping Groundwater at 90°C." *Scientific Basis for Nuclear Waste Management XXII, Symposium held November 30-December 4, 1998, Boston, Massachusetts, U.S.A.* Wronkiewicz, D.J. and Lee, J.H., eds. *556,* 431-438. Warrendale, Pennsylvania: Materials Research Society. TIC: 246426.

Finch, R.J.; Hawthorne, F.C.; and Ewing, R.C. 1998. "Structural Relations Among Schoepite, Metaschoepite, and Dehydrated Schoepite." *Canadian Mineralogist, 36,* 831-845. Ontario, Canada: Mineralogical Association of Canada. TIC: 246161.

Finch, R.J.; Miller, M.L.; and Ewing, R.C. 1992. "Weathering of Natural Uranyl Oxide Hydrates: Schoepite Polytypes and Dehydration Effects." *Radiochimica Acta, 58/59,* 433-443. München, Germany: R. Oldenbourg Verlag. TIC: 238032.

Finch, R.J.; Suksi, J.; Rasilainen, K.; and Ewing, R.C. 1996. "Uranium Series Ages of Secondary Uranium Minerals, with Applications to the Long-Term Storage of Spent Nuclear Fuel." *Scientific Basis for Nuclear Waste Management XIX, Symposium held November 27-December 1, 1995, Boston, Massachusetts.* Murphy, W.M. and Knecht, D.A., eds. *412,* 823-830. Pittsburgh, Pennsylvania: Materials Research Society. TIC: 233877.

Finn, P.; Hoh, J.C.; Wolf, S.F.; Surchik, M.T.; Buck, E.; and Bates, J.K. 1997. "Spent Fuel Reaction: The Behavior of the Epsilon-Phase over 3.1 Years." *Scientific Basis for Nuclear Waste Management XX, Symposium held December 2-6, 1996, Boston, Massachusetts.* Gray, W.J. and

Triay, I.R., eds. *465,* 527-534. Pittsburgh, Pennsylvania: Materials Research Society. TIC: 238884.

Finn, P.A.; Wronkiewicz, D.J.; Finch, R.J.; Hoh, J.C.; Mertz, C.; Emery, J.W.; Buck, E.C.; Fortner, J.; Wolf, S.F.; Neimark, L.A.; and Bates, J.K. 1998. *Yucca Mountain Project - Argonne National Laboratory, Annual Progress Report, FY 1997 for Activity WP1221 Unsaturated Drip Condition Testing of Spent Fuel and Unsaturated Dissolution Tests of Glass.* ANL-98/12. Argonne, Illinois: Argonne National Laboratory. ACC: MOL.19980818.0230.

Finn, P.A.; Wronkiewicz, D.J.; Hoh, J.C.; Emery, J.W.; Hafenrichter, L.D.; and Bates, J.K. 1993. *Test Plan for Reactions Between Spent Fuel and J-13 Well Water Under Unsaturated Conditions.* ANL-92/48. Argonne, Illinois: Argonne National Laboratory. ACC: HQX.19930318.0004.

Forsyth, R.S. and Werme, L.O. 1992. "Spent Fuel Corrosion and Dissolution." *Journal of Nuclear Materials, 190,* 3-19. Amsterdam, The Netherlands: Elsevier Science Publishers. TIC: 246372.

Frondel, C. 1956. "Mineral Composition of Gummite." *Journal of the Mineralogical Society of America, 41,* (7 and 8), 539-568. Washington, D.C.: Mineralogical Society of America. TIC: 246052.

Frondel, C. 1958. *Systematic Mineralogy of Uranium and Thorium.* Bulletin 1064. Washington, D.C.: U.S. Geological Survey. TIC: 246837.

Gabriel, U.; Gaudet, J.-P.; Spadini, L.; and Charlet, L. 1998. "Reactive Transport of Uranyl in a Goethite Column: An Experimental and Modelling Study." *Chemical Geology, 151,* p. 107-128. New York, New York: Elsevier Science Publishing. TIC: 246884.

Garrels, R.M. and Christ, C.L. 1959. "Behavior of Uranium Minerals During Oxidation." Part 6 of *Geochemistry and Mineralogy of the Colorado Plateau Uranium Ores.* Garrels, R.M. and Larsen, E.S., eds. Professional Paper 320. 81-89. Reston, Virginia: U.S. Geological Survey. TIC: 246367.

Giaquinta, D.M.; Soderholm, L.; Yuchs, S.E.; and Wasserman, S.R. 1997. "The Speciation of Uranium in a Smectite Clay: Evidence for Catalysed Uranyl Reduction." *Radiochimica Acta, 76,* (1/2), 113-121. Munich, Germany: R. Oldenbourg Verlag. TIC: 246886.

Giblin, A.M. 1980. "The Role of Clay Adsorption in Genesis of Uranium Ores." *Uranium in the Pine Creek Geosyncline Proceedings of International Uranium Symposium on the Pine Creek Geosyncline Sponsored by the Bureau of Mineral Resources, Geology and Geophysics and the Csiro Institute of Earth Resources in Co-Operation with the International Atomic Energy Agency and held in Sydney, Australia 4-8 June 1979.* Ferguson, J. and Goleby, A.B., eds. Pages 521-529. Vienna, Austria: International Atomic Energy Agency. TIC: 247117.

Glinka, Y.D.; Jaroniec, M.; and Rozenbaum, V.M. 1997. "Adsorption Energy Evaluation from Luminescence Spectra of Uranyl Ions UO_2^{2+} Adsorbed on Disperse Silica Surfaces." *Journal of*

Colloid and Interface Science, 194, 455-469. New York, New York: Academic Press. TIC: 246165.

Grambow, B. 1989. *Spent Fuel Dissolution and Oxidation: An Evaluation of Literature Data.* SKB Technical Report 89-13. Stockholm, Sweden: Swedish Nuclear Fuel and Waste Management Company. TIC: 208579.

Grambow, B.; Loida, A.; Dressler, P.; Geckeis, H.; Gago, J.; Casas, I.; de Pablo, J.; Giménez, J.; and Torrero, M.E. 1996. *Long-term Safety of Radioactive Waste Disposal: Chemical Reaction of Fabricated and High Burnup Spent UO2 Fuel with Saline Brines.* FZKA 5702. Final Report. Karlsruhe, Germany: Forschungszentrum Karlsruhe GmbH. TIC: 246887.

Grandstaff, D.E. 1976. "A Kinetic Study of the Dissolution of Uraninite." *Economic Geology and the Bulletin of The Society of Economic Geologists, 71,* (8), 1493-1506. El Paso, Texas: Economic Geology Publishing Company. TIC: 246339.

Gray, W.J. and Wilson, C.N. 1995. *Spent Fuel Dissolution Studies FY 1991-1994.* PNL-10450. Richland, Washington: Pacific Northwest Laboratory. ACC: MOL.19960802.0035.

Gray, W.J.; Leider, H.R.; and Steward, S.A. 1992. "Parametric Study of LWR Spent Fuel Dissolution Kinetics." *Journal of Nuclear Materials, 190,* 46-52. Amsterdam, The Netherlands: North-Holland Publishing Company. TIC: 238041.

Grenthe, I.; Fuger, J.; Konings, R.J.M.; Lemire, R.J.; Muller, A.B.; Nguyen-Trung, C.; and Wanner, H. 1992. *Chemical Thermodynamics of Uranium.* Volume 1 of *Chemical Thermodynamics.* Wanner, H. and Forest, I., eds. Amsterdam, The Netherlands: North-Holland Publishing Company. TIC: 224074.

Guenther, R.J.; Blahnik, D.E.; Campbell, T.K.; Jenquin, U.P.; Mendel, J.E.; Thomas, L.E.; and Thornhill, C.K. 1988. *Characterization of Spent Fuel Approved Testing Material ATM--103.* PNL-5109-103. Richland, Washington: Pacific Northwest Laboratory. ACC: NNA.19911017.0104.

Hawthorne, F.C. 1992. "The Role of OH and H2O in Oxide and Oxysalt Minerals." *Zeitschrift für Kristallographie, 201,* 183-206. Munchen, Germany: R. Oldenbourg Verlag. TIC: 246654.

Holland, H.D. 1978. "Physical and Chemical Transport in River Systems ." Chapter IV of *The Chemistry of the Atmosphere and Oceans.* New York, New York: John Wiley & Sons. TIC: 247069.

Isobe, H.; Murakami, T.; and Ewing, R.C. 1992. "Alteration of Uranium Minerals in the Koongarra Deposit, Australia: Unweathered Zone." *Journal of Nuclear Materials, 190,* 174-187. Amsterdam, The Netherlands: Elsevier Science Publishers. TIC: 246371.

Janeczek, J.; Ewing, R.C.; and Thomas, L.E. 1993. "Oxidation of Uraninite: Does Tetragonal U3O7 Occur in Nature?." *Journal of Nuclear Materials, 207,* 177-191. Amsterdam, The Netherlands: Elsevier Science Publishers B.V. TIC: 245943.

Johnson, L.H. and Werme, L.O. 1994. "Materials Characteristics and Dissolution Behavior of Spent Nuclear Fuel." *Materials Research Society Bulletin, 19,* (12), 24-27. Pittsburgh, Pennsylvania: Materials Research Society. TIC: 246655.

Langmuir, D. 1978. "Uranium Solution-Mineral Equilibria at Low Temperatures with Applications to Sedimentary Ore Deposits." *Geochimica et Cosmochimica Acta, 42,* (6), 547-569. New York, New York: Pergamon Press. TIC: 217857.

Markovic, M. and Pavkovic, N. 1983. "Solubility and Equilibrium Constants of Uranyl(2+) in Phosphate Solutions." *Inorganic Chemistry, 22,* (6), 978-982. Washington, D.C.: American Chemical Society. TIC: 246122.

Matzke, Hj. 1992. "Radiation Damage-Enhanced Dissolution of UO2 in Water." *Journal of Nuclear Materials, 190,* 101-106. Amsterdam, The Netherlands: Elsevier Science. TIC: 246435.

McEachern, R.J. and Taylor, P. 1998. "A Review of the Oxidation of Uranium Dioxide at Temperatures Below 400°C." *Journal of Nuclear Material, 254,* 87-121. Amsterdam, The Netherlands: Elsevier Science. TIC: 246427.

Murakami, T.; Isobe, H.; Ohnuki, T.; Sato, T.; Yanase, N.; and Kiyoshige, J. 1996. "Mechanism of Saléeite Formation at the Koongarra Secondary Uranium Deposit." *Scientific Basis for Nuclear Waste Management XIX, Symposium held November 27-December 1, 1995, Boston, Massachusetts.* Murphy, W.M. and Knecht, D.A., eds. *412,* 809-816. Pittsburgh, Pennsylvania: Materials Research Society. TIC: 233877.

Murakami, T.; Ohnuki, T.; Isobe, H.; and Sato, T. 1997. "Mobility of Uranium During Weathering." *American Mineralogist, 82,* 888-899. Washington, D.C.: Mineralogical Society of America. TIC: 246053.

Murrell, M.T.; Paviet-Hartmann, P.; Goldstein, S.J.; Nunn, A.J.; Roback, R.C.; Dixon, P.A.; and Simmons, A. 1999. "U-series Natural Analog Studies at Peña Blanca, Mexico: How Mobile is Uranium?." *Eos, Transactions (Supplement), 80,* (46), F1205. Washington, D.C.: American Geophysical Union. TIC: 246374.

Neck, V.; Konnecke, T.; Fanghanel, T.; and Kim, J.I. 1998. "Activity Coefficients and Pitzer Parameters for the Fission Product Ions Cs+ and TcO4- in the System Cs+/Na+/K+/Mg2+/Cl-/So42-/TcO4-/H2O at 25degrees C." *Radiochimica Acta, 83,* 75-80. Munchen, Germany: R. Oldenbourg Verlag. TIC: 246447.

Nguyen, S.N.; Silva, R.J.; Weed, H.C.; and Andrews, J.E., Jr. 1992. "Standard Gibbs Free Energies of Formation at the Temperature 303.15 K of Four Uranyl Silicates: Soddyite, Uranophane, Sodium Boltwoodite, and Sodium Weeksite." *Journal of Chemical Thermodynamics, 24,* (1-6), 359-376. New York, New York: Academic Press. TIC: 238507.

NRC (U.S. Nuclear Regulatory Commission) 1999. *Issue Resolution Status Report Key Technical Issue: Container Life and Source Term.* Rev. 2. Washington, D.C.: U.S. Nuclear Regulatory Commission. TIC: 245538.

NRC (U.S. Nuclear Regulatory Commission) 2000. *Issue Resolution Status Report Key Technical Issue: Total System Performance Assessment and Integration.* Rev. 2. Washington, D.C.: U.S. Nuclear Regulatory Commission. TIC: 247614.

O'Hare, P.A.G.; Lewis, B.M.; and Nguyen, S.N. 1988. "Thermochemistry of Uranium Compounds, XVII. Standard Molar Enthalpy of Formation at 298.15 K of Dehydrated Schoepite U03.0.9H2O. Thermodynamics of (Schoepite + Dehydrated Schoepite + Water)." *Journal of Chemical Thermodynamics, 20,* 1287-1296. New York, New York: Academic Press. TIC: 246154.

Parks, G.A. and Pohl, D.C. 1988. "Hydrothermal Solubility of Uraninite." *Geochimica et Cosmochimica Acta, 52,* 863-875. New York, New York: Pergamon Press. TIC: 240879.

Pearcy, E.C.; Prikryl, J.D.; Murphy, W.M.; and Leslie, B.W. 1994. "Alteration of Uraninite from the Nopal I Deposit, Pena Blanca District, Chihuahua, Mexico, Compared to Degradation of Spent Nuclear Fuel in the Proposed U.S. High-Level Nuclear Waste Repository at Yucca Mountain, Nevada." *Applied Geochemistry, 9,* 713-732. New York, New York: Elsevier Science. TIC: 236934.

Perez, I.; Casas, I.; Torrero, M.E.; Cera, E.; Duro, L.; and Bruno, J. 1997. "Dissolution Studies of Soddyite as a Long-Term Analogue of the Oxidative Alteration of the Spent Nuclear Fuel Matrix." *Scientific Basis for Nuclear Waste Management XX, Symposium held December 2-6, 1996, Boston, Massachusetts.* Gray, W.J. and Triay I.R., eds. *465,* 565-572. Pittsburgh, Pennsylvania: Materials Research Society. TIC: 238884.

Sandino, A. 1991. *Processes Affecting the Mobility of Uranium in Natural Waters.* Ph.D. thesis. Stockholm, Sweden: Royal Institute of Technology. TIC: 246941.

Sandino, A. and Bruno, J. 1992. "The Solubility of (UO2)3(PO4)2.4H2O(s) and the Formation of U(VI) Phosphate Complexes: Their Influence in Uranium Speciation in Natural Waters." *Geochimica et Cosmochimica Acta, 56,* 4135–4145. New York, New York: Pergamon Press . TIC: 246154.

Sandino, M.C.A. and Grambow, B. 1994. "Solubility Equilibria in the U(VI)-Ca-K-Cl-H2O System: Transformation of Schoepite into Becquerelite and Compreignacite." *Radiochimica Acta, 66/67,* 37-43. Munich, Germany: R. Oldenbourg Verlag. TIC: 246117.

Sato, T.; Murakami, T.; Yanase, N.; Isobe, H.; Payne, T.E.; and Airey P.L. 1997. "Iron Nodules Scavenging Uranium from Groundwater." *Environmental Science and Technology, 31,* 2854-2858. Washington, D.C.: American Chemical Society. TIC: 246507.

Sergeyeva, E.I.; Nikitin, A.A.; Khodakovskiy, I.L.; Naumov, G.B.; and Vernadskiy, V.I. 1972. "Experimental Investigation of Equilibria in the System UO3-CO2-H2O in 25-200[degrees]C Temperature Interval." *Geokhimiya, 11,* 1340-1350. Moscow, Russia: Maik Nauka. TIC: 246653.

Shannon, R.D. 1976. "Revised Effective Ionic Radii and Systematic Studies of Interatomic Distances in Halides and Chalcogenides." *Acta Crystallographica, A32,* ([5]), 751-767. Copenhagen, [Denmark: Munksgaard International Publishers]. TIC: 240561

Shoesmith, D.W. and Sunder, S. 1991. *An Electrochemistry-Based Model for the Dissolution of UO2.* SKB Technical Report 91-63. AECL-10488. Stockholm, Sweden: Swedish Nuclear Fuel and Management Company. TIC: 206581.

Shoesmith, D.W. and Sunder, S. 1992. "The Prediction of Nuclear Fuel (UO2) Dissolution Rates Under Waste Disposal Conditions." *Journal of Nuclear Materials, 190,* 20-35. Amsterdam, The Netherlands: Elsevier Science. TIC: 246431.

Smith, D.K., Jr. 1984. "Uranium Mineralogy." *Uranium Geochemistry, Mineralogy, Geology, Exploration and Resources.* De Vivo, B.; Ippolito, F.; Capaldi, G.; and Simpson, P.R., eds. p. 43-88. London, United Kingdom: Institution of Mining and Metallurgy. TIC: 246885.

Sowder, A.G.; Clark, S.B.; and Fjeld, R.A. 1996. "The Effect of Silica and Phosphate on the Transformation of Schoepite to Becquerelite and Other Uranyl Phases." *Radiochimica Acta, 74,* 45-49. Munich, Germany: R. Oldenbourg Verlag. TIC: 246119.

Stroes-Gascoyne, S. 1992. "Trends in the Short-Term Release of Fission Products and Actinides to Aqueous Solution from Used CANDU Fuels at Elevated Temperature." *Journal of Nuclear Materials, 190,* 87-100. Amsterdam, The Netherlands: Elsevier Science. TIC: 246434.

Stroes-Gascoyne, S.; Johnson, L.H.; Tait, J.C.; McConnel, J.L.; and Porth, R.J. 1997. "Leaching of Used CANDU Fuel: Results from a 19-Year Leach Test Under Oxidizing Conditions." *Scientific Basis for Nuclear Waste Manangement XX, Materials Research Society Symposium Held December 2-6, 1996, Boston, Massachusetts, U.S.A.* Gray, W.J. and Triay, I.R., eds. *465,* 511-518. Pittsburgh, Pennsylvania: Materials Research Society. TIC: 238884.

Stout, R.B. 1998. *Unsaturated Dissolution Tests of Spent Fuel and UO2.* Activity Plan D-20-43 REV 01. Livermore, California: Lawerence Livermore National Laboratory. ACC: MOL.19980803.0086

Stumm, W. and Morgan, J.J. 1981. *Aquatic Chemistry – An Introduction Emphasizing Chemical Equilibria in Natural Waters.* New York, New York: John Wiley & Sons. TIC: 208448.

Sturchio, N.C.; Antonio, M.R.; Soderholm, L.; Sutton, S.R.; and Brannon, J.C. 1998. "Tetravalent Uranium in Calcite." *Science, 281,* 971-973. Washington, D.C.: American Association for the Advancement of Science. TIC: 246116.

Thomas, L.E.; Einziger, R.E.; and Buchanan, H.C. 1993. "Effects of Fission Products on Air Oxidation of LWR Spent Fuel." *Journal of Nuclear Materials, 201,* 310-319. Amsterdam, The Netherlands: Elsevier Science Publishers. TIC: 242662

Vochten, R. and Van Haverbeke, L. 1990. "Transformation of Schoepite into the Uranyl Oxide Hydrates: Becquerelite, Billietite and Wölsendorfite." *Mineralogy and Petrology, 43,* 65-72. New York, New York: Springer Verlag. TIC: 246060.

Waite, T.O.; Davis, J.A.; Payne, T.E.; Waychunas, G.A.; and Xu, N. 1994. "Uranium(VI) Adsorption to Ferrihydrite: Application of a Surface Complexation Model." *Geochimica et Cosmochimica Acta, 58,* (24), 5465-5478. Oxford, England: Elsevier Science. TIC: 226322.

Walenta, K. 1985. "Uranotungstit, ein Neues Sekundares Uranmineral aus Dem Schwarzwald." *TMPM Tschermaks Mineralogische und Petrographische Mitteilungen, 34,* 25-34. New York, New York: Springer-Verlag. TIC: 246634.

Walenta, V.K. 1983. "Uranosilit, ein Neues Mineral aus der Uranlagerstatte von Mendenschwand im Sudlichen Schwarzwald." *Neues Jahrbuch für Mineralogie, Monatschefte,* 259-269. Stuttgart, Germany: E. Schweizerbart'sche Verlagsbuchhandlung. TIC: 246652.

Werme, L.O. and Spahiu, K. 1998. "Direct Disposal of Spent Nuclear Fuel: Comparison Between Experimental and Modelled Actinide Solubiluties in Natural Waters." *Journal of Alloys and Compounds, 271-273,* 194-200. Lausanne, Switzerland: Elsevier Science. TIC: 243085.

Wilson, C.N. 1988. "Summary of Results from the Series 2 and Series 3 NNWSI Bare Fuel Dissolution Tests." *Scientific Basis for Nuclear Waste Management XI, Symposium held November 30-December 3, 1987, Boston, Massachusetts.* Apted, M.J. and Westerman, R.E., eds. *112,* 473-483. Pittsburgh, Pennsylvania: Materials Research Society. TIC: 203662.

Wilson, C.N. 1990a. *Results from NNWSI Series 2 Bare Fuel Dissolution Tests.* PNL-7169. Richland, Washington: Pacific Northwest Laboratory. ACC: NNA.19900814.0048.

Wilson, C.N. 1990b. *Results from NNWSI Series 3 Spent Fuel Dissolution Tests.* PNL-7170. Richland, Washington: Pacific Northwest Laboratory. ACC: NNA.19900329.0142.

Wronkiewicz, D.J.; Bates, J.K.; Gerding, T.J.; Veleckis, E.; and Tani, B.S. 1992. "Uranium Release and Secondary Phase Formation During Unsaturated Testing of UO2 at 90°C." *Journal of Nuclear Materials, 190,* 107-127. Amsterdam, The Netherlands: North-Holland Publishing Company. TIC: 236558.

Wronkiewicz, D.J.; Bates, J.K.; Wolf, S.F.; and Buck, E.C. 1996. "Ten-Year Results from Unsaturated Drip Tests with UO2 at 90°C: Implications for the Corrosion of Spent Nuclear Fuel." *Journal of Nuclear Materials, 238,* (1), 78-95. Amsterdam, The Netherlands: North-Holland Publishing Company. TIC: 243361.

8.2 CODES, STANDARDS, AND REGULATIONS

AP-2.21Q, Rev. 0, ICN 0. *Quality Determinations and Planning for Scientific, Engineering, and Regulatory Compliance Activities.* [Washington, D.C.]: U.S. Department of Energy, Office of Civilian Radioactive Waste Management. ACC: MOL.20000802.0003.

ASTM C 1174-97. 1998. *Standard Practice for Prediction of the Long-Term Behavior of Materials, Including Waste Forms, Used in Engineered Barrier Systems (EBS) for Geological Disposal of High-Level Radioactive Waste.* West Conshohocken, Pennsylvania: American Society for Testing and Materials. TIC: 246015.

8.3 SOURCE DATA

LL010109312241.021. Spent Fuel Test Particle Analysis in Scientific Notebook SN 1635. Submittal date: 01/25/2001.

LL010305312241.022. TEM Analyses of Colloids from Scientific Notebook #1528. Submittal date: 03/20/2001.

LL991110351021.100. TEM Analyses of Colloids Formed During Corrosion Testing of Spent Fuel for Work Documented in SN 1528 and SN 867. Submittal date: 01/10/2000.

LL010305512241.024. Analyses of Colloids by TEM from Scientific Notebook #1355. Submittal date: 03/20/2001.

LL991001251021.090. Draft - CSNF Waste Form Degradation: Unsaturated Drip Tests - G2020 Analysis and Modeling Report . Submittal date: 10/04/1999.

ATTACHMENT I

OVERVIEW OF SELECTED RADIONUCLIDE RELEASE DATA FROM ANL UNSATURATED DRIP AND HUMID-AIR TESTS

A1. FUEL MATRIX DISSOLUTION IN ANL DRIP AND HUMID-AIR TESTS

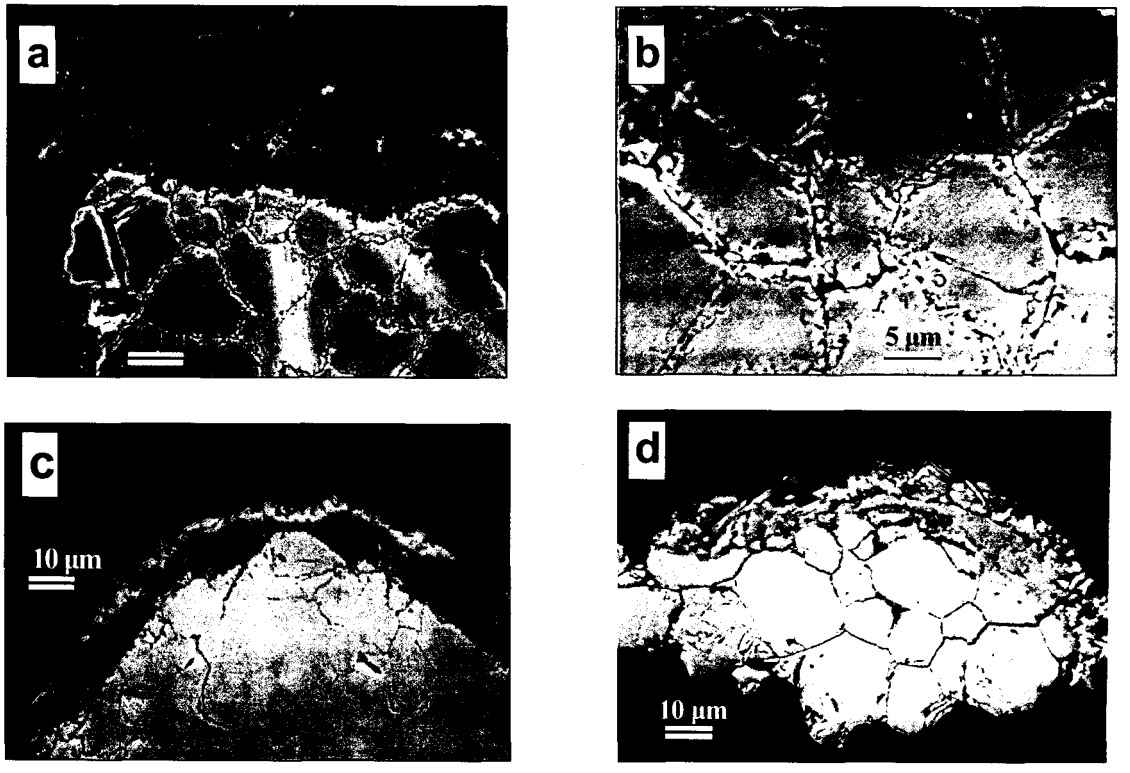
The mechanisms of fuel corrosion and the extent of matrix dissolution is important for understanding the releases of various radionuclides from spent fuel, and a brief discussion of matrix dissolution follows. Additional details on fuel dissolution mechanisms in the ANL unsaturated experiments are provided by Finch et al. (1999) and data on rates of radionuclide release are provided by CRWMS M&O (2000b). The spent-fuel matrix dissolves by two, possibly three modes: (1) dissolution through the outer surface of fuel fragments (general corrosion) (Figure A1), (2) dissolution along grain boundaries and defects associated with grain boundaries (Figures A1a, b), and (3) dissolution of micrometer-sized intergranular fuel particles (Figure A1b). The third mode is essentially equivalent general corrosion, i.e., dissolution of fine particulates. It is distinguished here because these fine particles are apparently generated during corrosion rather than being pre-existing features of unreacted fuel fragments. The first mode is evident in samples from all three types of experiment (humid-air, low drip rate, and high drip rate) (Figure A1), whereas the second and third seem less significant for LDR and humid-air experiments (Figures A1c and A1d, respectively).

Dissolution of fuel fragments in samples from all three types of experiment has proceeded through the outermost grains, with little or no preferential dissolution along adjacent grain boundaries (general dissolution). There is a distinct interface between inner and outer layers in samples from HDR experiments but no detectable difference in composition at the SEM scale. The physical significance of this interface is uncertain, but it may represent the original outer surface of the fuel; however, the degree to which the interface may have been displaced from its original position is uncertain. Some displacement might be expected because of the large volume difference between the original fuel and U(VI) corrosion products, and the narrowing of layers near the corners of some fragments suggests expansion of the replacement layer relative to the original volume of fuel that was dissolved and replaced (Figure A1c).

Dissolution along fuel-grain boundaries (mode 2) is observed in samples contacted by the largest volumes of dripping groundwater (HDR experiments) (Figure A1b). Dissolution along grain boundaries extends at least 20 or 30 grains deep (> 200 μm) and possibly throughout entire fragments from HDR experiments. There seems much less dissolution along grain boundaries in samples from LDR and humid-air experiments, where gaps between grains penetrate only a few grains deep (~10-30 μm) (Figures A1c and A1d, respectively). Dissolution of defects near grain boundaries appears minimal for fuel reacted in LDR and humid-air experiments; however, specimens from low-drip and humid-air experiments with fuel grains are difficult to obtain and observations are limited.

The "worm-like" texture observed near fuel-grain boundaries in samples from HDR experiments may be caused by preferential dissolution along defects (Figure A1b). These curvilinear features penetrate 1 to 2 μm into each grain and may be responsible for fragmentation observed between

fuel grains, especially in samples from HDR experiments. Micrometer- to submicrometer-sized fuel particles have been observed in all polished samples. These small particles commonly occur between the larger fuel grains, although some fuel grains appear to have fragmented entirely into smaller pieces. The smallest particles are most abundant along grain boundaries in the HDR samples, where dissolution along defects may weaken the outer 1-2 μm of the grains. Weakening of grain-to-grain contacts, caused by dissolution along defects, may also explain the disaggregation of one large fuel fragment during the 3.7-year sampling (Finn et al. 1997). These submicrometer-sized fuel particles may help to increase pathways available for infiltration of water to fragment interiors and can dramatically increase the reactive surface area of fuel samples.



NOTE: (a) Back-scattered electron (BSE) image of a polished section through a fuel particle (bright contrast) from an HDR experiment with a corrosion layer (intermediate contrast) predominantly composed of Na-boltwoodite (ATM-103 HDR 3.7 yr). (b) BSE image of a polished section showing curvilinear features at fuel-grain boundaries, which may result from dissolution along defects. Note fragmentation of grains along boundaries (ATM-103 HDR 3.7 yr). (c) BSE image of a polished section and corrosion layer formed in an LDR experiment (ATM-103 LDR 4.1 yr). (d) BSE image of a polished section with a corrosion layer of uranyl oxyhydroxides formed in a humid-air experiment (ATM-103 humid-air 4.1 yr). Darkest contrast (black) in all images is epoxy.

Figure A1. Back-Scattered Electron Images of Corroded Spent Fuel from ANL Drip Tests

A2. NEPTUNIUM

The dose contribution from Np-237 becomes significant only beyond 10,000 years. Crystal chemical similarities between oxysalts of Np(V) and U(VI) indicate that substantial substitution of Np(V) into some U(VI) corrosion products is possible; however, Np(V) can substitute for U(VI) only if (1) charge-balance mechanisms are available and (2) dissolved Np and U exist together in solution such that they can coprecipitate. Solution data from most studies on the oxidative dissolution of spent UO_2 fuels indicate that Np is released congruently from the UO_2 matrix. Most studies on the behaviors of radionuclides released from dissolving nuclear fuels report only solution analyses, some identify solids, but few analyze those solids for radionuclides. Thus, few experiments allow us to correlate both secondary precipitates and Np concentrations in solution. If U(VI) solids have precipitated, apparent congruent release of U and Np is most readily explained if both elements are controlled by the same solid(s). Whether Np enters into U(VI) solids depends, at least in part, on the solid (which depends in turn on experimental conditions). Some studies have assumed that Np (and other "missing" radionuclides) is retained in fuel-corrosion products; however, without positive identification of specific radionuclides in specific solids, such assumptions remain only speculative. Although, several studies have identified some of the corrosion products formed in spent fuel experiments (e.g., by XRD or SEM), to our knowledge, only the solids formed in the ANL unsaturated tests have been examined for the presence of radionuclides.

Np has been released to solution at nearly constant average rates in both HDR experiments since the first year of reaction (Figure A2). Following initial rapid releases of Np within the first year, average rates of release have been remarkably constant in both HDR experiments, averaging approximately 3.3×10^{-6} and 1.6×10^{-6} fraction-Np per year for ATM-103-HDR and ATM-106-HDR, respectively (Figure A2). Although cumulative release fractions of Np from the two experiments differ by approximately a factor of ten after nearly five years with 0.12% of Np released in ATM-103-HDR, compared with 0.0112% Np released in ATM-106-HDR, nearly 3/4 of the released Np was recovered from the ATM-103-HDR test in the first sampling interval (0.085% of inventory for ATM-103, compared to 0.000002% for ATM-106 in the same sampling interval).

Uranium has shown remarkably similar release behavior to that of Np. Both experiments exhibit similarly early rapid U releases, followed by slow and steady releases since the end of the first year or so (ATM-103 shows a small, but brief increase after about 1.5 years of reaction) (Figure A2). As for Np release in ATM-106-HDR, the vast majority of total U was released in this experiment within the first year (0.017% of U released before the end of the first year, compared with 0.018% total U released after nearly five years). The cumulative release of U in the experiment with ATM-103-HDR has not been quite as constant, but U release has been remarkably steady–and slow–for the past three years. Both HDR experiments exhibit average U release rates similar in magnitude to average Np release rates during the same period; i.e., 2.9×10^{-6} and 1.6×10^{-6} fraction-U per year for ATM-103-HDR and ATM-106-HDR, respectively.

For comparison, releases of Tc in both experiments have been relatively rapid and, since 1.5 years of reaction for ATM-106-HDR, have remained remarkably constant (Figure A3). In fact, the five-year-average Tc release rates from both experiments are approximately equal to

(ATM-106) or exceed (ATM-103) the initial release rates of Np and U during initial rapid releases during the first year.

A2.1 Analytical Detection Limits for Solids Analyses

Because of the importance of accurately determining whether Np and U may have coprecipitated in uranyl alteration products during the corrosion of spent UO_2 fuel, a discussion of measurement uncertainties is provided here. Two techniques were used to measure Np/U molar ratios in solid corrosion products from the ANL drip and humid-air experiments: ICPMS and EELS. ICPMS analyses are obtained from solutions made by dissolving solid samples in nitric acid, whereas EELS analyses are performed on small single crystals (tens of nanometers to a few micrometers across) in a TEM. In both cases a spectrum is recorded, with peaks that correspond to either a characteristic mass (ICPMS) or energy shift (EELS). The data from these two techniques, therefore, represent peak intensities, and confidence about whether a particular peak is observed or not depends on the ratio of peak intensity to background intensity (signal-to-noise ratio). The absolute intensity of a peak represents a concentration. An ICPMS measurement can only be related to concentration if the mass of the original solid sample is known; for example, the concentration (e.g., in ppm) of Np in the solid is given by

$$[Np]_{concentration} = [Np]_{measured}/(\text{sample mass})$$

The solids from the ANL drip tests that were examined by ICPMS were so small that their masses could not be measured accurately on a five-place balance (i.e., to within 10 μg). Thus, the largest uncertainty in determining the absolute concentrations of Np in solid corrosion products from the ANL high drip-rate experiments analyzed by ICPMS is known only with very large uncertainty. On the other hand, the mass (and therefore molar) ratio of Np/U is known with a high degree of precision and accuracy. This is because the concentration ratios are determined thus:

$$[Np]/[U] = \{[Np]_{measured}/(\text{sample mass})\} \div \{[U]_{measured}/(\text{sample mass})\}$$

and the value of the sample mass and therefore, the elemental concentration, is not necessary for accurately knowing the Np/U ratio for the sample.

Whereas it is not possible to determine the actual mass of material being analyzed by TEM-EELS, quantitative interpretation of an observed peak intensity from an EELS spectrum in terms of an elemental concentration requires comparison with the corresponding peak intensity obtained from a "standard" material of known composition (and which has a similar matrix). However, no suitable standard is currently available for TEM-EELS measurements of Np in a U-oxide matrix. In the case of analyzing for Np in DS, EELS peak intensities and intensity ratios for Np and U in DS can be compared with those obtained from unreacted fuel, but the fuel is not an appropriate Np standard because the overall Np concentration of the fuel is only known from ORIGEN-code calculations, which do not apply strictly to specific regions of a fuel grain. Thus, the signal-to-noise ratio for the Np EELS peak is such that it can be stated with confidence that the DS sample contains Np (because the EELS peak is clearly above background), and that the Np concentration in DS is comparable to that of the fuel, but the actual concentration of Np in

DS cannot be quantified with certainty. However, an argument similar to that made for the determination of mass ratios from ICPMS measurements also applies to EELS measurements: knowledge of the actual concentration is not necessary for knowing the Np/U ratio of the solid being analyzed; only the ratios of the peak intensities are necessary for determining Np/U ratios, and peak intensities are known accurately. Thus, Np/U ratios are known with a high degree of confidence for both ICPMS and EELS measurements, although the absolute concentrations are not.

Finally, it is emphasized that the Np/U *ratio* of a compound forms the basis by which it can be inferred whether Np and U have coprecipitated congruently in solid corrosion products. If they have, the Np/U ratio in a corrosion product will be the same as in unreacted fuel, regardless of the actual Np concentration in the solid.

A2.2 Is There a Deficit of Np Released to Solution in the ANL High Drip-Rate Tests on Spent Fuel?

A persistent question that has been raised asks whether reported Np releases in the ANL high drip-rate experiments on spent UO_2 fuels are accurate or whether apparent deficits of Np released to solution are being misinterpreted, since the magnitude of the Np deficit is based on the assumption that Tc release is a reasonably accurate "marker" for the dissolution of the spent fuel matrix. This uncertainty arises because the assumption that Tc is a reliable marker has been called into question. The following discussion is intended to demonstrate that Np releases are lower than the amount expected from congruent release, even if Tc is not a suitable marker of matrix dissolution.

As shown in Figure A2, the release of uranium practically stopped within a year or so after the experiments were initiated. Releases of many elements into solution during early stages of the experiments are commonly explained by the dissolution of very small (< 1 μm) particles (sometimes called fines) with high specific surface areas. In addition, some of the incongruency in the releases of some elements might have been due to the dissolution of corrosion products formed during storage and handling of the fuels used in the experiments. However, once fuel fines and possible pre-existing corrosion products have dissolved, all elemental releases (from those solids) should slow down.

The early disappearance of rapidly dissolved solids cannot explain the dramatic decrease in the rates at which U and Np (and other actinides) are recovered in the leachates. The continued corrosion of the fuel matrix after the first year of reaction is evident from visual observations of the surfaces of fuel fragments in both HDR experiments. At the time when actinide releases to solution slowed dramatically, fuel fragment surfaces were primarily black, possibly with a few incipient precipitates of yellow corrosion products just visible along fragment edges (Finn et al. 1997). Since that time, fuel-fragment surfaces have become increasingly covered by a thickening layer of yellow material. This yellow layer has been identified as being composed of U-bearing solids, primarily Na- and Ca-uranyl silicates (Na-boltwoodite and uranophane-beta). The only source for the uranium required to form these uranyl silicates is the spent fuel matrix. It is, therefore, clear that the matrix has continued to react, with uranium entering into solution to re-precipitate as uranyl silicates. Although the mass of U that has precipitated as U corrosion

products cannot be independently quantified, it is certain that not all U from the spent fuel matrix has been released to solution in either HDR experiment, i.e., U is being "held up." This is undisputed.

Given that the spent fuel matrix is dissolving and has apparently been doing so for the duration of the drip and humid-air experiments, rates of U release to solution for all unsaturated drip and humid-air experiments (measured since the first year) definitely *underestimate* the rate of matrix dissolution. Average U releases to solution must also underestimate the average rates at which elements contained within the fuel matrix are dissolved. These additional elements may be released to solution at various rates, depending on their effective solubilities under experimental conditions. However, any element that is released to solution at or below the rate at which U is released (on a fractional basis) must be somewhere other than in the (now dissolved) fuel matrix or in solution; that is, these elements are "retained" somehow.

By comparing the plots in Figure A2, we can readily see that average rates of release of Np to solution in both HDR experiments have remained closely similar to the average releases of U since the early rapid stage of elemental releases slowed after the first year of reaction. Thus, if it is assumed that Np is contained entirely within the fuel matrix (and is uniformly distributed), Np must be retained to about the same degree as U during the last four years of reaction. In fact, the cumulative fractional releases of U and Np for ATM-106-HDR after nearly five years are comparable (0.018% and 0.011%, respectively) and have continued to follow similar release behaviors during the entire test interval (Figure A4). The Np fractional release for ATM-103-HDR exceeds that of U; however, this is entirely attributable to early rapid release of Np. The relative fractions of U and Np released since the 1.3-year sampling interval are similar for this experiment, with about three times as much of the U inventory being released (0.003% and 0.001% of U and Np, respectively) (CRWMS M&O 2000b). This compares with approximately 2% of the Tc inventory being released over the same interval, a one-thousand-fold difference.

Estimating the actual amount of Np that has reacted is difficult because one needs to monitor the release of an element that is released to solution as the fuel matrix dissolves. The spent fuel matrix is greater than 95% UO_2. If not for the fact that much of the U that enters solution during dissolution of the spent fuel matrix re-precipitates as U(VI) corrosion products, U would be the most appropriate marker of matrix dissolution. In fact, flow-through dissolution experiments can successfully monitor matrix dissolution from U releases because U does not reach saturation with "secondary" phases. In fact, under the conditions of the ANL unsaturated tests, most actinides and many fission products appear to reach saturation and be retained at the fuel, either as solid corrosion products or, perhaps, by adsorption to fuel surfaces or to the Zircaloy cup. Two radionuclides that are released to solution most rapidly are Tc and I, and estimates of the extent of matrix dissolution in the ANL unsaturated tests have used Tc as the "marker" element (Finn et al. 1997). Unfortunately, both Tc and I are known to not be in the fuel matrix but are in separate phases that occur on or near grain boundaries and other defects. The fraction of inventory located in such readily accessible places is uncertain but is probably less than one to perhaps a few percent (Gray et al. 1992). The release of Tc from the ANL unsaturated tests has remained relatively constant for about five years; however, Johnson and Werme (1994) note that constant Tc release is common in fuel experiments (e.g., Forsyth and Werme 1992). They point out that Tc releases from fuel may not correspond well with dissolution of the fuel matrix but is

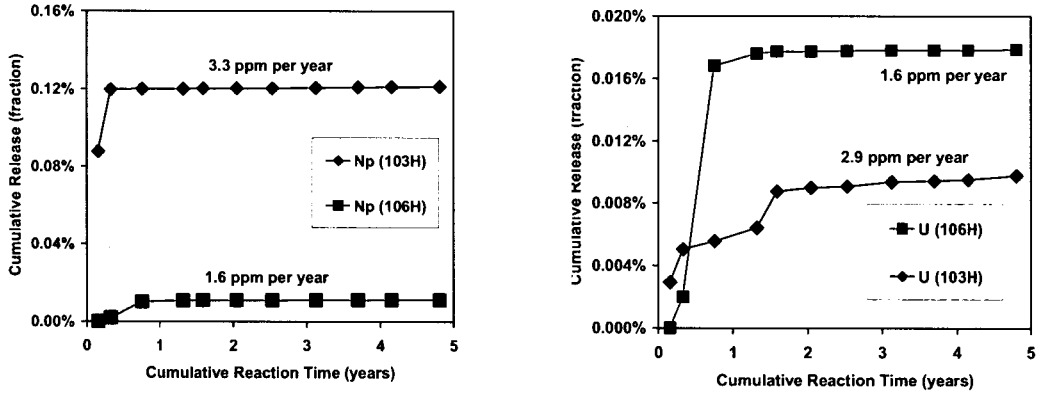
controlled by the kinetics of the oxidative dissolution of ε-Ru particles. In fact, Finn et al. (1997) demonstrated that ε-Ru particles are reactive under the test conditions at ANL, although the assumption is that ε-Ru particles can only react when the matrix surrounding them has dissolved. However, ε-Ru particles embedded within the fuel matrix may be available to corrosive attack by the ability of water to penetrate along defect and interconnected fission gas bubbles within an otherwise minimally corroded matrix (Johnson and Werme 1994).

There is, therefore, significant concern that Tc can overestimate the extent of dissolution of the spent fuel matrix, and it is useful to compare the releases of Tc with those of Np and U for the HDR experiments. Technetium is assumed to derive entirely from ε-Ru particles that react upon exposure following dissolution of the surrounding spent-fuel matrix, and because it is highly soluble, Tc release is used as a marker for the dissolution of the spent fuel matrix. The only possible alternative explanation for releases of Tc that are much higher than U and Np is that essentially all Tc is being derived from dissolution of ε-Ru particles along grain boundaries. This seems an unlikely scenario, although it must remain as a working hypothesis. It is true that Tc-bearing epsilon particles decorate grain boundaries in ATM-103 fuel (Guenther et al. 1988), and SEM examinations of one disaggregated spent-fuel fragment indicate substantial groundwater attack along grain boundaries and along defects that intersect grain boundaries (Finch et al. 1999, Fig. A1). This suggests that reported Tc releases may, in fact, overestimate the extent of matrix dissolution, a suggestion that is also supported by the apparent slowing of Tc release in the ATM-103-HDR experiment during the last three years (Figure A3). On the other hand, estimates of the reaction-layer thicknesses on several reacted fuel particles that have been examined by SEM offer some support that the approximate magnitude of Tc release is similar to the magnitude of matrix dissolution. Reaction-layer thicknesses appear to represent at least some degree of general corrosion through the outer surfaces of fuel fragments. The thickness of the original fuel that may have dissolved via general corrosion is difficult to estimate with much precision; however, thickness of the reaction layers in all experiments (drip and humid-air) are comparable and range between approximately 5 and 50 μm. Thinning of reaction layers near the corners of particles suggests some degree of expansion, and the thinnest regions of reaction layers at these corners are commonly about 2–3 μm thick on particles that had reacted for 3.7 years. If it is assumed that 2.5 μm represents a minimum estimate for the thickness of the fuel matrix that has dissolved from fragment surfaces, then after approximately 3.7 years of reaction, approximately 0.5% of the initial mass of fuel would have dissolved via general corrosion.

So even the lowest reasonable estimate of the mass of fuel reacted, ~0.5%, is greater than the total fraction of Np that has been released in ATM-103-HDR (i.e., 0.12%), and the conclusion that Np is being retained to approximately the same degree as U is valid. Furthermore, whereas the retention of Np or U cannot be quantified at this time, a substantial fraction of U is known to be retained in U-bearing corrosion products on the surfaces of fuel fragments. The obvious inference is that a substantial fraction of Np is being retained as well.

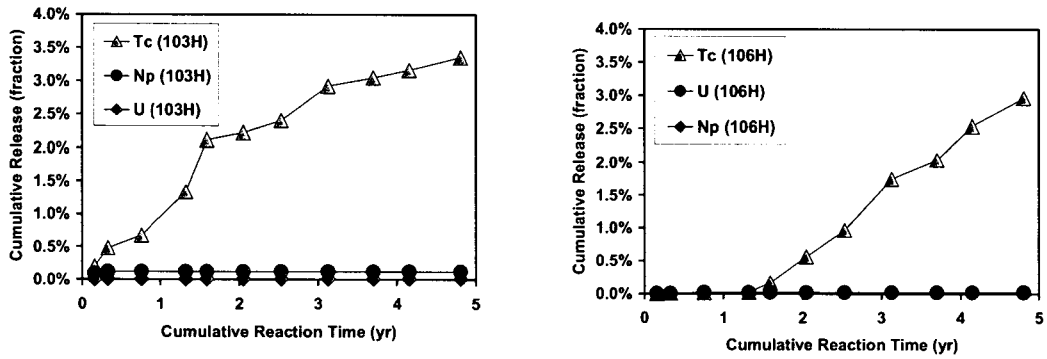
Figure A5 illustrates the Np/U ratio in solution for the LDR and HDR tests. This ratio has remained close to the value in the fuel with notable exceptions during the first two sampling intervals when Np release exceeded U release on a fractional basis, and during the 3.7-year sampling interval when U releases were somewhat low but Np releases remained nearly constant

(cf. Figure A4). Figure A6 compares the fractional releases of Np with those of Tc and U for the HDR and LDR tests. Although there is some scatter in the HDR data, U and Np releases plot near the line that indicates congruent release; congruency for these two elements is even clearer for the two LDR tests. Np is clearly retained in the HDR tests compared to Tc, as well as for the LDR test on ATM-106 (Figure A6); however, Np and Tc are released with nearly perfect congruency for LDR test for ATM-103. Cumulative fractional releases of Np and U are illustrated for the LDR and humid-air tests in Figure A7. The releases in these tests, especially for the humid-air tests, are exceedingly low, and releases to solution may well be transport-limited.



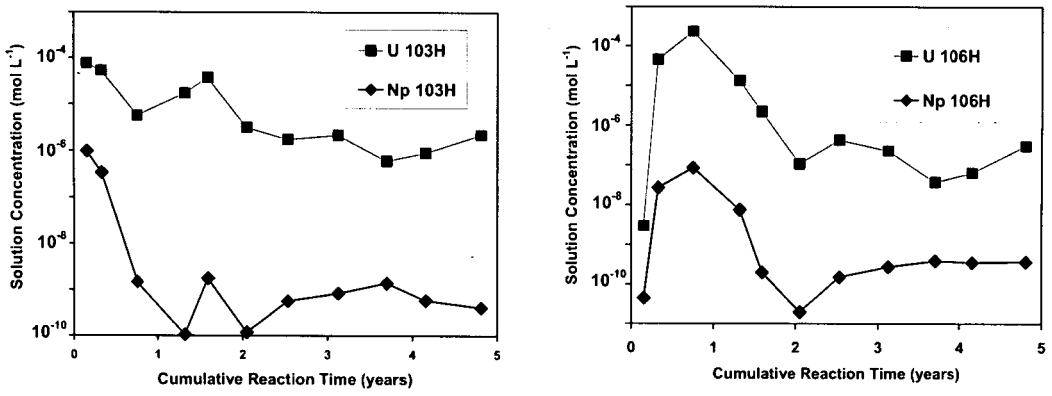
NOTE: Cumulative releases of U and Np in HDR tests, illustrating similar release rates for both elements (Figure A4). Release rates calculated from least-squares fit to approximately collinear data (i.e., by ignoring initially steep slopes in each plot).

Figure A2. Cumulative Releases of U and Np in HDR Tests



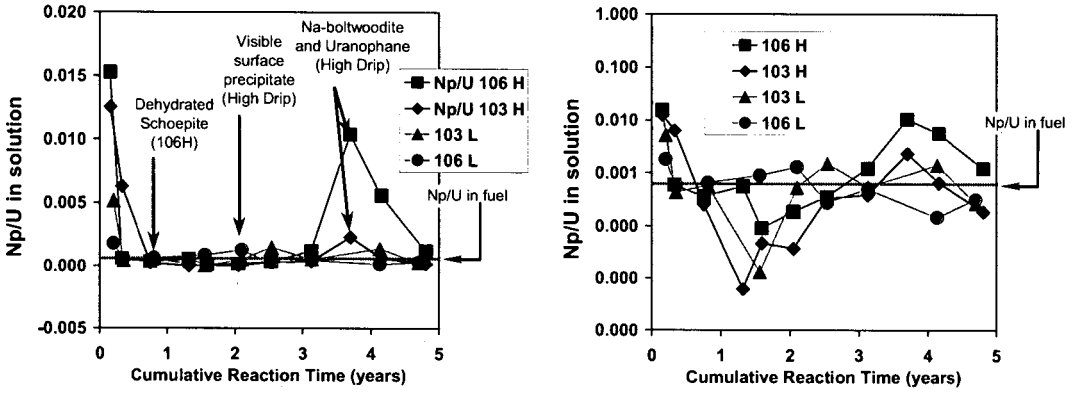
NOTE: Cumulative U, Np, and Tc release as total fraction of inventory, illustrating large gap between Tc releases and releases of U and Np.

Figure A3. Cumulative U, Np, and Tc Releases in ANL Drip Tests



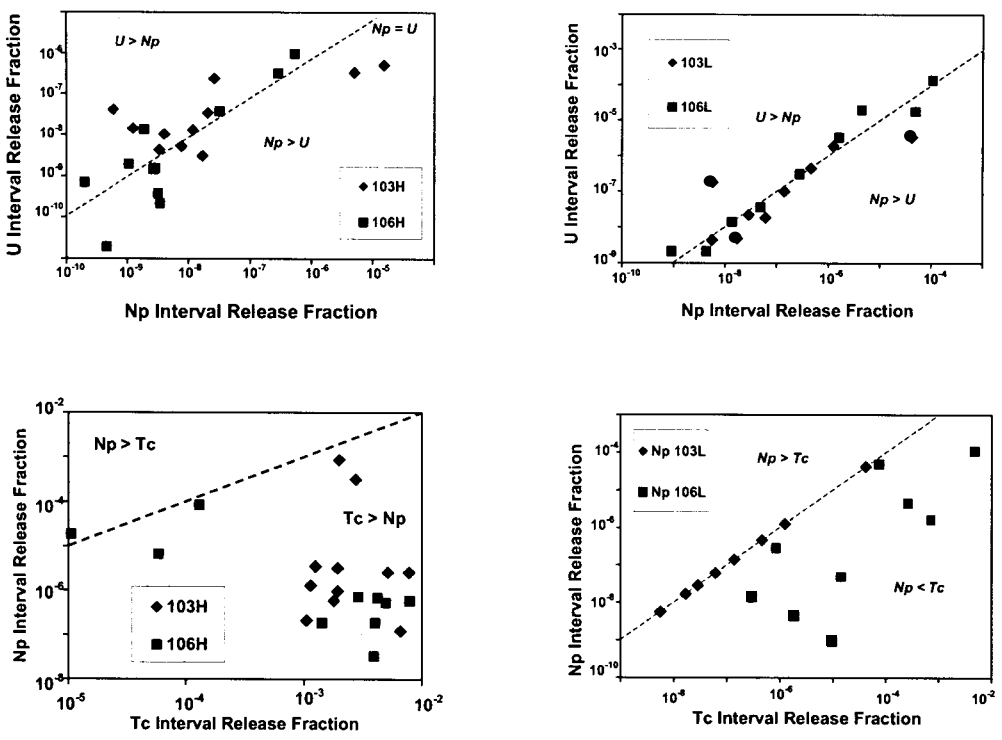
NOTE: Molar concentrations of Np and U in solution, ANL HDR Tests (left, 103H; right, 106H)

Figure A4. Molar Concentrations of Np and U in Solution, ANL HDR Tests



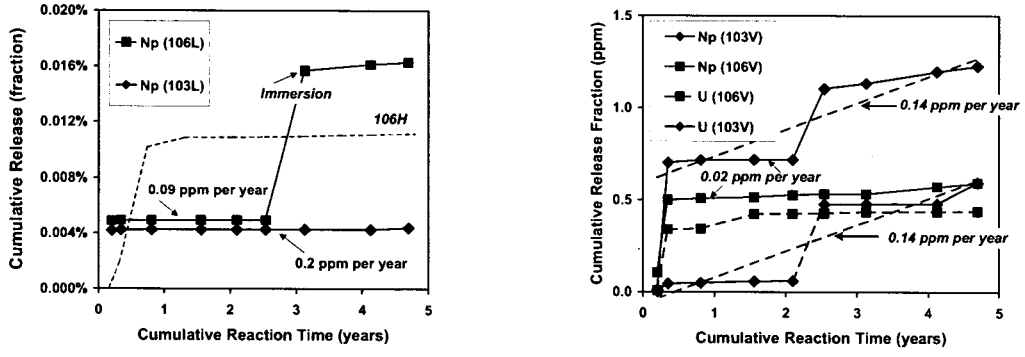
NOTE: Molar ratios Np/U in solution for all ANL Unsaturated Tests. Labels indicate significant observation at some sampling intervals (see text). Left, linear plot; right, logarithm illustrating changes not evident on the linear plot.

Figure A5. Molar Ratios Np/U in Solution for All ANL Unsaturated Tests



NOTE: Comparisons of U, Np, and Tc releases in HDR (left) and LDR (right) tests. Dashed line corresponds to congruent release (i.e., equal fractions of inventory). Np and U show approximately congruent release (top), whereas Np is released incongruently with respect to Tc in all but one LDR test (103L) (bottom).

Figure A6. Comparisons of U, Np, and Tc Releases in ANL HDR and LDR Tests



NOTE: "Immersion" corresponds to a brief immersion of reacted fuel fragments in the leachate during sampling. Similar jump in 103 humid-air tests is not due to a similar effect and is unexplained.

Figure A7. Np Releases in ANL LDR and Humid-Air Tests

A3. TECHNETIUM

The fission products Mo, Tc, Ru, Rh, and Pd are incompatible in the UO_2 structure, and they exsolve from UO_2 to form particles of the five-metal alloy known as ε-Ru. Microscopic examinations of unreacted LWR fuels reveal that ε-Ru particles commonly decorate grain boundaries and other defects (Thomas et al. 1993). It is currently unknown what proportion of ε-Ru particles are readily accessible to groundwater attack during oxidative corrosion. One possibility is that ε-Ru particles cannot react with groundwater until the adjacent UO_2 matrix dissolves. Under anoxic or reducing conditions, Tc is released from fuels approximately congruently with U (Stroes-Gascoyne 1992; Grambow et al. 1996). However, under these conditions, Tc may be oxidized from the metal to Tc(IV), which may re-precipitate as insoluble TcO_2. Also, ε-Ru particles may not be as reactive under these conditions as in more oxidizing environments.

Finn et al. (1997) demonstrated that ε-Ru particles are reactive under the HDR-test conditions, releasing Mo and Tc when exposed to dripping groundwater in the ANL unsaturated drip tests. Finn et al. (1997) explained the reactivity of ε-Ru particles by the accumulation of radiolytic products within thin water films condensed on fuel surfaces and along grain boundaries that have been penetrated by water, leading to relatively aggressive oxidizing conditions. Tc is released to solution in ANL drip tests faster than all elements except I-129. Both fuels in the HDR tests released approximately 3% of their Tc inventories to solution within about five years (Figure A8). Tc releases from low drip-rate and humid-air experiments are substantially lower than those in HDR experiments, but equal or exceed other elements, except I. UO_2 matrix dissolution rates in HDR experiments, calculated by assuming that 3% of the UO_2 matrix has dissolved after five years, appear to be, within the uncertainties of extrapolating to relevant conditions, comparable to dissolution rates measured in single-pass flow-through experiments on spent UO_2 fuels exposed to carbonated water (Gray and Wilson 1995).

Flow-though experiments are designed to measure "intrinsic" dissolution rates, which are considered to represent maximum rates of fuel dissolution. Therefore, based on Tc release, spent fuel exposed to dripping groundwater at 90°C (conditions that may exist in a repository) appears to dissolve at or near the intrinsic dissolution rate, despite the existence of a thickening layer of corrosion products formed on the surface.

The conclusion that corroded fuel continues to dissolve as fast as fuel in flow-through experiments suggests that corrosion products do little or nothing to inhibit the oxidative dissolution of fuel. This conclusion seems contrary to results from some electrochemical studies of UO_2 and spent-fuel corrosion, which indicate that surface precipitates can "poison" reactive surface sites on UO_2. Uninhibited fuel-dissolution rates in groundwater also seem contrary to certain batch and flow-though experiments that indicate a reduction in *apparent* dissolution rates of UO_2 and spent fuels exposed to simulated groundwaters with dissolved Ca, Mg and Si. Most of these experiments use large volumes of water in which radiolytic species might diffuse or be washed away from the surface of dissolving fuel, and the accumulation of radiolytic species in

thin water films on fuel surfaces has been suggested as an explanation for the apparent rapid dissolution of fuel and ε-Ru particles in HDR experiments (Finn et al. 1997).

Microscopic examinations of corroded fuels from drip experiments with water-injection rates that differ from each other by an order of magnitude demonstrate that the degree of general corrosion is independent of injection rate (fuels corroded in humid-air experiments without added groundwater also appear corroded to the same degree as fuels in drip experiments). Micrographs also indicate that fuel dissolution has occurred along fuel-grain boundaries in HDR experiments, a feature not evident from microscopic examinations of fuel fragments from experiments conducted at LDR. Releases of Tc in LDR experiments are only about one hundredth of Tc releases in HDR experiments. However, fuel fragments from one LDR experiment that were immersed in low ionic strength groundwater for several minutes released nearly 1% of their Tc inventory, a result that suggests that limited flow paths explain one-third of the apparent Tc deficit in LDR experiments compared with HDR experiments. The remaining Tc released in HDR experiments (2% of inventory) may, therefore, come from ε-Ru particles along fuel-grain boundaries.

A few batch experiments with small water volumes (0.5 mL) and powders of single fuel grains (0.2 g) have also been conducted at ANL. These experiments recreate thin films of water similar to those believed to exist on fuel fragments in drip and humid-air experiments. Virtually all the grain boundaries are exposed to groundwater in these batch experiments, so grain boundaries account for essentially all of the reactive surface area. Also, total surface areas of fuel powders in batch experiments are comparable to initial reactive surface areas in drip experiments. Early results from these batch experiments (29, 43, and 57 days) demonstrate that Tc is released as fast or faster from fuel powders for which grain boundaries are fully exposed than from fuel fragments in the drip experiments (Figure A8). This is consistent with a significant proportion of Tc being released from ε-Ru particles located along grain boundaries.

Technetium has not been reported in secondary products from any studies of fuel corrosion, suggesting that, under oxidizing conditions, essentially all Tc released from spent fuel remains in solution. EELS spectra of the uranyl silicate, β-uranophane, from a HDR test at ANL reveal only a trace amount of Tc in this phase, close to the detection limit for EELS (Finn et al. 1998).

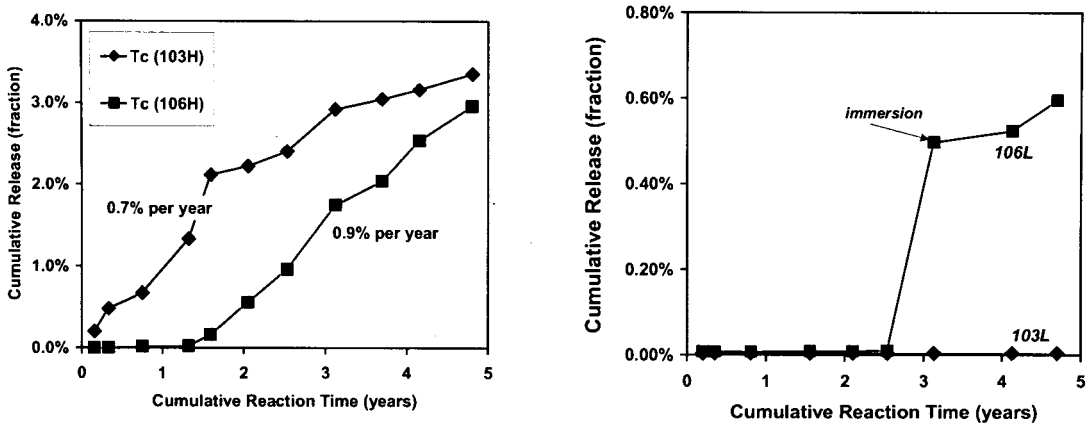
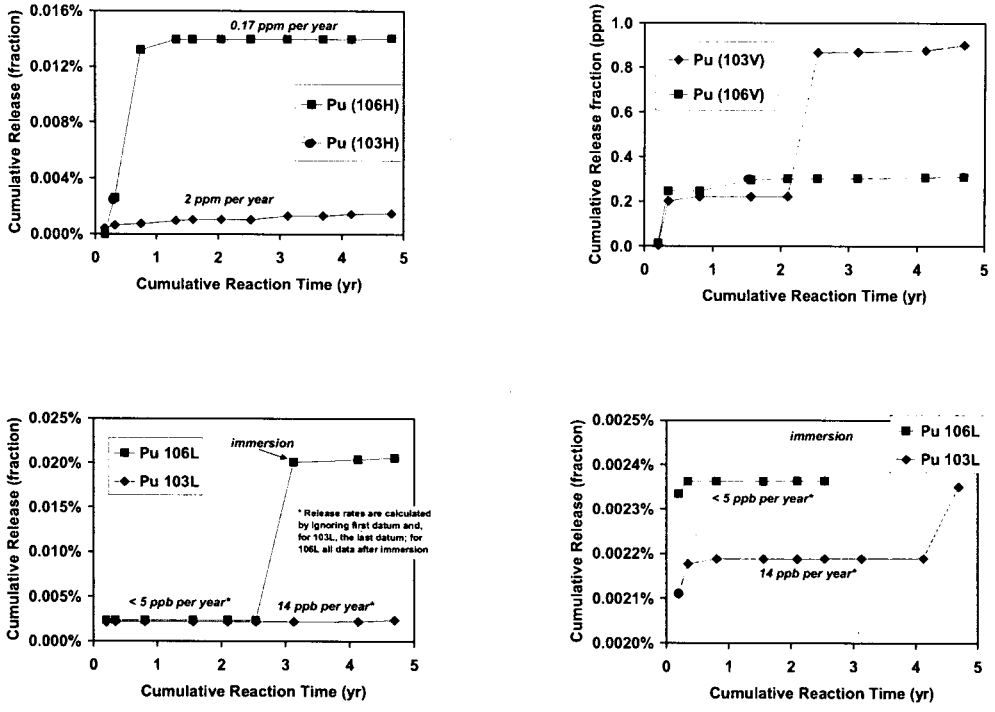


Figure A8. Cumulative Tc Release as Fraction of Inventory in HDR Tests and LDR Tests at ANL

A4. PLUTONIUM

After early releases that may reflect rapid dissolution of fines, Pu has been almost entirely retained. Releases to solution after one year are measured in terms of parts per million per year, although some deviations are apparent (Figure A9). One such excursion is apparent for the LDR test on ATM-106 when, at the 3.1 year sampling interval, the sample was immersed for a few minutes, releasing most of the Pu released in this test. A similar excursion, but of much smaller magnitude, is apparent for the humid-air test on ATM-103 (Figure A9), but this is not well understood.

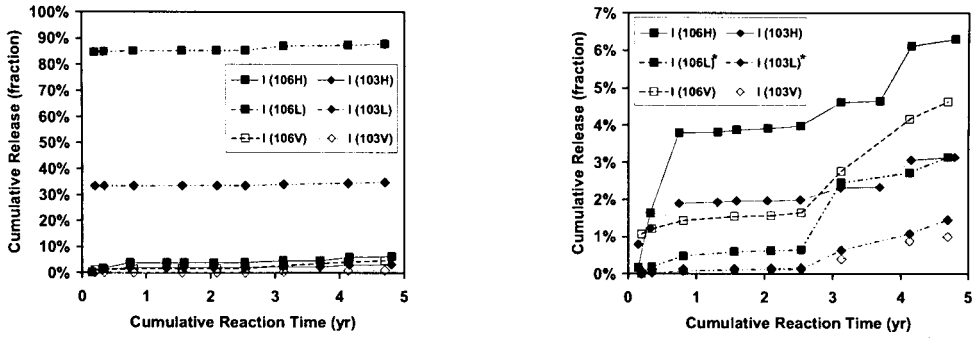


NOTE: Cumulative releases of Pu (fraction of inventory) for all ANL unsaturated tests (HDR, top left; humid air, top right; LDR bottom). Release rates are calculated by at least square fit to the data, as for Figure A2. Release rates are calculated for both LDR tests by ignoring first datum and for 103L, the last datum; for 106L, all data after immersion are ignored. Figure at lower right is an expanded view of that on the lower left.

Figure A9. Cumulative Releases of Pu (fraction of inventory) for all ANL Unsaturated Tests

A5. IODINE

Iodine exhibits essentially complete release, without evidence of retention in corrosion products (Figure A10). Qualitatively, I release in HDR and humid-air experiments is comparable to that of Tc release in both HDR tests. Although the initial reported releases for I from the two LDR tests is suspect, considering the large fractional releases during the first sampling interval, I releases in the LDR tests after the initial datum have been consistent with the other test types and are comparable to Tc releases in HDR tests. A potentially large fraction of I is believed to be located along grain boundaries, as for Tc. Both these radionuclides may, therefore, be useful indicators of grain-boundary penetration by water; however, it is uncertain to what degree their releases reflect matrix corrosion.

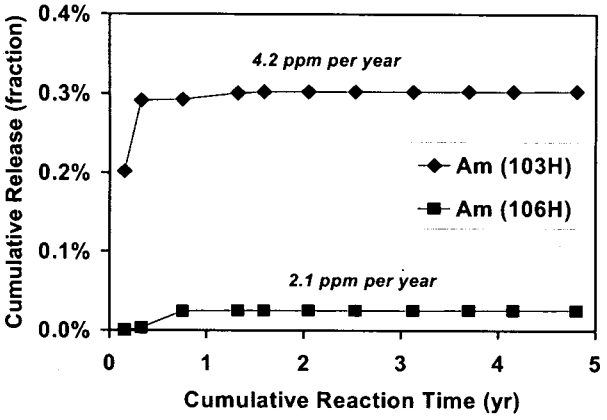


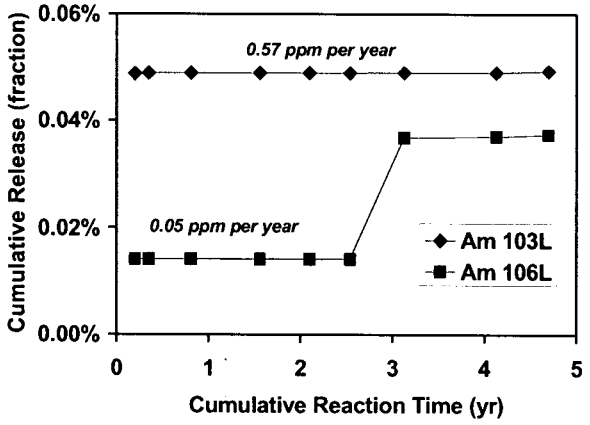
NOTE: Data at left are plotted by ignoring the first data points for both HDR tests in order to demonstrate similar behaviors since that time. Note that release rates for I-129 show little or no dependence on drip rate.

Figure A10. Cumulative Releases of I (fraction of inventory) for all ANL Unsaturated Tests

A6. AMERICIUM

There is strong evidence for retention in the ANL unsaturated tests. Figure A11 illustrates the cumulative releases of Am for the three test series, HDR, LDR and humid air. After the first year, releases have been consistently low for all tests, with fractional releases averaging approximately 4 ppm per year or less in the two HDR tests, less than 1 ppm per year in the LDR and humid-air tests. An Am-bearing solid has been identified, and it is a poorly crystalline residue that has precipitated on surfaces of UO_2 fuel grains in the drip experiments. In addition to Am, this solid residue contains U, Pu, lanthanides and Zr.





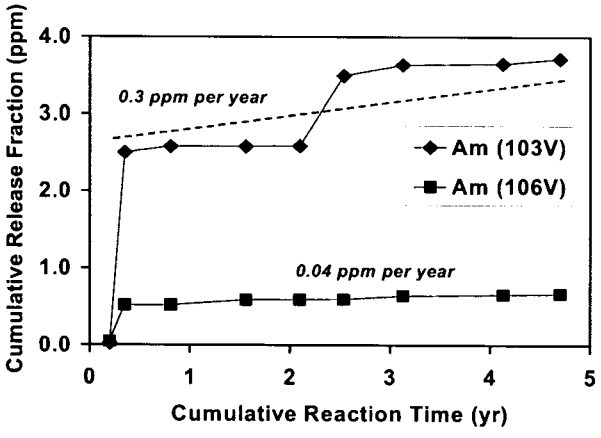


Figure A11. Cumulative Releases of Am in Unsaturated Tests at ANL

A7. SELENIUM

There are no data.

A8. PROTACTINIUM

There are no data.

A9. CARBON

There are no data.

ATTACHMENT II

PARAGENESIS OF URANIUM MINERALS IN NATURE

B1. OXIDATIVE CORROSION OF URANINITE IN NATURE

Frondel (1958) described the natural oxidative alteration of uraninite as follows: partial oxidation of U^{4+} to U^{6+} without decomposition of the uraninite structure, although the uraninite commonly displays a change in color from black to dark brown and a change in luster from submetallic to "dull or pitchlike." Frondel (1958) noted that, at this stage and as alteration progressed, there was commonly "some degree of hydration, and uranium and especially thorium may be [lost to groundwater]" relative to Pb. Further alteration, which Frondel (1958) considered as a "second type," resulted in the complete conversion of uraninite into U(VI) minerals, the compositions of which depended primarily on the composition of the local groundwaters.

By analogy with synthetic UO_2, several authors have proposed that the early stages of oxidation and alteration of uraninite proceed through intermediate uranium oxides such as U_3O_7 or U_3O_8. However, these oxides are unknown in nature. Whether these oxides occur as thin (~1 μm) layers on uraninite has been proposed but has never been demonstrated (Janeczek et al. 1993). The formation of hydrated, X-ray amorphous U^{6+} hydroxides from uraninite has been postulated, and given names such as "hydronasturan" and "urghite" (Finch and Murakami 1999), but these are poorly described and not considered valid species.

The initial oxidation and subsequent dissolution of uraninite has not been studied in detail, although the oxidation, dissolution, and corrosion of synthetic UO_2 (and UO_2 nuclear fuels) have been examined in great detail (Casas et al. 1993a; 1993b; 1993c; Forsyth and Werme 1992; Shoesmith and Sunder 1992; Gray et al. 1992; Einziger et al. 1992; Bruno et al 1992; Matzke 1992; Wronkiewicz et al. 1992; 1996). Because of the structural similarity of UO_2 to that of uraninite, the oxidation and geochemical behavior of uraninite has often been assumed to be identical to that of synthetic UO_2 (Parks and Pohl 1988). This is probably true to a limited degree, but the presence of elements besides U and O can affect the alteration behavior of uraninite (Grandstaff 1976), of irradiated (spent) UO_2 fuels (Thomas et al. 1993; Einziger et al. 1992), and of doped uranium oxides (Thomas et al. 1993).

The slow diffusion of oxygen into the UO_2 structure necessitates that most oxidation studies of UO_2 be performed at elevated temperatures (~150 to > 800°C). [The diffusion coefficient of oxygen in UO_2 at 25°C is on the order of 10^{-23} to 10^{-25} $m^2 \cdot s^{-1}$ (Grambow 1989).] Even slow kinetics of oxygen diffusion may be unimportant over geologic time spans, because interstitial sites in ancient uraninites probably become saturated with oxygen in all but the most reducing environments. The question of whether uranium oxides that form in nature, especially during weathering, resemble those synthesized at elevated temperatures, has been the subject of some debate (e.g., Janeczek et al. 1993).

The mechanisms by which synthetic UO_2 oxidizes in water may differ from those by which it oxidizes in dry air. For example, Grambow (1989) reports that the activation energy for weight

gain in water is approximately one-third of that in dry air (21-42 $kJ \cdot mol^{-1}$ in water versus ~110 $kJ\ mol^{-1}$ in air). X-ray photo-electron spectroscopy has shown that the earliest stages of aqueous oxidation of synthetic UO_{2+x}, prior to dissolution, probably mimic those of air oxidation (Shoesmith and Sunder 1991). Whether this is true for uraninite is uncertain, but recent studies indicate that the oxidation pathway of impure UO_2 (i.e., Gd-doped UO_2) differ from that of pure UO_2 (Thomas et al. 1993; Einziger et al. 1992). Inferring the oxidation and corrosion behavior of uraninite from that of pure UO_2 must, therefore, be done carefully. Despite potential discrepancies, however, the oxidation of synthetic UO_2 is a useful analogue for the oxidation behavior of uraninite, and studies on the low temperature oxidation of UO_2 in aqueous solutions provide insight into crystal chemical and micro-structural changes occurring in uraninite during oxidative corrosion (Wronkiewicz et al. 1996).

B2. REPLACEMENT OF URANINITE BY URANYL OXYHYDROXIDES

Finch and Ewing (1992) described a simplified reaction for the early-stage oxidative corrosion of uraninite at Shinkolobwe (all U is retained in solid uranyl oxyhydroxides, schoepite and vandendriesscheite):

$$U^{4+}_{0.48}U^{6+}_{0.39}(Y,Ce)_{0.02}Pb_{0.09}Ca_{0.02}O_{2.27} + 0.24O_2 + 1.57H_2O + 0.10H^+ \Rightarrow$$
$$0.03375[(UO_2)_8O_2(OH)_{12}](H_2O)_{12} + 0.06Pb_{1.5}[(UO_2)_{10}O_3(OH)_{11}](H_2O)_{11} + 0.02Ca^{2+} + 0.02(Y,Ce)^{3+}.$$

Because of the uncertain role of Na and K in the structure of uraninite, these two elements have been ignored in the above reaction.

The above reaction represents a simplified view of the natural system and is written without dissolved silica or carbonate. Unless silica and carbonate concentrations are considerably elevated, however, these species do not play an important role in the earliest stages of uraninite corrosion; thus this reaction reflects the observed initial corrosion of uraninite. The minerals on the right, schoepite and vandendriesscheite, are the corrosion products observed in contact with altered uraninites from numerous occurrences. This is not to suggest that dissolved constituents in groundwater do not affect the corrosion of uraninite. Silica- and carbonate-bearing waters alter the early-formed uranyl oxyhydroxides, resulting in observed paragenetic relationships. It is believed that kinetic factors best explain why uranyl oxyhydroxides form early and are subsequently altered to uranyl silicates. This may not be quite correct, but much remains unknown about the conditions of formation for uranyl oxyhydroxides and other uranyl minerals.

The following paragenetic sequence is most common at weathered uraninite deposits:

1. Dissolution of uraninite and precipitation of hydrated uranyl oxyhydroxides, Pb-poor and Pb-free

2. Alteration of the early-formed hydrated uranyl oxyhydroxides to uranyl silicates and curite, removing dissolved Si from groundwater and preferential loss of uranium. Some uranium precipitates within voids and fractures as the uraninite continues to dissolve, but

most migrates to the exterior of the uraninite to precipitate as a rind of hydrated uranyl oxyhydroxides, ianthinite, schoepite, and becquerelite.

3. The replacement of hydrated uranyl oxyhydroxides in the corrosion rind repeats the sequence.

B3. URANYL-MINERAL PARAGENESIS

Uranyl Oxy-hydroxides–The uranyl oxyhydroxides form in U-rich aqueous solutions and develop early during the oxidation and corrosion of uraninite-bearing ore deposits, most commonly at or near the surface of corroded uraninite. Alteration of the uranyl oxyhydroxides is ubiquitous, and the question of their long-term stability under different environmental conditions is pertinent to understanding the often-complex assemblages of uranyl minerals. The formation and alteration of the uranyl oxyhydroxides partially determine reaction paths for the alteration of uranium ore deposits in an oxidizing environment, and they help control the dispersion or fixation of uranium in nature.

The uranyl oxyhydroxides may be represented by the general formula:

$$M_n[(UO_2)_xO_y(OH)_z](H_2O)_m \, .$$

M represents divalent cations, commonly Ca^{2+}, Pb^{2+}, Ba^{2+}, and Sr^{2+}, although K^+-bearing phases are also known. Uranyl oxyhydroxides form early during the alteration of uraninite. Therefore, these minerals play an important role in the early paragenesis of uranyl minerals and influence the alteration of uranium ore deposits under oxidizing conditions. The alteration of uranyl oxyhydroxides is ubiquitous, largely owing to dehydration as well as interactions with carbonate-, silica-, and phosphate-containing groundwaters.

Uranyl oxyhydroxides are stable in groundwaters in the absence of aqueous ligands such as CO_3, SO_4, and VO_4. However, where uraninite (and UO_2) are undergoing rapid oxidative dissolution, local U concentrations can quickly reach saturation with respect to uranyl oxyhydroxides. These minerals apparently precipitate readily from solution, whereas uranyl silicates apparently do not, even where dissolved Si concentrations should be adequate to stabilize their formation. Thus, uranyl minerals formed from U-saturated groundwaters commonly alter to the more insoluble uranyl silicates. This paragenesis was dramatically demonstrated experimentally by Wronkiewicz et al. (1992; 1996) where unirradiated UO_2 pellets were reacted with Si-saturated water at 90°C. The reasons for kinetic constraints on the precipitation of many uranyl minerals are uncertain. Precipitation of uranyl oxyhydroxides may require little atomic rearrangement of uranyl solution complexes, compared with atomic rearrangements required to precipitate uranyl silicates or phosphates. Most uranyl carbonate and uranyl sulfate solution complexes might be expected to precipitate as minerals without much atomic rearrangement, especially many uranyl tricarbonates, the structures of which commonly contain the uranyl tricarbonate ion, $(UO_2)(CO_3)_3^{4-}$, which is identical to the solution complex. However, uranium concentrations required to precipitate most uranyl carbonates and sulfates are much higher than for uranyl oxyhydroxides (with the exception of rutherfordine, which is relatively insoluble). Uranyl

oxyhydroxides may, therefore, have the lowest solubilities among those minerals for which precipitation kinetics do not present significant barriers to formation.

The uranyl oxyhydroxides, schoepite, ianthinite, vandendriesscheite and fourmarierite form early within the voids formed by dissolution. These minerals incorporate U and Pb from the uraninite and H_2O and oxygen from groundwater. As the dissolution of uraninite progresses, fractures and gaps formed by dissolving uraninite become conduits for the penetration of groundwaters. Interaction of groundwaters with early-formed uranyl oxyhydroxides results in their replacement by uranyl silicates and carbonates and by Pb-enriched uranyl oxyhydroxides.

Uranyl Silicates–Uranyl silicates are moderately insoluble in most natural groundwaters. Because of the ubiquity of dissolved Si in most groundwaters, uranyl silicates are the most abundant group of uranyl minerals. Uranophane, the most common uranyl mineral and possibly the most common U mineral after uraninite, precipitates from near neutral to alkaline groundwaters that contain dissolved Si and Ca. When exposed to low ionic strength meteoric waters (low carbonate and pH below ~7), uranophane may be replaced by soddyite (Finch 1997), a phenomenon also observed in experimental dissolution studies of uranophane in deionized water (Casas et al. 1994). Sklodowskite is observed being replaced by kasolite where radiogenic Pb that accumulates within the sklodowskite reaches sufficient levels to be exsolved and reprecipitated as kasolite. This appears to be independent of changes in water compositions but rather a result of the durability of sklodowskite, which persits long enough to accumulate radiogenic Pb in substantial amounts (Isobe et al. 1992). Replacement of other uranyl silicates has not been documented, a reflection, perhaps, of their durability. Uranophane and soddyite can persist in some environments for more than one hundred thousands years (Finch et al. 1996).

Several especially Si-rich minerals are known, the most important being the weeksite group with a U:Si ratio of 1:3. These minerals are relatively rare and occur, like uranyl di- and tri-carbonates and uranyl sulfates, where evaporation rates are relatively high. Their formation in arid environments probably reflect evaporation of Si-rich waters of relatively high pH in which Si concentrations can reach quite elevated values. Unlike the uranyl carbonates and silicates with similar parageneses, however, the weeksite-group minerals do not seem to dissolve readily upon re-exposure to low ionic strength waters. Like uranophane, when exposed to carbonate-free waters, they may lose some Ca and Si preferentially, altering to more U-rich minerals such as uranophane or soddyite. In more alkaline waters, they may lose U preferentially, altering to amorphous or microcrystalline silica.

Uranosilite is a very unusual mineral, with U:Si of 1:7. No data are available on its stability or solubility, although it is relatively insoluble in weak hydrochloric acid (Walenta 1983). Uranosilite is known from only one locality, the Menzenschwand U mine in Germany, where it occurs intimately intergrown with the uranyl peroxides studtite and metastudtite (Walenta 1983). The conditions necessary for the precipitation of uranosilite are unknown, although the fact that it occurs with studtite suggests it may be stable only in highly oxidizing environments. Dehydration does not affect the structure.

Uranyl Carbonates–Uranyl di- and tri-carbonates tend to form only where evaporation is high. Most of these minerals tend to be ephemeral, dissolving readily when re-exposed to low ionic

strength waters. Solution uranyl carbonate complexes are quite stable and are probably the most important solution complexes responsible for U migration in oxidizing environments. They are important in near neutral to alkaline waters (pH > 7). Thus, precipitation of uranyl carbonate minerals usually reflects evaporation of alkaline waters. An exception is the formation of some monocarbonates, rutherfordine, joliotite, blatonite, urancalcarite, and wyartite. These minerals probably precipitate from low ionic strength waters where (at least local) pCO_2 values are elevated, relative to atmospheric values ($pCO_2 > 10^{-3.5}$ atm). Elevated pCO_2 most commonly results from organic respiration, transpiration, and decomposition. Such waters tend to have relatively acid pH values (pH < 6 or 7). Unlike the uranyl di- and tri-carbonates, the uranyl monocarbonates are relatively insoluble. The solubility of rutherfordine, for example, is comparable to that of schoepite (Grenthe et al. 1992), and rutherfordine may persist in some environments for several tens to hundreds of thousands of years (Finch et al. 1996). Also, the recent discovery that two naturally occurring uranyl monocarbonates incorporate U(V) suggests that similar phases may be able to incorporate Np(V) without difficulty. The formation conditions for wyartite are poorly understood; however, it occurs with rutherfordine, ianthinite (another mixed-valence uranyl mineral), and other uranyl oxyhydroxides. Wyartite II is apparently a dehydration product of wyartite and may not form directly from solution.

B3.1 Other Uranyl Minerals

Uranyl Sulfates–Uranyl sulfates are important only where sulfides are being oxidized, providing dissolved sulfate to groundwater that can complex with UO_2^{2+} to form stable uranyl sulfate complexes in solution. Waters where uranyl sulfates are important tend to be somewhat acidic, with pH values below approximately 6 (Garrels and Christ 1959; Finch and Murakami 1999). Like the uranyl di- and tri-carbonates, uranyl sulfates are ephemeral and redissolve upon exposure to low ionic strength waters.

Uranyl Selenites–Uranyl selenites exhibit similar parageneses to those of uranyl sulfates and uranyl arsenates, occurring in the vicinity of where Se(II)-bearing sulfide minerals are undergoing oxidation. Selenium in all known uranyl selenites occurs as Se(IV), in the form of the selenite ion, SeO_3^{2-}. No data are available on the solubilities of these minerals, only a few of which are known. Given the chemical similarities between S(VI) and Se(VI), it seems likely that most uranyl selenates may be relatively soluble; however, this cannot be stated with any certainty. As noted above, radiogenic Se from corroded spent fuel will probably not reach concentrations sufficient to precipitate uranyl selenites, and minor Se may replace Si in uranyl silicates.

Uranyl Phosphates–Uranyl phosphates help limit U concentrations in many natural waters. They generally have solubilities below those of the uranyl silicates and are associated with a wide range of weathered uranium deposits. Uranyl phosphates are known to precipitate from groundwater where U concentrations are in the range 10^{-8} to 10^{-9} mol/kg (Dall'aglio et al. 1974), values that approach the solubility of uraninite in reducing environments. Uranyl phosphates are commonly found well removed from any uranium source (Frondel 1956; 1958). In groundwaters where log $\{[PO_4^{3-}]_T/[CO_3^{2-}]_T\} > -3.5$, uranyl phosphate complexes predominate over uranyl carbonate complexes (Sandino and Bruno 1992). Apatite controls the phosphate concentrations in many natural waters, keeping phosphate activities below 10^{-7} mol/kg^{-1} above pH = 7 (Stumm

and Morgan 1981). Synthesis experiments show that the phosphate concentrations necessary to precipitate uranyl phosphates can be quite high [on the order of 10^{-2} mol/kg (Sandino 1991; Markovic and Pavkovic 1983)]. Uranyl phosphates are typically most stable below approximately pH 5, where apatite solubility increases.

Phosphate is a ubiquitous anion in surficial environments. Dissolved phosphate concentrations in most river waters are on the order of 20 ppb, and dissolved U concentrations are typically less than 0.3 ppb (Holland 1978), suggesting that most rivers are well below saturation with respect to uranyl phosphates. Sorption of U onto Fe and Mn oxyhydroxides and clay minerals is an important mechanism influencing U migration in natural waters. Groundwater concentrations of Si may also influence U adsorption if dissolved Si competes with U for surface sites on goethite, as demonstrated experimentally by Gabriel et al. (1998). The chemical forms of U adsorbed on various minerals have been examined by several authors. For example, Waite et al. (1994) modeled the adsorption of U as mononuclear uranyl complexes on ferrihydrite surfaces, and extended X-ray-absorption fine-structure spectroscopy shows that U may be sorbed either as outer-sphere uranyl complexes on smectite (Dent et al. 1992) or as inner-sphere complexes, which may influence subsequent reduction of U (Giblin 1980; Giaquinta et al. 1997). Glinka et al. (1997) found that U sorbed weakly onto colloidal silica as outer-sphere complexes. Uranium sorption on Fe and Mn oxyhydroxides has long been known to be an important process. A combined experimental and modeling study by Bruno et al. (1995) suggested that U may coprecipitate on Fe(III) oxyhydroxides surfaces as schoepite or DS. Murakami et al. (1997) examined a sample from Koongarra by high-resolution transmission electron microscopy and found microcrystals of saléeite, 10-50 nm across, within a microvein of goethite or hematite, a few nm wide. The sample was from a region where the groundwater is far below saturation with respect to saléeite (Mg = 13 ppm, P < 5 ppb, U = 30 ppb). Murakami et al. (1997) explained the crystallization of saléeite microcrystals (microcrystallization) as follows. Ferrihydrite is formed early during weathering of ferrous minerals (Murakami et al. 1996). Dissolved P from groundwater is incorporated onto or into ferrihydrite by adsorption, coprecipitation, or both. Phosphorous in ferrihydrite is then released during the transformation (Ostwald ripening) of ferrihydrite to goethite and hematite. In addition to this localized source of P, locally available U (which can strongly sorb onto fine- grained ferric oxyhydroxides) results in precipitation of saléeite microcrystals directly on the surfaces of goethite and hematite. Sato et al. (1997) reported microcrystals of torbernite on Fe oxyhydroxide nodules at Koongarra, and Buck et al. (1997) identified microcrystals of meta-autunite in U-contaminated soils at Fernald, Ohio, USA. Microcrystallization is, therefore, a potentially important mechanism by which U can be immobilized in natural environments for long periods.

Uranyl Arsenates–Uranyl arsenates occur most commonly where arsenide(II) minerals and as-bearing sulfide(II) minerals are being oxidized. Thus, uranyl arsenates commonly occur in the same localities as uranyl sulfates. However, unlike the sulfates, uranyl arsenates are quite insoluble. In fact, they are structurally related to the uranyl phosphates and display virtually identical physical properties, including low solubilities. Some uranyl arsenates also exhibit reversible dehydration (Cejka 1999).

Uranyl Vanadates–Uranyl vanadates comprise, perhaps the most insoluble of the uranyl minerals (Garrels and Christ 1959). Uranyl vanadates are important U ores in the Colorado

Plateau of the US. Uranyl vanadates are so stable that it is considered likely that they will form wherever dissolved U comes in contact with waters containing dissolved vanadate ions. The uranyl vanadates occur where reduced U minerals (e.g., uraninite, coffinite, or brannerite) and reduced V minerals (e.g., montroseite) are undergoing oxidation. Vanadium(V) may also be derived from V(III)-bearing rocks, such as shales and other clay-rich rocks that also commonly contain organic matter in which both U and V are reduced. The structural stabilities of uranyl vanadates is also manifested by the abilities of most to rehydrate reversibly (Cejka 1999).

Uranyl Molybdates–There are no data, but parageneses are similar to that of the vanadates, formed where reduced Mo(II) minerals are being oxidized. In addition to uranyl molybdates, several U-Mo minerals are known in which U or Mo or both are in a reduced state.

Uranyl Tungstates–Only one is known, uranotungstite, for which there is no thermodynamic data, but it is probably relatively insoluble in most groundwaters, as are many tungstate minerals. Uranotungstite is known from only one locality (Walenta 1985).

Uranyl Tellurates–There are no data. They are probably relatively insoluble. These minerals lack of H_2O; so dehydration is not a factor.

B4. ALTERATION OF URANYL MINERALS

B4.1 Dehydration Reactions and the Structural Role of H_2O in Uranyl Minerals

Virtually all minerals that contain the uranyl ion, $(UO_2)^{2+}$, also contain substantial amounts of structurally bound H_2O, as well as OH^- ions and a few minerals may contain H_3O^+ ions. Many uranyl minerals are weathering products, formed at low-temperatures in near-surface aqueous environments, and structurally bound molecular H_2O strongly influences the structural and thermodynamic stabilities of these minerals. The hydroxonium ion, H_3O^+, may occur in some uranyl minerals, but it has never been verified, and it is an unusual constituent in mineral structures (Hawthorne 1992). Structurally bound H_2O groups most commonly occur in interstitial (interlayer) sites in mineral structures, where they may be bonded to an interlayer cation, or they may occupy sites in which H_2O groups act as an H-bond "bridge" only. The ease with which H_2O groups may be removed from interstitial sites depends on bonding environments, and H_2O groups that are H-bonded only appear to be lost most readily (Finch et al. 1998). Numerous uranyl minerals display significant structural changes caused by the loss of structurally bound H_2O groups. Such structural changes are the reason that many uranyl minerals dehydrate irreversibly, although some uranyl sulfates, vanadates, and, rarely, uranyl phosphates are known to hydrate and dehydrate reversibly. No uranyl oxyhydroxides are known to dehydrate reversibly, a significant fact, since these minerals are commonly the earliest to form during corrosion of uraninite in weathering environments.

The removal of structurally bound H_2O groups from interlayer sites requires significant re-adjustment of local bonding arrangements and commonly results in phase transformations or even complete structural decomposition. For these reasons, most dehydration reactions among the uranyl minerals are irreversible, even at near-ambient temperatures. Furthermore, the relatively low energies required to remove H_2O groups from the interlayer sites in many of these

structures results in narrow temperature ranges over which each mineral stable with respect to other uranyl phases with more or less H_2O.

Perhaps the most dramatic and best understood effect of dehydration is that experienced by the loss of H_2O from schoepite. Schoepite, $[(UO_2)_8O_2(OH)_{12}]\cdot 12H_2O$, transforms slowly in air at ambient temperature to metaschoepite, $[(UO_2)_8O_2(OH)_{12}]\cdot 10H_2O$ ($UO_3\cdot 2H_2O$). The transformation is characterized by a 2% decrease in the ***a*** cell dimension. There may be a slight decrease in the ***b*** cell dimension, but there is no significant change in the ***c*** cell dimension. The observed unit-cell changes may be due to the loss of one-sixth of the interlayer H_2O groups in schoepite, and this must result in changes to H-bonding arrangements. Differences in unit cell volumes induce strain to crystals for which the transformation to metaschoepite is incomplete, and stored strain energy may be sufficient to rapidly drive the transformation of schoepite to DS when exposed to an external stress (e.g., heat or mechanical pressure). The complete transformation of schoepite to DS is:

$$[(UO_2)_8O_2(OH)_{12}](H_2O)_{12} \Rightarrow 8[(UO_2)O_{0.25}(OH)_{1.5}] + 12H_2O$$

DS is a defect structure-derivative of α-$UO_2(OH)_2$. Crystals that undergo dehydration change from translucent yellow schoepite to opaque yellow, polycrystalline DS ± metaschoepite. The complete transformation occurs in three steps: (1) loss of interlayer H_2O from schoepite, causing collapse of the layers, (2) atomic rearrangement within the sheets from a schoepite-type arrangement to a configuration which may be similar to that of metaschoepite, and (3) a second rearrangement to the defect α-$UO_2(OH)_2$-type sheet. Finch et al. (1998) proposed that the formula of DS be written $(UO_2)O_{0.25x}(OH)_{1.5+2x}$ to reflect the observed non-stoichiometry and irreversible dehydration reactions of schoepite and metaschoepite.

Some important physical effects of minerals dehydration include the expansion of gaps between grain boundaries (caused by reductions in molar-volume due to dehydration) and reductions in grain sizes (due to structural changes). These phenomena increase the available pathways for penetration of groundwater into corrosion rinds that form on many altered uraninites in nature. Reductions in grain sizes also increases the reactive surface area of minerals exposed to subsequent infiltration of groundwater. No evidence for rehydration of dehydrated uranyl oxyhydroxides is apparent where water has recontacted previously dehydrated uranyl minerals (Finch et al. 1992). Instead, the pre-existing minerals dissolve along grain boundaries, and minerals such as soddyite and uranophane commonly replace the dehydrated minerals. Reprecipitation of schoepite in contact with DS is apparently uncommon, and Finch et al. (1992) suggest that DS may inhibit the formation of schoepite. Indeed, schoepite, though common, is not an abundant mineral where uraninite is undergoing weathering (Frondel 1958). Uranyl oxyhydroxides with additional cations, such as Ca (becquerelite), K (compreignacite), Ba (billietite) and Pb (numerous Pb-uranyl oxyhydroxides are known) are more common and persistent than schoepite. Becquerelite is, in fact, one of the most common uranyl minerals in uraninite-bearing deposits undergoing weathering reactions.

B4.2 Groundwater Alteration

Precipitated early during uraninite alteration, the uranyl oxyhydroxides alter as they continue to interact with groundwaters. Their alteration may include complete dissolution, e.g., where carbonate or sulfate complexes are available or replacement by uranyl silicates or carbonates (commonly rutherfordine). At uraninite deposits where carbonates are abundant, dissolved carbonate concentrations and pH can increase during interaction with the host rocks. Above a pH of about 8, the dissolution of schoepite in the presence of bicarbonate can release U to solution:

$$[(UO_2)_8O_2(OH)_{12}](H_2O)_{12} + 24\ HCO_3^{2-} \Rightarrow 8\ UO_2(CO_3)_3^{2-} + 32\ H^+ + 14\ H_2O$$

Where pH remains relatively low (< 6), schoepite may be replaced by rutherfordine if groundwater pCO_2 increases due to biological respiration and decomposition:

$$[(UO_2)_8O_2(OH)_{12}](H_2O)_{12} + 8CO_{2\,(g)} \Rightarrow 8\ UO_2CO_3 + 16\ H_2O$$

The alteration of becquerelite and many other uranyl oxyhydroxides is essentially identical to that of schoepite, with UO_2^{2+} being solubilized in carbonate groundwaters, except where pCO_2 exceeds atmospheric levels, under which conditions, rutherfordine or one of several uranyl carbonates illustrated in Figure 3 may become stable. Becquerelite is more stable than schoepite at higher $\{Ca^{2+}\}/\{H^+\}^2$ values (Figures 3 and 4) and so, perhaps, is more resistant to dissolution. In low ionic strength, low pH, non-complexing waters (e.g., fresh rain water), becquerelite may dissolve incongruently by losing Ca preferentially to U (Casas et al. 1994), possibly to form schoepite:

$$4\ Ca[(UO_2)_6O_4(OH)_6](H_2O)_8 + 8\ H^+ + H_2O \Rightarrow 4\ Ca^{2+} + 3\ [(UO_2)_8O_2(OH)_{12}](H_2O)_{12}$$

If the activity of dissolved silica is sufficient, UO_2^{2+} can complex with silicic acid to precipitate as uranyl silicates. Whether soddyite or uranophane forms depends on the activity ratio, $\{Ca^{2+}\}/\{H^+\}^2$. Low pH, Ca-poor waters favor formation of soddyite; for example, replacing schoepite:

$$[(UO_2)_8O_2(OH)_{12}](H_2O)_{12} + 4\ H_4SiO_4 \Rightarrow 4\ (UO_2)_2SiO_4(H_2O)_2 + 12\ H_2O$$

or becquerelite:

$$Ca[(UO_2)_6O_4(OH)_6](H_2O)_8 + 2\ H^+ \Rightarrow 3\ (UO_2)_2SiO_4(H_2O)_2 + Ca^{2+} + 6\ H_2O$$

More alkaline, Ca-bearing waters favor formation of uranophane, assuming carbonate concentrations remain relatively low:

$$[(UO_2)_8O_2(OH)_{12}](H_2O)_{12} + 4\ Ca^{2+} + 8\ H_4SiO_4 \Rightarrow 4\ Ca(UO_2)_2(SiO_3OH)_2(H_2O)_5 + 8\ H^+ + 12\ H_2O$$

and

$$Ca[(UO_2)_6O_4(OH)_6](H_2O)_8 + 2\,Ca^{2+} + 6\,H_4SiO_4 \Rightarrow 3\,Ca(UO_2)_2(SiO_3OH)_2(H_2O)_5 + 8\,H^+ + H_2O$$

The above reactions constitute some of the more important replacement reactions that occur as groundwaters interact with corrosion rinds of uranyl oxyhydroxides. The alteration of the Pb-uranyl oxyhydroxides is slightly different from that of the Pb-free minerals, and their alteration will be considered in the next section.

Comparable reactions are relevant for the replacement of uranyl oxyhydroxides by minerals such as uranyl phosphates, arsenates, and vanadates. However, in the presence of these ions, the uranyl oxyhydroxides tend to be rare or non-existent (Garrels and Christ 1959; Langmuir 1978).

The alteration of uranyl silicates is less commonly reported than that of the uranyl oxyhydroxides. Uranyl silicates are less soluble than oxyhydroxides in most natural waters and tend to be less vulnerable to groundwater attack. However, as for becquerelite, uranophane may dissolve incongruently in fresh waters, releasing Ca^{2+} and silica, and precipitating soddyite. The replacement of uranophane by soddyite has been observed in natural samples from the Shinkolobwe mine (Deliens 1977), as well as experimentally (Casas et al. 1994):

$$Ca(UO_2)_2(SiO_3OH)_2(H_2O)_5 + 2\,H^+ \Rightarrow (UO_2)_2SiO_4(H_2O)_2 + Ca^{2+} + H_4SiO_4 + 3\,H_2O$$

As far as is known, the reverse reaction has not been reported.

The interaction of uranyl silicates with strongly complexing solutions, such as alkaline bicarbonate waters, might result in the preferential release of U, which would increase the Si:U ratio in the residual solid, and might help explain compositional uncertainties for minerals such as "ursilite."

The following sequence summarizes observed U mineral paragenesis at many oxidized uraninite deposits:

1. Dissolution of uraninite and precipitation of uranyl oxyhydroxides: becquerelite, schoepite, (ianthinite) and vandendriesscheite. These minerals tend to first precipitate within voids and fractures in uraninite as it dissolves. Deliens (1977) noted that the earliest-formed uranyl oxyhydroxides tend to be very fine grained.

2. Replacement of earlier-formed uranyl oxyhydroxides by uranyl silicates and replacement of Pb-poor minerals by Pb-enriched uranyl minerals. In weakly complexing waters, some U is transported short distances to precipitate on the outer surfaces of corroding uraninite as a coarsely crystalline rind of uranyl oxyhydroxides schoepite and becquerelite (± ianthinite). Monocarbonates such as rutherfordine may also precipitate where pCO_2 values are sufficient.

3. The continued replacement of both coarse and fine-grained uranyl oxyhydroxides repeats the alteration sequence. Uranyl phosphates commonly form relatively late.

The dehydration and alteration of uranyl oxyhydroxides notwithstanding, schoepite and becquerelite may persist for many thousands of years. Uranium-series activity ratios for several

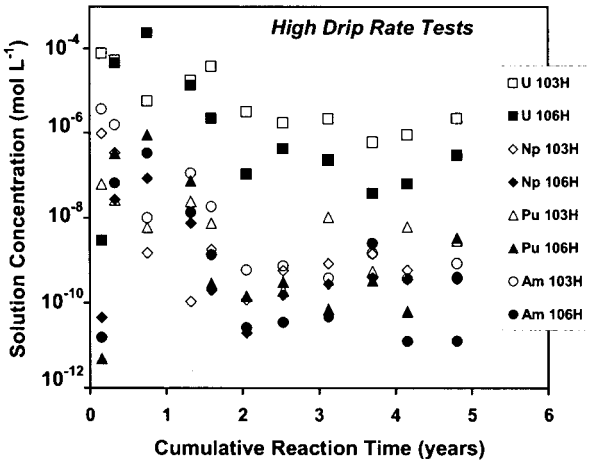
uranyl minerals from the Shinkolobwe mine in southern Democratic Republic of Congo indicate that these minerals did not experience significant preferential loss of U since their formation more than 100,000 years ago. The minerals examined included rutherfordine, schoepite, becquerelite, and uranophane. No correlation was found between mineral species and mineral age (Finch et al. 1996). Finch et al. (1996) concluded that the oxidative dissolution of primary uraninite maintains locally high dissolved U, keeping waters supersaturated with respect to most uranyl minerals and providing an inexhaustible source of dissolved U^{6+} for new mineral precipitation and growth. These results suggest that, as long as uraninite persists in an oxidizing environment, the assemblage of secondary uranyl minerals is determined by local groundwater chemistry (including transitory changes) but not necessarily towards formation of uranyl minerals with lower solubilities.

ATTACHMENT III

USE OF EXEMPT SOFTWARE IN AMR.ANL-EBS-MD-000019

Graphical Plots of Data

Microsoft Excel 97 SR-1 was used to prepare all figures in the AMR. Figures 1, 8, 9, A2, A3, A4, and A6 through A11 show graphical plots of raw data from the data tables in DTN: LL991001251021.090. No formulas, functions or mathematical operations were used on data values from the input source. As an example, Figure 1 (Section 6.4) is reproduced below.



Development of the Least-Squares Fits

In addition to plots of data, Figures A2 and A6 though A11 also show least-squares fits through the data. Microsoft Excel 97 SR-1 was used to calculate the least-squares fits by using the conventional least-squares method, which is explained briefly here. Each release fraction (y_i) that is associated with a sampling interval (x_i), as reported in LL991001251021.090, defines a data point in each figure. The data was modeled by a straight line of the form, $\hat{y} = mx + b$, where $\hat{y}$ is the calculated release fraction (dependent variable), x is the sampling interval in units of time; e.g., years (independent variable), b is the intercept (value of y for x = 0), and m is the rate of release (i.e., the slope of the line in fraction released per unit time). The difference between each estimated value, $\hat{y}_i$, and each measured value, y_i, was calculated and the difference was squared. The squares of these differences were summed over the range of data to be fitted to the model equation in each figure. The best-fit equation is calculated by adjusting the values of m and b in order to minimize the function

$$\sum_{i=1}^{n}(y_i - \hat{y}_i)^2 = \sum_{i=1}^{n}(y_i - mx_i - b)^2 .$$

Obtaining the best values for *m* and *b* may be accomplished by trial and error, which was done for Figures A2, and A6 though A11 by using the SOLVER routine in MS Excel 97. All of the input data for calculating the least-squares fit were obtained from data tables in LL991001251021.090. No mathematical manipulations of the data were performed.

Molar Ratios of Actinides in Solution

Figures 2 and A5 show molar ratios of selected actinides in solution. These figures were calculated by simply dividing the concentration (mol L^{-1}) reported for each transuranium actinide (Np, Pu, Am) by the concentration (mol L^{-1}) reported for uranium (U) from each sampling interval; all data are from data tables in DTN: LL991001251021.090.

An example is provided by Figure A5 (Attachment I), which is reproduced below. Data for a representative calculation is given in Table C1.

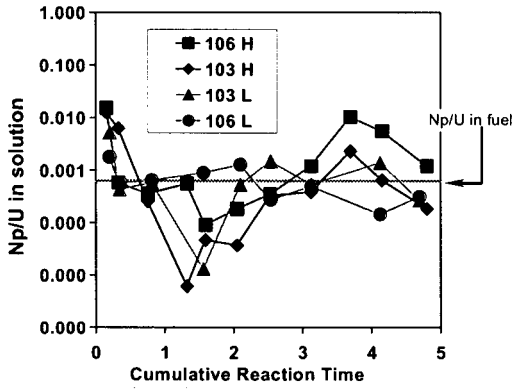


Table C1. Drip Test Data from LL991001251021.090 Used To Calculate the Line "103H" in Figure A5

Years	Np 103H	U 103H	Np/U 103 H
0.16	9.77E-07	7.78E-05	1.26E-02
0.33	3.37E-07	5.36E-05	6.29E-03
0.75	1.47E-09	5.76E-06	2.56E-04
1.32	1.06E-10	1.74E-05	6.11E-06
1.59	1.78E-09	3.81E-05	4.67E-05
2.05	1.19E-10	3.20E-06	3.72E-05
2.53	5.75E-10	1.75E-06	3.28E-04
3.13	8.39E-10	2.18E-06	3.84E-04
3.70	1.39E-09	6.04E-07	2.31E-03
4.16	5.87E-10	9.05E-07	6.48E-04
4.81	4.08E-10	2.20E-06	1.86E-04

Equilibrium Phase Boundaries: Example Calculation for Figures 3, 4, 6, and 7

Figures 3, 4, 6 and 7 display equilibrium phase boundaries between stability fields for two solids (i.e., uranium minerals) that are in equilibrium with water that has compositions spanning the range of values indicated on the ordinate and abscissa. Each line defines the locus of water chemistries along which two solids and the water are in equilibrium. Note that implicit in these stability diagrams is that the concentration of dissolved uranium in the water is always equal to that required to stabilize the solid in each stability field shown.

The equilibrium line between soddyite and uranophane is defined by the reaction between the two minerals in the presence of water containing the elements in the solids, such that the change in the Gibbs free energy of the reaction (ΔG_{rxn}) is zero; vis:

$$\text{SODDYITE} + Ca^{2+}_{(aq)} + H_4SiO_{4\,(aq)} = \text{URANOPHANE} + 2H^{+}_{(aq)}$$

$$\Delta G_{rxn} = -RT\ln K_{so} = \Sigma\Delta G_{products} - \Sigma\Delta G_{reactants}$$

Where,

R is the gas constant (8.314 J mol^{-1} K^{-1}), T is (for the diagrams in Figures 3, 4, 6, and 7) temperature (in Kelvin): (298.15 K, which is 25°C), and K_{so}, the solubility constant for the reaction specified, is defined by the following equation:

$$K_{so} = \frac{a^2_{H+} a_{uranophane}}{a_{Ca^{2+}} a_{H4SiO4} a^3_{H2O} a_{soddyite}}$$

in which a_i is the thermodynamic activity of species i.

Because, for pure solids and dilute aqueous solutions, $a_{uranophane}$, $a_{soddyite}$, a_{H2O}, are equal to 1, K_{so} (for this reaction) simplifies to:

$$K_{so} = \frac{a^2_{H+}}{a_{Ca^{2+}} a_{H4SiO4}}$$

or, by taking the logarithm and rearranging, we get the following equation, which is a straight line (in the form of $y = mx+b$, where $m = -1$ and $b = \log_{10}K_{so}$):

$$\log_{10} a_{H4SiO4} = \log_{10} K_{so} - \log_{10} \frac{a^2_{H+}}{a_{Ca^{2+}}}$$

Furthermore, from the first relation defined above, we know that

$$\log_{10} K_{so} = -\frac{\Sigma\Delta G_{rxn}}{\ln 10 \times RT} = -\frac{\Sigma\Delta G_{products} - \Sigma\Delta G_{reactants}}{2.303 \times RT}.$$

We calculate $\Sigma\Delta G_{rxn}$ (see Table C2) by using the ΔG_i values in Table 6 in the AMR and, for dissolved species and water, by using values reported in Grenthe et al. (1992).

Table C2. Values for Gibbs Free Energies of Formation Used in This Document

Species	ΔG_i (kJ mol^{-1})	Source
Soddyite	-3658.0	Table 6 of AMR
Uranophane	-6210.6	Table 6 of AMR
Ca^{2+}	-552.806	Grenthe et al. (1992)
$H_4SiO_{4\,(aq)}$	-1307.735	Grenthe et al. (1992)
H_2O	-237.14	Grenthe et al. (1992)
H^+	0	By convention (see, e.g., Grenthe et al. 1992)

Which gives:

$$\Delta G_{rxn} = \Sigma\Delta G_{products} - \Sigma\Delta G_{reactants}$$

$$= [-6210.6 + 0] - [-3658.0 - 552.806 - 1307.735 + 3(-237.14)]$$

$$= 19.361 \text{ kJ mol}^{-1}$$

Therefore, we define the straight line given by the equation

$$\log_{10} a_{H4SiO4} = 3.39 - \log_{10} \frac{a_{H+}^2}{a_{Ca^{2+}}}.$$

In order to plot the equilibrium phase boundary between soddyite and uranophane, we calculate a unique value for $\log_{10}K_{so}$ for any arbitrary value of $\log_{10} \frac{a_{H+}^2}{a_{Ca^{2+}}}$ that we choose. We choose two endpoints and connect them to define a line on the diagram (this line is the equilibrium phase boundary). The endpoints are calculated by choosing the abscissa and calculating the ordinate to give the number pairs $(\log_{10} \frac{a_{H+}^2}{a_{Ca^{2+}}}, \log_{10} a_{H4SiO4})$. The values calculated thus, and used in Figure 3, define the end points on the boundary between soddyite and uranophane; they are (6.205, -2.813) and (7.913, -4.521).

The same methodology was used to calculate all phase boundaries illustrated in Figures 3, 4, 6, and 7.